University of Stavanger

Faculty of Science and Technology

MASTER'S THESIS

Study program/ Specialisation: Master of Science: Biological Chemistry	Autumn-spring semester, 2019-2020 Open access
Writer: Geir Magne Risbakken Bringsjord	Geir R. Bringsjord ..... (Writer's signature)
Faculty supervisors: Emil Lindbäck	
Thesis title: Synthesis of tacrine- and coumarin-isocryptolepine hybrids as potential dual binding site acetylcholinesterase inhibitors	
Credits (ECTS): 60 points	
Key words: Alzheimer's disease, Tacrine, Isocryptolepine, Coumarin, Acetylcholinesterase	Pages: 97 (Including Appendix) Enclosure: Spectroscopic data Stavanger, 10th August 2020

Front page for master's thesis
Faculty of Science and Technology
Decision made by the Dean October 30th 2009

UNIVERSITY OF STAVANGER

MASTER'S THESIS

Synthesis of tacrine- and coumarin-isocryptolepine hybrids as potential dual binding site acetylcholinesterase inhibitors

Author:
Geir Magne Risbakken Bringsjord

Supervisor:
Emil Lindbäck

August 10, 2020

University of
Stavanger

Abstract

This project presents the synthesis of tacrine and coumarin scaffolds armed with an alkyl-chain of varying length with an azido functionality and isocryptolepine scaffold armed with a terminal alkyne.

The synthesis of these compounds lead to the successful synthesis of the potential dual binding site acetylcholinesterase inhibitors, a tacrine-cryptolepine hybrid with a 3 carbon-linker and a coumarin-isocryptolepine hybrid with a 4 carbon-linker assembled *via* copper-catalyzed azide-alkyne cycloaddition (CuAAC). The attempted synthesis of the same hybrids with different linker-length (6 and 8) were not successful.

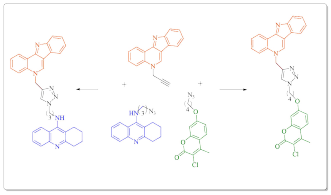

Acknowledgements

All work conducted on this thesis was done at the University of Stavanger, Department of Chemistry, Bioscience and Environmental Technology, Norway, as part of my Master's Degree in Biological Chemistry.

First and foremost, I would like to express my sincere gratitude to Associate Professor Dr. Emil Lindbäck for his constant guidance and support throughout the entirety of this project. I would also like to thank him for giving me the opportunity to work on such an exciting project.

Secondly, I would like to thank PhD student Vebjørn Eikemo and PhD student Katja S. Håheim for all of your constant help and support. You probably do not realize how much your presence during this year has meant to me. I would also like to thank PhD student Marianne Bore Haar, and although our time together was shorter, you always had the time to help whenever I would have an inquiry. I would also like to thank fellow MSc-student Kristin Lende for all of the fun we had in the lab and for being a great sparring partner. You all made my time at the lab so much better, and for that I am grateful.

Furthermore, thanks to Associate Professor Dr. Kåre B. Jørgensen for his help with the NMR instrument when it was in need, which at times felt more often than not.

Finally, a big thanks to my friends and family for their relentless support in my time of presence, and for all of their understanding in my time of absence. Special thanks to my wonderful girlfriend, Julie Andersen. Your support and love throughout this project is what kept me going at times.

Selected abbreviations and acronyms

ACh	Acetylcholine
AChE	Acetylcholinesterase
AChEI	Acetylcholinesterase inhibitor
AD	Alzheimer's disease
Aβ	Amyloid-β protein
Ar	Aryl
BuChE	Butyrylcholinesterase
CAS	Catalytic anionic site
ChE	Cholinesterase
CuAAC	Copper(I)-catalyzed azide-alkyne cycloaddition
DFT	Density functional theory
DCM	Dichloromethane
DMF	Dimethylformamide
DMSO	Dimethyl sulfoxide
FTIR	Fourier transform infrared spectroscopy
hAChE	Human AChE
Hz	Hertz
HMBC	Heteronuclear multiple bond correlation spectroscopy
HSQC	Heteronuclear single-quantum correlation spectroscopy
h	Hour(s)
LRMS	Low resolution mass spectrometry
MW	Microwave
MAO	Monoamine oxidase
MTDL	Multi-target-directed-ligand
NFTs	Neurofibrillary tangles
S_NAr	Nucleophilic aromatic substitution reaction
PAS	Peripheral anionic site
PE	Petroleum ether
R_f	Retardation factor
tcAChE	*Torpedo californica* AChE

Contents

1 Introduction

1.1 Alzheimer's disease

Among many diseases affecting modern societies, dementia is one of the most serious health problems of today. The number of cases worldwide is estimated at 50 million, a number which is projected to reach 152 million already by 2050.[1] With a current globally estimated cost of care of about $1 trillion and an expected cost of about $2 trillion by 2030, dementia may both weaken social and economical development and could potentially overwhelm the health and social services.[1,2] The leading form of dementia, accounting for about 60-80% of cases, is Alzheimer's disease (AD). The disease is a neurodegenerative disorder characterized by a progressive loss of neurons which may affect learning ability, speech, behaviour, memory, the motor system and other cognitive functions.[3–5] A description of AD was first published in 1907 by Alois Alzheimer, and even today the principal features that he described of aggregation of extracellular amyloid-β protein (Aβ), also known as plaques, and paired filaments of intracellular hyperphosphorylated τ protein, also known as neurofibrillary tangles (NFTs), are still required for pathological diagnosis and are considered the two main hallmarks of the disease.[6,7] Other neuropathological features of AD include synaptic alteration, microgliosis, inflammation and glial cell dysfunction.[8–11]

Despite huge efforts by both pharmaceutical companies and the scientific community, no cure for AD has yet to be found. In the period of 2002-2012, 431 AD trials, whereas 83 reached Phase 3, were performed.[12] According to an online database provided by the U.S. National Library of Medicine,[1] almost 1000 clinical trials related to AD are either recruiting or ongoing. However, no new drug has been approved since the US Food and Drug Administrations (FDA) approval of the *N*-methyl-D-aspartate(NMDA)-receptor antagonist memantine in 2003.[13,14]. The only other therapeutic options available on the market today are the three acetylcholinesterase inhibitors (AChEIs) donepezil, rivastigmine and galantamine (Figure 1).[15,16] However, all of the aforementioned approved drugs only serve as palliative treatment, resulting only in a temporary symptomatic relief. In fact, in about 90% of cases the drugs will already seize to have a positive effect after just more than 3 years.[17]

[1] https://clinicaltrials.gov/ct2/home

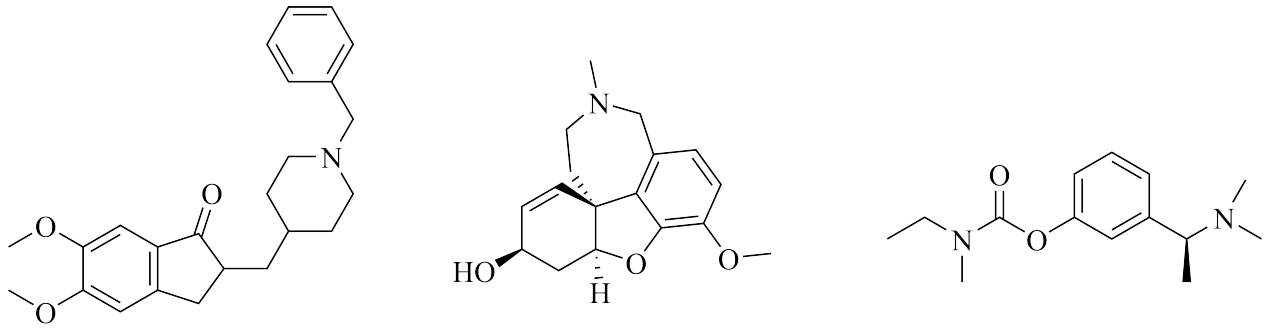

Figure 1: The three acetylcholinesterase inhibitors donepezil, galantamine and rivastigmine.

1.1.1 History and progress of Alzheimer's disease hypotheses

The reason behind the therapeutic majority of AChEIs on the market is rooted in the cholinergic hypothesis. The support for the hypothesis came in the 1970s as significant deficits of choline acetyltransferase, the enzyme responsible for the synthesis of the neurotransmitter acetylcholine (ACh), was reported in cases regarding AD.[18,19]. Subsequent discoveries of decreased choline uptake[20] and additional research relating ACh to memory, learning, and other cognitive functions, led to the rise of the cholinergic hypothesis.[21,22] According to the hypothesis normal cognitive functions might reoccur if acetylcholinesterase (AChE), the enzyme mainly responsible for the hydrolysis of ACh, could be inhibited.[23] Crystal structural studies on AChE from the electric fish (*Torpedo californica*) (tcAChE)[24,25] have shown that the enzyme consists of two binding sites: the catalytic anionic site (CAS) and the peripheral anionic site (PAS), lined with multiple conserved aromatic residues. In more recent times this has been confirmed by studies on recombinant human AChE as well.[26,27] The two binding sites are connected by a $\sim$20 Å deep, and $\sim$5 Å narrow gorge, located at the bottom and at the mouth of the gorge, respectively (Figure 2).[24,28] The CAS region of hAChE includes the catalytic triad (Ser203-His447-Glu334), oxyanion hole (Gly121, Gly122 and Ala204), the choline binding site (Trp86, Tyr337, Phe338), and the acyl pocket (Phe295 and Phe297,) all of which serve a role in the binding of substrates[29]. The PAS consists of the aromatic residues Trp286, Tyr124, Tyr72 and Tyr341 and functions as a relay station temporarily binding to the substrates and subsequently leading them towards the CAS.[30,31] The discovery and further research on the two active sites in AChE eventually led to the "bivalent strategy", suggesting that a dimer of pharmacophores tethered by a suitable linker would be able to bind to both the PAS and CAS of AChE, promoting a significant increase in binding affinity and consequently a greater inhibition of AChE.[32] The active-site gorge of AChE is known to display a certain conformational flexibility. This is displayed as binding of different bifunctional ligands can induce

sidechain rotations (of varying degree) allowing binding to the AChE despite structural differences between the bivalent ligands, which in turn allows for greater diversity in the designs of potential dimers.[33,34] With this in mind: Most of todays approved drugs have a heterocyclic system, indicating the activity of heterocyclic based compounds as important in inhibiting the ChEs.[35] Compounds with tricyclic and heterocyclic system such as *tacrine* and *coumarin* are able to interact with both the CAS and PAS of the ChEs through hydrophobic interactions and by binding to the aryl group of different amino acids through π-π bond-stacking.[36–38]

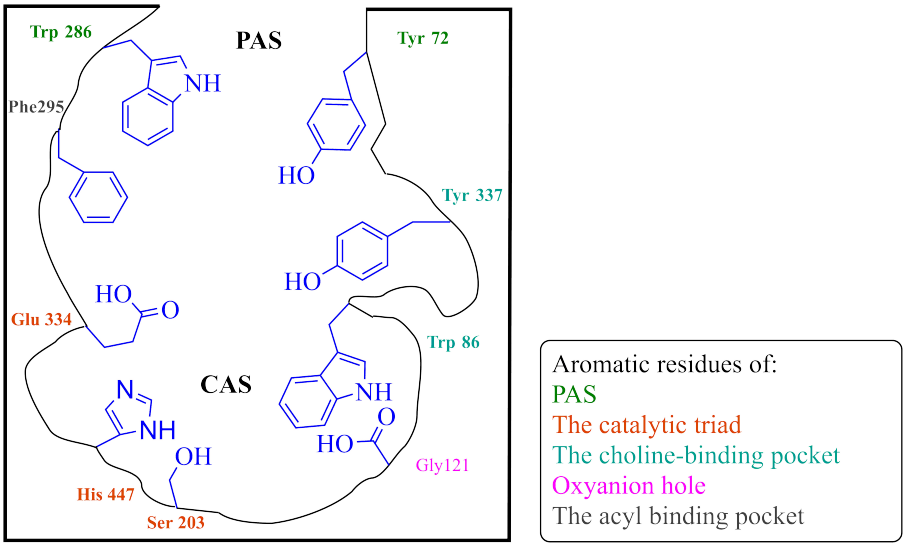

Figure 2: Illustration of the structure of hAChE, including some of the aromatic residues present.[30,39]

Besides AChE, one other type of cholinesterase (ChE) exists, and that is butyrylcholinesterase (BuChE). Despite AChE and BuChE being encoded by different genes, they share a 65% amino acid sequence homology.[40,41]. The main difference between the two ChEs is the replacement of aromatic with aliphatic amino acid residues in BuChE.[41] This structural difference also leads to differences in their susbtrate specificity; AChE is highly selective for ACh while BuChE is less selective and is able to metabolize several different molecules including a number of various neuropeptides.[42] The volume of the CAS in BuChE is considerably larger (roughly $\sim$200 Å) than the one found in AChE, which allows BuChE to bind bulkier inhibitors than AChE.[43] Despite the differences, BuChE also possess the ability to hydrolyse ACh. The hydrolysis of ACh yields choline and acetic acid and leads to the termination of its function as a neurotransmitter.[41] Interestingly, BuChE binds to ACh less efficient at low concentrations, but highly efficient at elevated ones.[44] This is relevant in the context of AD, because as the level of AChE declines or remains unaffected, the level of BuChE increases in the AD brain.[45] In addition, it has also been confirmed that BuChE serve a vital role in cognitive functions and

has been found to associate with both Aβ plaques and NFTs in both mouse models and human tissue.[46,47] This could imply that dual inhibition of both AChE and BuChE may serve as an appropriate therapeutic target for the treatment of AD.[41,48]

For almost 30 years another hypothesis has emerged as the dominant model of AD pathogenesis; the amyloid cascade hypothesis.[49,50] The hypothesis postulates that one of the hallmarks of AD, Aβ aggregates, is the fundamental cause of the disease.[51] Disocoveries of mutations in the genes influencing Aβ production in patients with early-onset familial AD[52,53] and the detection of a similar mutation in patients with Downs syndrome, of which a majority develop at least early symptoms of AD after the age of 40, supported this hypothesis.[54,55] The major components of Aβ are $A\beta_{1-40}$ and $A\beta_{1-42}$.[56] The plaques generated from $A\beta_{1-42}$ lead to severe neuronal toxicity[57] meaning the prevention of $A\beta_{1-42}$ aggregation could serve as a potential strategy in the treatment of AD. However, results from studies on potential amyloid cascade players have so far been disappointing.[58,59] One approach to lowering toxic Aβ aggregation which is still of interest today, is the inhibition of βsecretase, the β-site APP cleaving enzyme I (BACE1). BACE1 is responsible for the *N*-terminal cleavage of the APP, leading to the production of Aβ peptide and making BACE1 a potential target in AD treatment.[60,61]

In recent years, studies have shown that AChE may play a role in accelerating Aβ formation via amino acids located in the proximity of the PAS.[62] Studies have confirmed that AChEIs that are able to bind to either exclusively to the PAS, or bind to both the CAS and PAS binding sites, can inhibit Aβ aggregation.[63,64] It has also been presented evidence of AChE impacting another hallmark of AD through dysregulation of hyperphosporylated τ.[65] This has brought new life to the use of AChEIs in the development of AD drugs.[66]

Another potential therapeutic target in the treatment of AD is monoamine oxidase (MAO). MAO is classified as two isoforms, MAO-A and MAO-B, distinguished on the basis of their substrate specificity and their sensitivity towards specific inhibitors.[67] MAOs are enzymes responsible for oxidative deamination of neurotransmitters like histamine, tyramine and dopamine.[68,69] The deamination process instigated by MAO produces hydrogen peroxide (H_2O_2), which in turn can trigger the production of oxidative free radicals.[70,71] Whereas inhibitors of MAO-A are used as antidepressants[72], inhibitors of MAO-B can be used to treat neurodegenerative disorders like Parkinson's disease and AD[73,74]. The MAO-B activity has been shown to increase with age, especially in AD patients. The increase in hydrogen peroxide and oxidative free radicals can lead to and induce mitochondrial and neuronal damage.[75,76] It is therefore of no surprise that several selective MAO-B inhibitors have been demonstrated to retard the fur-

ther neurodegeneration in AD[77,78]. More recent research also suggests that MAO-B plays a role in the formation of Aβ plaques, further supporting selective MAO-B inhibition as a viable target for the treatment of AD.[79]

In addition to what has already been discussed a large body of research have described a number of pathogenic mechanism underlying the causes of AD, including, but not limited to: neuroinflammmation, mitochondrial dysfunction, dysregulation of iron metabolism, calcium theory, oxidative stress and metabolic disruption of biometals.[80–85] The multifactorial nature of AD is seen as the main cause of the lacklustre results of early anti-AD drug development.[86] It furthers suggests that the conventional standard of 'one drug, one target' may not be a suitable strategy in the treatment of AD. This spawned the "multifactorial hypothesis", which is the basis of the multi-target-directed-ligand (MTDL) strategy.[87] The strategy aims to develop a single molecule, often by combining two distinct pharmacophores connected by a suitable linker able to target a number of the key pathogenic mechanisms suggested to be vital in the progression of AD. Preferably each pharmacophore also retains its ability to interact with its specific site(s) on the target resulting in greater effectiveness compared to single-targeting drugs.[88–91] The MTDLs also have the advantage of lower probability of drug-drug interactions, and higher patient adherence, which is important for a neurodegerenative disease like AD.[92] A review of the literature reveals that the most common approach when designing MTDLs is to combine an AChEI with another pharmacophore providing the new molecule with biological properties beyond AChE inhibition.[93,94] This is most commonly achieved by combining a known AChEI with a pharmacophore with known BACE1 and/or MAO inhibition properties, metal chelating properties or NO-releasing activities[95]

The vast number of hypotheses and strategies attempting to explain and combat the multifactorial disorder of AD has led to a wide array of research on different design strategies and possible pharmacophores in the search for a cure, evidenced by the numerous comprehensive reviews published on the matter.[96–100] This project will focus on just a few out of the vast number of potential AD pharmacophores (Figure 3): *Tacrine*, mainly due to its well-known ability to inhibit AChE by binding to the CAS, but also due to its ability to inhibit BuChE.[98] *Coumarin*, due to the large number of potential analogs, resulting in a wide range of biological activities in regards to both AD specifically (MAO-, BACE1- and AChE-inhibition)[101], but also in a general sense (anti-coagulant[102], antioxidant[103], etc.). *Iocryptolepine*, due to its unknown potential as a possible AChEI, in combination with it being a natural product with well established biologcal activities[104,105]. *The 1,2,3-triazole ring*, due to its excellent properties in regards to medicinal chemistry (stable to hydrolysis, metabolic degradation and

redox)[106] and its potential to form hydrogenbonds and π-π stacking interactions, which is especially interesting in regards to AD due to potential bonding with aromatic residues in the AChE gorge.[107]

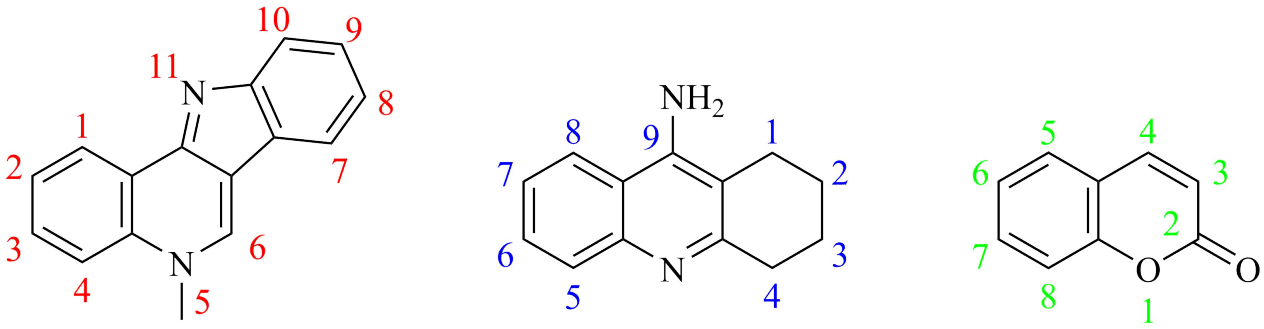

Figure 3: The basic form of the pharmacophores and linker moiety addressed in this project

1.2 Tacrine and its role in the treatment of Alzheimer's disease

Tacrine (1,2,3,4-tetrahydro-9-acridinamine or Cognex®) (Figure 3) is a 1,2,3,4-tetrahydroacridine substituted by an amino group at position 9 and a member of the chemical class of acridines. As one of several acridines, tacrine was first synthesized by the Australian chemists Adrien Albert and Walter Gledhill, at the university of Sydney in the 1940s.[108,109] Although overshadowed by the British discovery of Penicillin, tacrine quickly demonstrated the ability to cross the blood brain barrier and to inhibit AChE with potency in the nanomolar range.[110]. Later research confirmed that this also was true in regards to BuChE aswell, however the binding was even more selective.[111] Tacrines ability to inhibit AChE eventually lead to testing on AD patients[112], which in turn lead to tacrine being approved by the FDA as the first AChEI in 1993, as a reversible, non-competitive inhibitor.[113] However it was soon established that tacrine expressed hepatotoxic responses in patients, especially towards the liver and gastrointestinal tract.[114,115]. Other side-effects included nausea, diarrhoea and anorexia which led to the eventual withdrawal of tacrine from the US market in 1998.[116] However, in the wake of the proposed MTDL strategy, tacrine has re-emerged as an interesting ligand in the development of AD drugs. This is attributed to its classical pharmacophore structure, low molecular weight, synthetic accessibility and its inhibitory properties towards both AChE and BuChE. In tcAChE the binding is displayed through parallel π - π stacking interaction between the benzyl ring of tacrine and the aromatic ring of Trp84 near the bottom of CAS and between the charged nitrogen of the piperidine ring and the phenyl ring on Phe330.[25,117] It is suggested that the cyclic nitrogen of tacrine is protonated when bound to the enzyme due to observed hydrogen

bonding between the cyclic nitrogen and the carbonyl oxygen of His440, highlighting the importance of the basic nitrogen atom of tacrine.[24,118] Crystal structures of the tacrine-AChE complex has shown that tacrine by itself binds solely to the CAS.[25]

More importantly, combining tacrine with another moiety have shown to extend the biological profile of tacrine and overcome some of the hepatotoxicity side effects associated with the use of it.[119–121] An extensive number of tacrine derivatives have already been discussed in great detail in multiple reviews[98,117,122–124]. Here, only a few will briefly be presented (Figure 4) (Table 1).

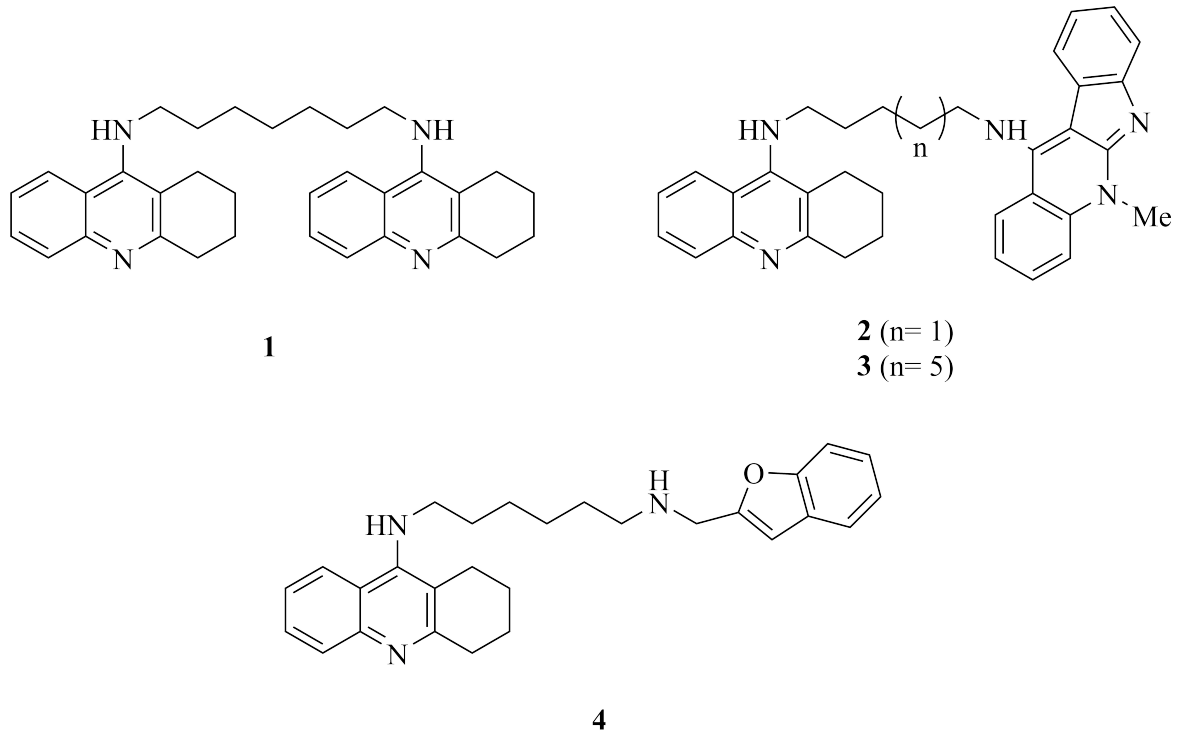

1

2 (n= 1)
3 (n= 5)

4

Figure 4: Structures of some tacrine derivatives presented in literature[36,125,126]

Table 1: Inhibition of hAChE and hBChE activities and AChE-mediated Aβ aggregation by some published tacrine derivatives (Figure 4) compared with tacrine.

Compound	hAChE[a]	hBuChE[a]	$A\beta_{1-42}$ self-aggregation[b]
	IC_{50} [nM]	IC_{50} [nM]	(% inhibition)
Tacrine	350[125]	40[125]	<5, 10 μM[125]
1	0.81[36]	5.66[36]	53.4, 100 μM[36]
2	53.0[125]	21.8[125]	19.7, 10 μM[125]
3	0.95[125]	2.29[125]	26.5, 10 μM[125]
4	0.86[126]	2.18[126]	58.4, 10 μM[126]

[a]IC50 values represent the concentration of inhibitor required to decrease enzyme activity by 50% and are the mean of atleast two independent measurements, each performed in triplicate; [b]Percent inhibition with inhibitor at given μM concentration.

The search for new and promising tacrine derivatives began with research on simple tacrine homodimers. The research group of Pang[32] wanted to prove that additional binding sites in tcAChE (Trp279, Tyr70, Phe290) near the PAS would make it possible for a tacrine homodimer to not only bind to CAS, but to the PAS of AChE as well. This interaction has later been reported as cation-π and π - π interactions.[127] The most promising of the synthesized homodimers of the group of Pang[32] was the compound bis(7)-tacrine (**1**), which connects the two tacrine units through a heptamethylene bridge. The compound was reported to be about a 1000-fold more potent than tacrine in inhibiting rat brain AChE serum[32] and about 400-fold more potent in hAChE serum (Figure 1).[125] Furthermore, the group also investigated the importance of the length of the linker in making potent dimers directed towards AChE.[32] The results showed that the linker at some point (depending on the structure of the dimer) would be too long, not being able to bind to both PAS and CAS, or too short, probably leading to a form of crowding at the bottom of AChE.[32]

An evidence of the importance of the linker length is illustrated by the tacrine-neocryptolepine derivatives **2** and **3**, where **3** is a more potent inhibitor than **2** of both hAChE (50-fold) and BuChE (10-fold).[125] It was reported that **2** was only able to bind to residues at PAS and the mid-gorge, whereas for **3** the neocryptolepine moiety bonded to the PAS region while the tacrine moiety was oriented towards the CAS region of the enzyme, ensuring a stronger binding. Finally, the tacrine-benzofuran hybrid **4**[126] presents an example of how a heterodimer consisting of tacrine and another pharmacophore can possess characteristics beyond inhibition of AChE and Aβ self-aggregation, as compound **4** additionally showed significant inhibition of human BACE1. Importantly, a common denominator for all four compounds (1-4) is that they

all exhibited significantly lower hepatotoxicity when compared to that of tacrine.

1.2.1 Synthesis of tacrine and tacrine derivatvies from the literature

A review of the literature reveals that the most common strategy when preparing quinoline derivatives, such as tacrine and its derivatives, is the use of the Friedländer condensation reaction.[128–130] The Friedländer synthesis is a reaction wherein quinoline derivatives traditionally are synthesized from a condensation reaction between an aromatic 2-amino-substituted aldehyde or ketone with an aldehyde or ketone bearing α-methylene functionality in the presence of a protic acid, a Lewis acid or a base, but has in more recent years come to include several variations.[128]

One such variation was presented by the group of McKenna (Scheme 1).[131] A Friedländer type condensation of 2-aminobenzonitrile (**5**) and cyclohexanone (**6**) is mediated by the Lewis acid boron trifluoride diethyl etherate (BF_3OEt_2) to yield tacrine (**7**). Although several ketones have been reported to participate in this reaction, the mechanism has not been thoroughly studied.[129]. The synthetic route of McKenna is presented in combination with a mechanistic suggestion by Costa *et al.*[128] (Scheme 1). An initial Lewis acid mediated imine formation (i) yielding intermediate **SC1** is followed by imine-enamine tautomerism (ii) activated by Lewis acid coordination and the following formation of **SC2**. The weakly basic nitrile of **SC2** is suggested to be activated by the Lewis acid leading to the intramolecular addition (iii) of the enamine carbon to the nitrile group affording **SC3**. Finally, imine-enamine tautomerism (iv) during or prior to work-up with base affords tacrine (**7**). The synthetic route of McKenna *et al.* was later used by the group of Xie[132], which reported a yield of 92%.

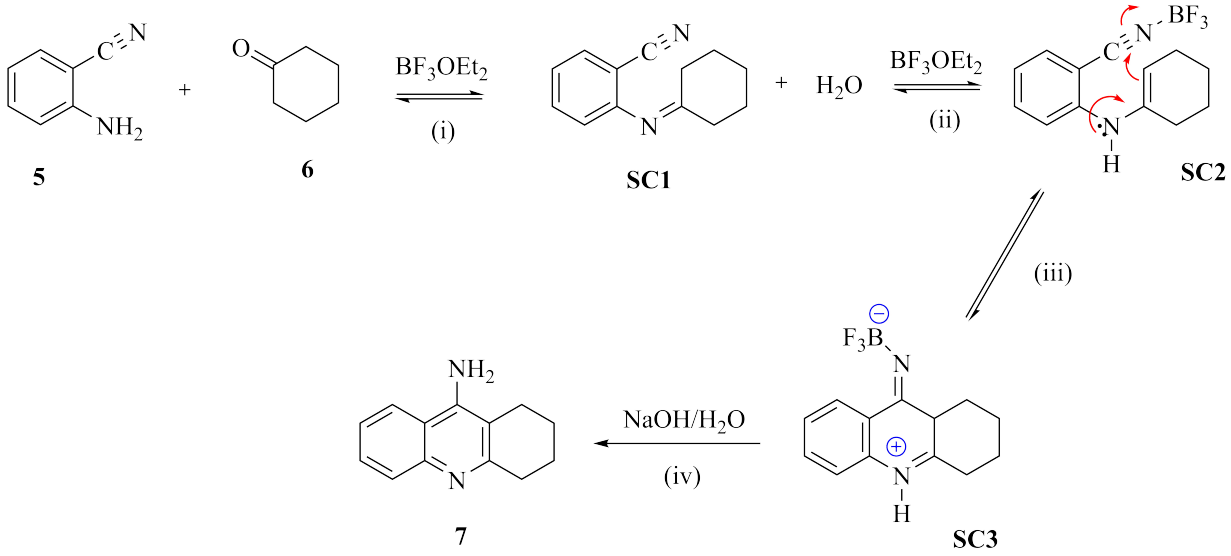

Scheme 1: Synthesis of tacrine (**7**) through a Friedländer type condensation, as described by McKenna *et al.*[131] in combination with a suggested mechanism for the reaction.[128]

Another popular method for synthesizing tacrine and potentially tacrine derivatives is the Niementowski quinoline synthesis reaction between anthranilic acid (**8**) and cyclohexanone (**6**), followed by a simultaneous $POCl_3$-mediated chlorination of the aromatic hydroxyl-group yielding 9-chloro-1,2,3,4-tetrahydroacridine (**9**).[129] Compound **9** has been extensively used as a starting point in the synthesis of several tacrine analogues,[118,133,134] as well as in this project. An example of this strategy was presented by the group of Oukoloff (Scheme 2).[135] From the initial synthesis of **9**, a synthetic strategy towards transforming **9** in to a tacrine scaffold **13** with a 2-methylene bridge armed with an azide functional group was presented. The first step is a S_NAr reaction of **9** facilitated by the addition of 3-amino-1-propanol and heat to obtain compound **10**. This is followed by two more substitution reactions, first $SOCl_2$ and heat yield **12**, before finally yet another substitution reaction with NaN_3 mediated by heat yield **13**.

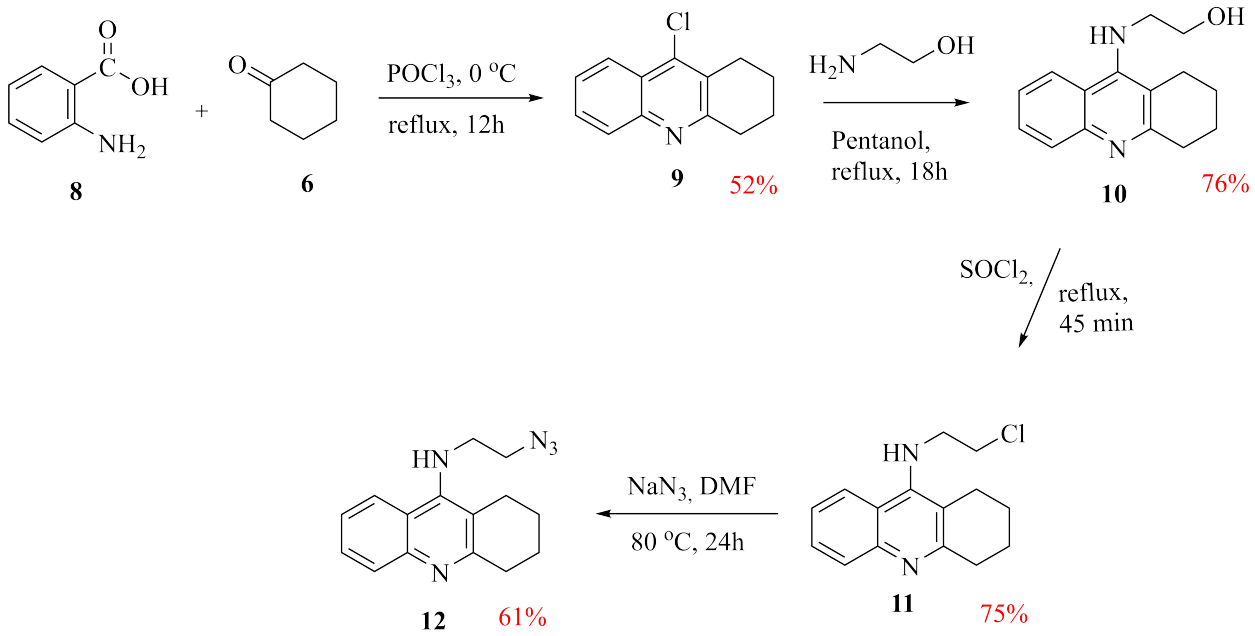

Scheme 2: Synthetic strategy towards the synthesis of a tacrine derivative armed with a 2 methylene bridge and an azido-functionality **13**, as reported by Oukoloff *et al.*.[135]

A review of the literature reveals that for the synthesis of tacrine derivatives armed with a longer linker (∼5C+), another approach is more commonly employed.[136]. This strategy is here presented by the work of the group of Wieckowska[136] where the addition of the desired dibromoalkane in the presence of a strong base facilitates a S_NAr reaction yielding a tacrine analog armed with a methylene-bridge (5-8) with a halide at the end. The terminal halide allows for furter functionalization of the linker, as shown already (Scheme 2).

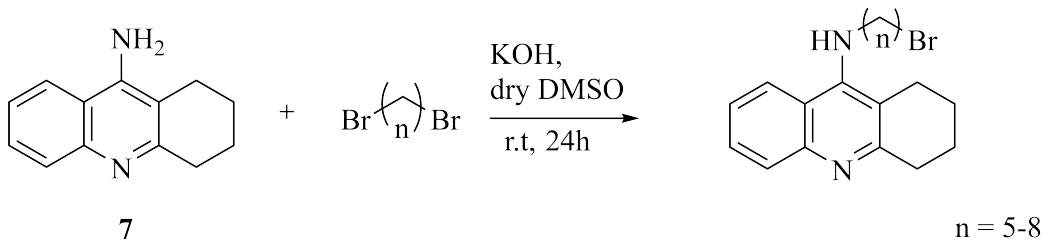

Scheme 3: Synthetic strategy towards arming tacrine with a longer linker (5-8).[136]

In regards to the Niementowski reaction; due to similarities to the Friedländer reaction, the two mechanisms suggested for that reaction have been proposed for the Niementowski quinoline synthesis as well. Although, since the Niementowski quinoline synthesis involves the condensation of an aldehyde or ketone with an anthranilic acid, the mechanistic pathway involving initial formation of a Schiffs base is suggested to be favored (Scheme 4).[137]

Starting from anthranilic acid **8** and a ketone/aldehyde partner (**N1**), an initial formation of the Schiff base (**N2**) is followed by an intramolecular aldol reaction to give the hydroxy imine (**N3**). The reaction is finalized by the loss of water, functioning as the driving force of the reaction, leading to ring closure and the formation of the quinoline product (**N4**).[137] The alchol-group (red) of **N4** is the chlorination target of $POCl_3$ in the synthesis of **9**.

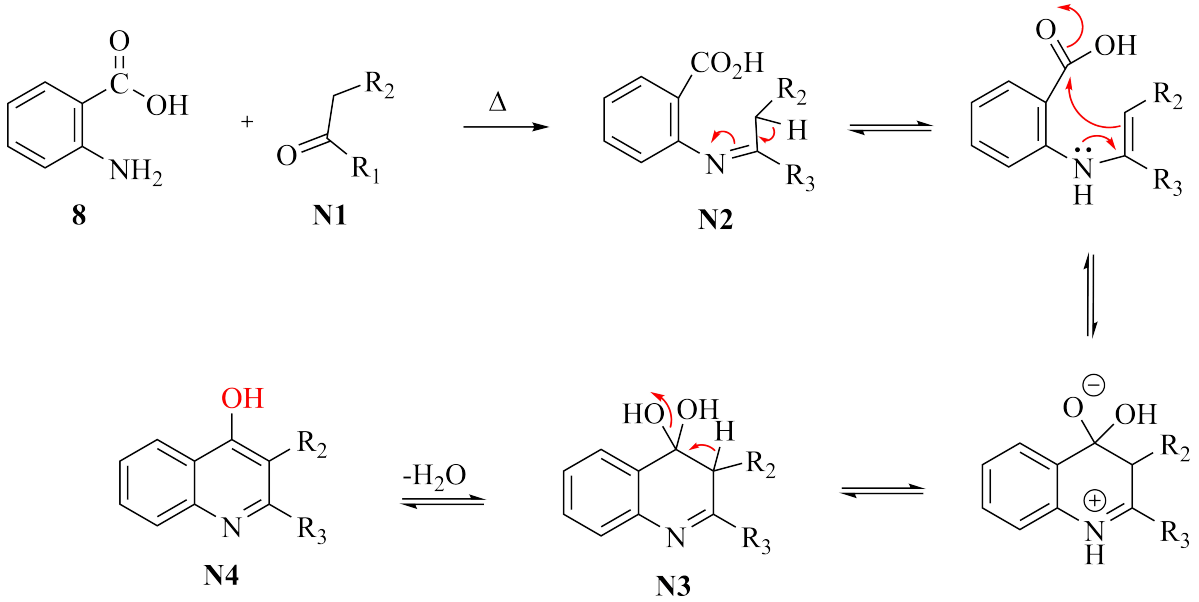

Scheme 4: Suggested mechanistic pathway of the Niementowski quinoline synthesis involving the initial formation of a Schiffs base.[135]

1.3 Coumarins and their potential in Alzheimer's disease treatment

Coumarin (2*H*-chromen-2-one or 2*H*-1-benzopyran-2-one) (Figure 3) is the simplest member of the chemical group of benzopyrones known as coumarins. Coumarin was first isolated in 1820 as a natural product from Tonka beans (*Dipteryx odorata*) and initially mistaken for benzoic acid.[138] Because of its pleasant odour, it has been used in perfumes and flavourings since 1868.[139] Coumarins represent an important family of phytochemicals and synthetic oxygen-containing heterocycles consisting of fused benzene and α-pyrone rings. Substitution reactions of coumarin can occur at any of the six available sites, which offers many possible permutations by both substitution and conjugation. This could explain why so many coumarin derivatives occur naturally[140] but also opens up for a wide array of coumarins with different functionalities and activities. Some of the reported biological activities of coumarins include anti-inflammatory,[140] anti-oxidant,[103] anti-bacterial,[141] anti-tumor,[142] and anticoagulant[143]. It is suggested that naturally based compounds, such as coumarins, are better tolerated in the body compared to synthetic chemicals.[144] This in combination with the wide array of biologi-

cal activities has made coumarins immensely popular in the world of pharmaceuticals in recent years. In regards to this project the reported anti-AD properties of coumarins is however of particular interest.[145,146]

Studies have shown that both naturally occurring as well as chemically synthesized coumarin analogs and coumarin hybrids exhibits potent AChE inhibitory activity. It has been reported that the inhibitory activity is exercised mainly through interactions with the PAS of AChE through π-π stacking interactions.[101,147,148] Studies have also revealed that novel coumarin analogs are capable of inhibiting Aβ aggregation, and that functionalization of the aromatic center can manipulate the inhibition mechanism.[149] Furthermore, coumarin analogs have also been identified as potent and selective MAO-B inhibitors, especially for 7-substituted coumarins with additional substitution in the 3- and/or 4-position.[150–154] Furthermore, coumarin analogs have also been reported as to have potency towards the inhibition of BACE1.[155–157] This has made coumarin analogs highly interesting as scaffolds in designing new bivalent AChEIs and MTDLs in regards to AD treatment. Here, a few will briefly be presented (Figure 5) (Table 2).

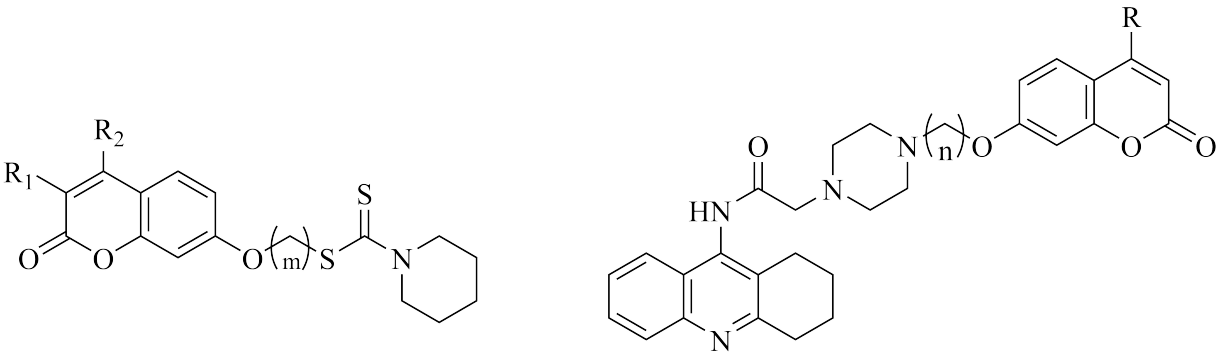

13a R_1 = H, R_2 = H, m = 4
13b R_1 = Me, R_2 = H, m = 4
13c R_1 = Cl, R_2 = Me, m = 4

14a R = Me , n = 2
14b R = Me , n = 3
14c R = MeO, n = 2

Figure 5: Structures of some coumarin hybrids from literature.

The group of He[158] designed and synthesized a series of coumarin-dithiocarbamate hybrids wherein they tested the effect of di-substitution on the coumarin scaffold in the 3C- and 4C-position with the linker armed at the hydroxyl group at the 7C-position (Figure 5). The results showed that compound **13c** was the most potent AChEI (IC_{50} = 0.061 nM) out of the synthesized hybrids as well as a potent MAO-B inhibitor (IC_{50} = 0.363). Xie and his group[132] designed and synthesized a series of tacrine-coumarin hybrids where they tested mono-substitution in the 4C-position. They discovered that hybrid **14a**, methyl-substituted in 4C with a two carbon linker was the most potent and promising inhibitor of both ChEs.

(eeAChE = 0.092 nM, eqBuChE = 0.234 nM) In addition, a majority of the compounds, including **13a-13c**, was also found to inhibit self-induced Aβ-aggregation.[132]

Table 2: Inhibition of ChEs and hMAO-B of some published coumarin hybrids (Figure 5).

Compound	eeAChE[a] IC_{50} [nM]	eqBuchE[a] IC_{50} [nM]	hMAO-B[a] IC_{50} [nM]
Donepezil[b]	0.041[158]	4.22[158]	-
Rasagiline[c]	-	-	0.138[158]
13a	0.218[158]	31.06[158]	8.84[158]
13b	0.367[158]	33.11[158]	4.36[158]
13c	0.061[158]	31.26[158]	0.363[158]
14a	0.092[132]	0.234[132]	-
14b	0.130[132]	0.628[132]	-
14c	0.150[132]	5.14[132]	-
Tacrine[b]	0.269[132]	0.042[132]	-

All values of IC_{50} are shown as mean of three independent experiments; [a]From electric eel (ee), equine serum (eq) and human serum; [b]Known AChEI; [c] Known MAO-B inhibitor.

1.3.1 Literature protocols for coumarin synthesis

The literature describes several possible methods involved in the synthesis of coumarins including Pechmann condensation reaction[159], Knoevenagel condensation[160], Wittig reaction[161], Claisen rearrangement[162], Perkin reaction[163] and Baylis–Hillman reaction[164]. More recently, microwave[165] and solid-phase[166] have been used to success in combination with already established methods. Of these, the Pechmann condensation reaction has been most widely employed for the synthesis of coumarins in large parts due to its preparative simplicity and inexpensive starting materials.[167] The method involves an acid-mediated condensation of phenols with β-keto esters conducted with a strong Brønsted acid or a Lewis acid, usually requiring high temperatures as well.[168]

Pisani and his group[169] presented the synthesis of ethyl (7-hydroxy-2-oxo-2*H*-chromen-4-yl)acetate (**17**) using standard Pechmann reaction conditions (Scheme 5. Resorcinol (**15**) and diethyl 1,3-acetonedicarboxylate (**16**) were condensated, mediated by a Brønsted acid (H_2SO_4) and heat, yielding **14**.

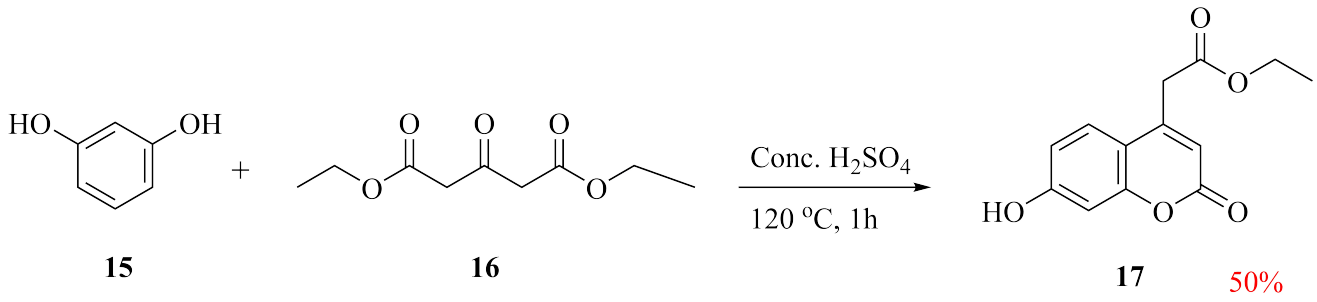

Scheme 5: Synthesis of the coumarin analog ethyl(7-hydroxy-2-oxo-2H-chromen-4-yl)acetate (**17**) using standard Pechmann reaction conditions as described by Pisani *et al.*.[169]

More recently, Zak *et al.*[170] presented a strategy to synthesize numerous coumarins in great yields and with excellent regioselectivity. The strategy is here represented by the synthesis of 3-chloro-7-hydroxy-4-methylcoumarin (**19**) (Scheme 6). Resorcinol (**15**) and ethyl 2-chloroacetoacetate (**18**) reacts in the presence of trifluoroacetic acid as a catalyst under microwave (MW) irradiation yielding the desired coumarin analog **19** by a Pechmann condensation reaction. Using this strategy, different coumarin derivatives were prepared simply by changing the acetoacetate derivative.

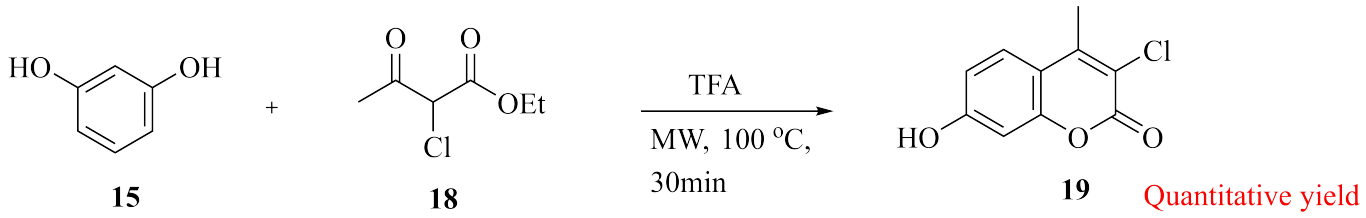

Scheme 6: Synthesis of the coumarin analog 3-chloro-7-hydroxy-4-methylcoumarin (**19**) by a MW-assisted Pechmann condensation as described by Zak *et al.*.[170]

A review of the literature also reveals that the presence of an OH-group in the 7-position is commonly exploited as a means to attach a linker of desired length to a coumarin analog, through the application of Williamson ether synthesis.[132,171,172] The group of Jiang presented an example of this strategy (Scheme 7).[173] The alcohol group of 7-hydroxy-4-methyl-2*H*-chromen-2-one (**20** is deprotonated in the presence of the base. From here, through a S_N2 reaction, the newly formed alkoxide attacks one of the electrophilic carbons of the dibromoalkane, expels the halide and an ether is formed. The result is a coumarin analog with a linker of desired length. The halide connected to the terminal end of the linker opens up for the potential addition of functionality to the linker, as previously shown in Scheme 2.

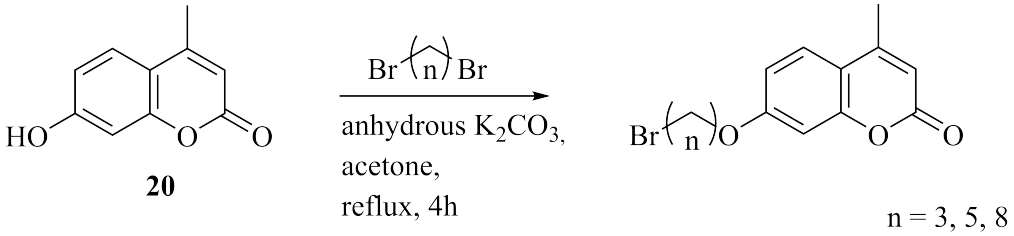

Scheme 7: Synthetic strategy towards arming 7-hydroxy-4-methyl-2*H*-chromen-2-one (**20**) by utilizing Williamson ether synthesis as described by Jiang *et al.*.[173]

1.4 Isocryptolepine, an antimalarial agent as a potential Alzheimer's disease pharmacophore

In recent years, the tetracyclic indoloquinoline alkaloids, composed of a fused quinoline and indole moiety, have attracted considerable attention due to promising antibacterial, antiplasmodial, antitumoral and antimalarial activity.[174,175] The roots of the West African climbing vine *Cryptolepis sanguinolenta* have for centuries been used in folk medicine for the treatment of malaria, bacterial infections and hepatitis.[105,174,176] Examinations of the plant proved it to be a great natural source of several indoloquinolines, of which particularly neocryptolepine, cryptolepine, and isocryptolepine have received considerable attention over the years (Figure 6).

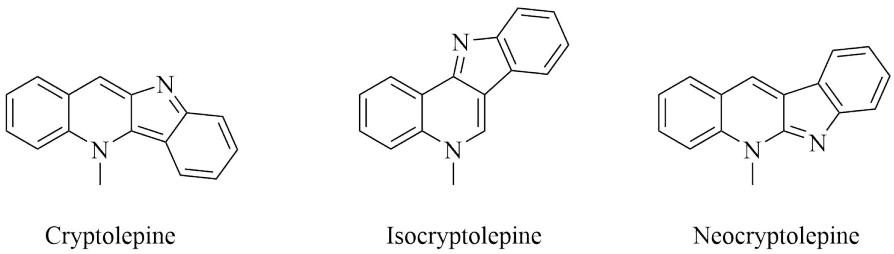

Figure 6: The most notable bioactive compounds isolated from *Cryptolepis sanguinolenta*

.

Although intensely studied in the field of antimalarial research due to their wide potential in several pharmacological applications, little to no research have been conducted on these alkaloids in the field of AD research despite their underlying potential from structure alone (nitrogen containing heterocycle).[177,178] An exception to this is the recent work of Wang *et al.*, wherein a neocryptolepine-tacrine hybrid **3** was synthesized and reported as an exceptionally potent bivalent AChEI (Figure 4). Very recently Nuthakki and his group also reported the ChE inhibitory activity of both cryptolepine and its derivative 2-bromocryptolepine.[179] Cryptolepine was additionally also reported to display inhibition of BACE1 and drug transporter

P-glycoprotein induction activity. The latter of which has emerged as a possible strategy to increase Aβ clearance from AD brains.[180] The limited, but promising research on other indoloquinolines in regards to AD might propose a possible role for isocryptolepine in the context of AD research as well. In addition, as a natural product, isocryptolepine has the advantage as an appropriate starting point due to natural products inherent multi-target profile, evolutionary selectivity and biological pre-validation.[181–183] This combined supports the idea of isocryptolepine as a potentially interesting scaffold in the context of AD research and in regards to the development of both bivalent ligands and MTDLs.

1.4.1 Synthesis of isocryptolepine in the literature

A number of total syntheses of isocryptolepine have been described in the literature over the years. Some of the most common syntheses include Fischer indole cyclisation[184], Pictet-Spengler cyclization[185], Graebe-Ullman reaction,[186] and palladium-catalyzed coupling reactions[187]. A common denominator for most of them is the use of either indoles or quinolines as starting materials.[105]

Helgeland and Sydnes[188] recently presented an effective and concise synthesis (Scheme 8) of isocryptolepine (**21**) using readily available starting materials. 3-Bromoquinoline (**21**) is coupled to 2-aminophenylboronic acid hydrochloride (**22**) under optimized Suzuki-Miyaura cross-coupling conditions applying $PdCl_2$(dppf) as the catalyst. The base (K_2CO_3) was introduced in a mixture of EtOH/water. The coupling product **23** was then subjected to a tandem C-H activation and intramolecular C-N bond formation into the ring system yielding **24**. Finally, (**24**) was regioselectively *N*-methylated to yield isocryptolepine (**25**). Recent efforts by Haaheim *et al.* have further improved the yield of the tetracyclic ring-system **24**.[189]

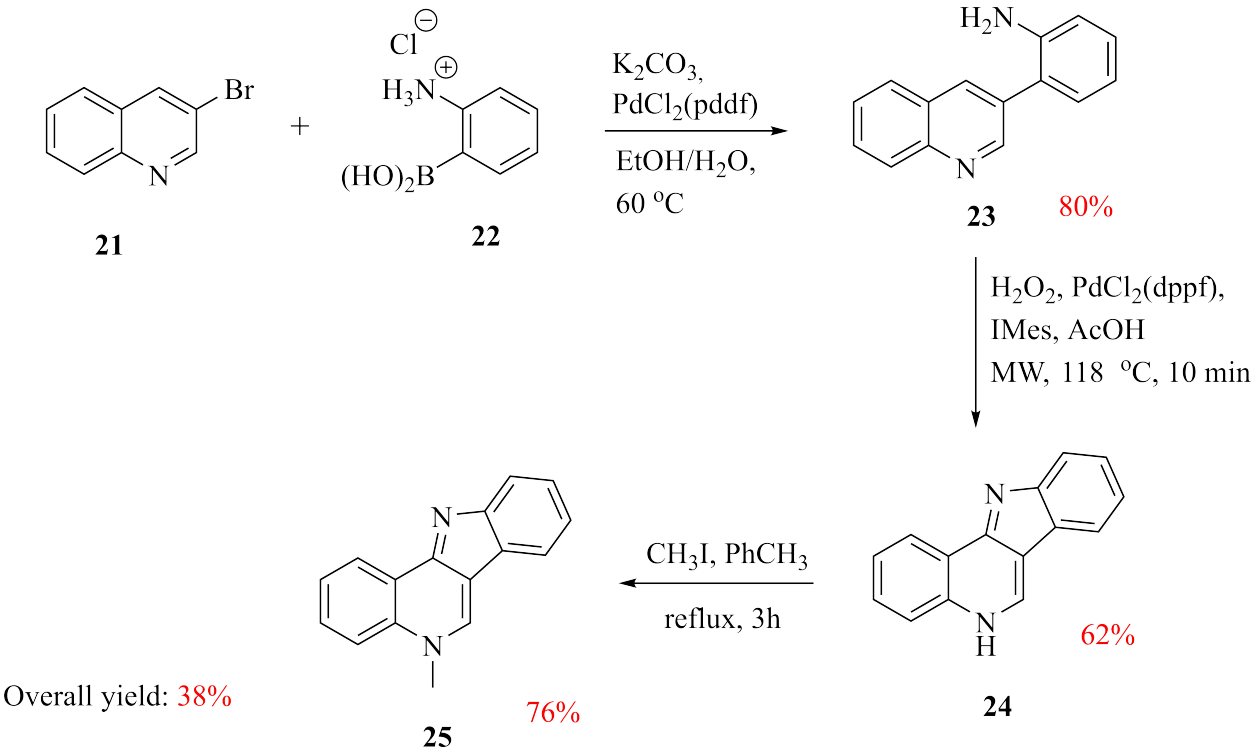

Scheme 8: Total synthesis of isocryptolepine (**25**) as conducted by Helgeland and Sydnes.[188]

The group of Timári[190] developed a synthetic route towards isocryptolepine (**25**) (Scheme 9. The biaryl **27** was obtained through a Suzuki-Miyaura cross-coupling reaction between *N*-pivaloylaminophenylboronic acid (**26**) and 3-bromoquinoline (**21**). The Piv-protective group was then removed by acid hydrolysis to obtain biaryl amine **23**. Subsequent diazotization of molecule **23** followed by treatment with sodium azide provided **28** in a Sandmeyer type reaction. Thermal cyclization was achieved by refluxing **28** in *ortho*-dichlorobenzene yielding the indoloquinoline **29**. Finally, regioselective *N*-methylation was achieved by reacting **29** with dimethyl sulfate (Me_2SO_4) in acetonitrile (CH_3CN) yielding isocryptolepine (**25**).

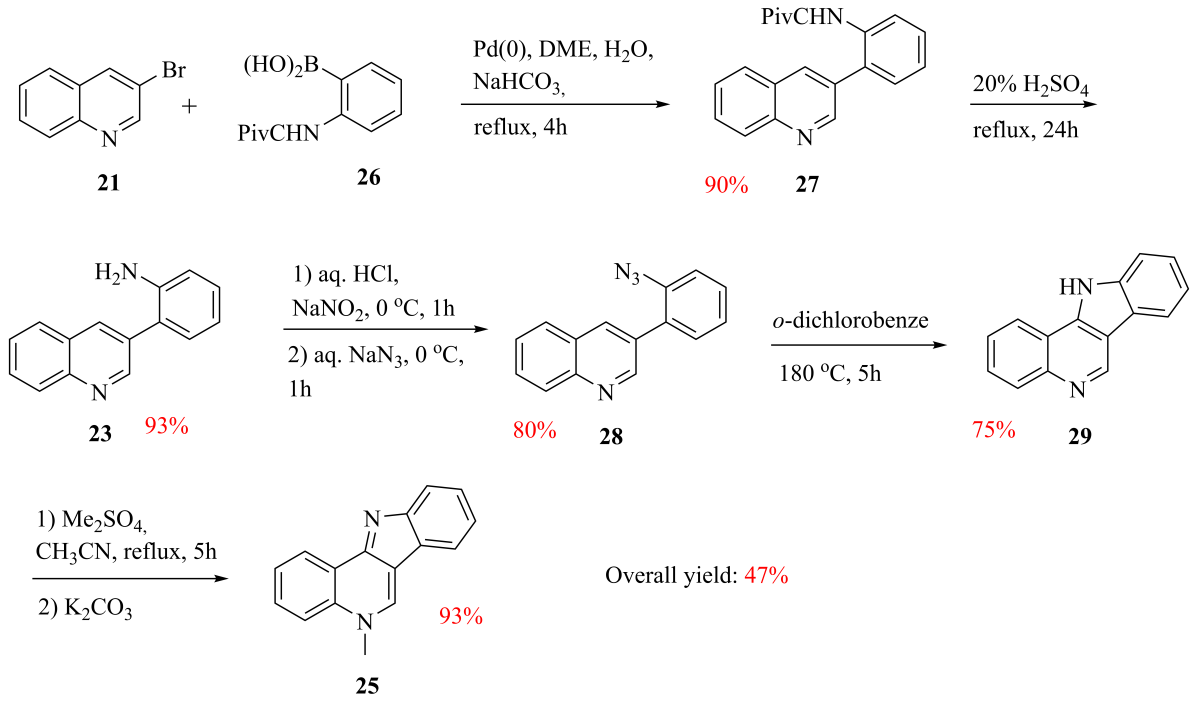

Scheme 9: Total synthesis of isocryptolepine (**21**) as described by Timári *et al.*.[190]

Singh *et al.*[191] have proposed a mechanism for the one-pot diazotization-azidation-cyclization (Scheme 9) of **24** yielding iscocryptolepine precursor (**25**). After the amine **23** is transformed into the corresponding aryl azide **28** under standard Sandmeyer-type conditons, the azide is collapsed in refluxing *ortho*-dichlorobenzene to give the isocrpyptolepine precursor as the major product (Scheme 10). Presumably the cyclization proceeds via a thermally induced nitrene insertion mechanism starting off with the expulsion of nitrogen gas from the moleule. Subsequent annulation and a 1,5-shift yields the isocryptolepine precursor **25**.

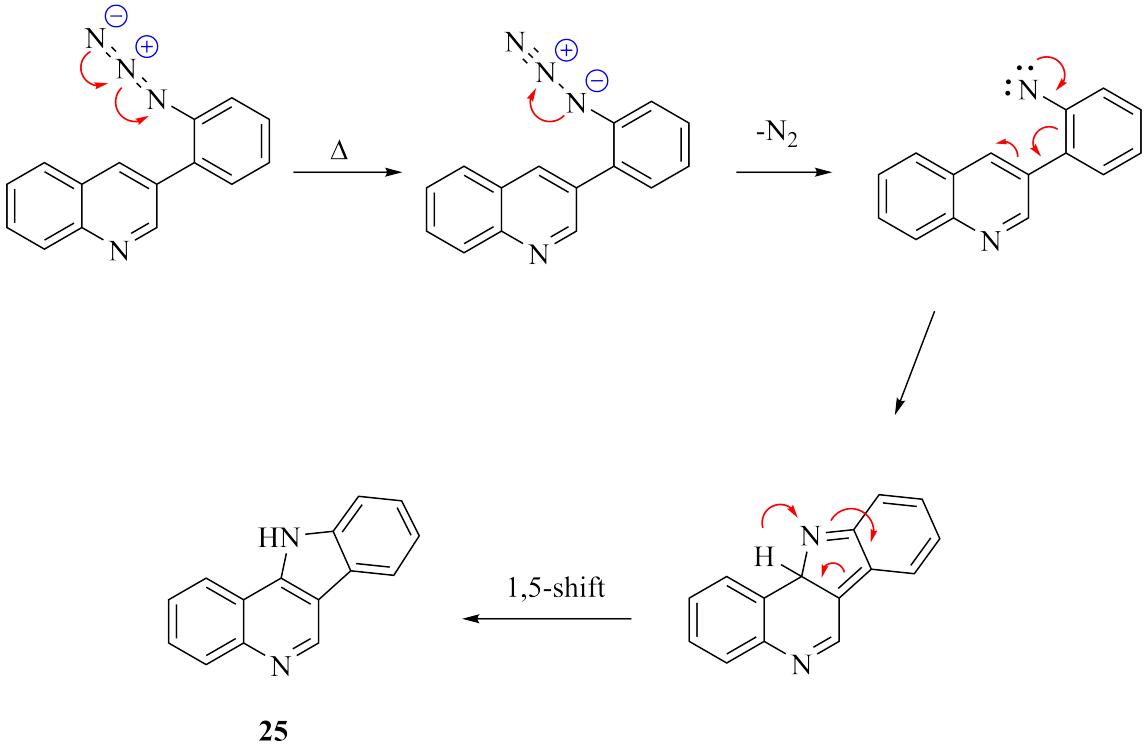

25

Scheme 10: Proposed mechanism[7] of the one-pot diazotization-cyclization of **19** to yield **25** as described by Singh *et al.*.

In regards to this project, the *N*-methylation step described in the two reactions above (Scheme 8, 9) is of particular interest, as modifications to this step could allow for the possible introduction of a linker-moiety to the heterocyclic nitrogen, which in turn could allow for the incorporation of isocryptolepine (**25**) to a bivalent ligand.

1.5 Suzuki-Miyaura cross-coupling reaction

One of the most popular techniques utilized in the synthesis of a variety of biaryls, to further obtain useful compounds such as pharmaceuticals and natural products, is the Suzuki-Miyaura C-C cross coupling.[192–195]. In fact, it is reported as the second most frequently used reaction in drug discovery and development only trailing amide formations.[195] The popularity stems from the large number of advantages associated with the reaction, such as the abundance of readily available starting materials, its water stability, its high regio- and stereoselectivity, tolerance to a broad range of functional groups (amines, ketones, heterocycles, etc.), high product yields, the minimal amount of catalyst required and of course its low toxicity.[196,197] The reaction is generally best described as a metal-catalyzed addition of an aryl (Ar), alkenyl or alkynyl halide (or triflate), to either organoboranes, organoboronic acids, organoboronate esters or potassium trifluoroborates in the presence of a base.[198–200] Some examples of bases

often used in the Suzuki-Miyaura cross coupling are NaOH, K_2CO_3, NaOAc and *t*-BuOK.[200] Although some studies have reported the use of nickel[201] as a potential catalyst, the most commonly employed catalyst in the Suzuki-Miyauara cross-coupling reaction is the palladium catalyst.[202] The palladium catalyst is most often employed in a complex aided by different types of ligands.[202] This structure enhances the stability of the reaction and contributes to the effectiveness of the catalytic cycle..[198,202]

The role of the base, palladium, and its intermediates in the catalytic cycle of the Suzuki-Miyaura cross coupling has been extensively studied over the years.[203] The cycle is comprised of three main steps: (i) oxidative addition, (ii) transmetallation and (iii) reductive elimination (Scheme 11).[200] In the oxidative addition step (i), the arylhalide, coordinates to the palladium species forming an organopalladium complex, [L_2-Pd-Ar^1X]. The mechanism of the transmetallation step (ii) and in particular the role of the base in the step, has been heavily debated over the years. Two pathways have typially been proposed: Path A and Path B.[204]. Path A, "the boronate pathway": Initiated by the conversion of an organoboron compound by attack of a base to form the nuchleophilic tetra coordinated boronate complex. The activated nucleophilic boronate complex in turn attacks the palladium-halide complex, [L_2Pd-Ar^1X], creating [L_2Pd-Ar^1Ar^2]. Path B, "oxo-palladium pathway": Hydrolysis of the palladium halide complex [L_2Pd-Ar^1X] yields the [L_2Pd-Ar^1OH] complex. The [L_2Pd-Ar^1OH] complex in turn reacts with a neutral tri-coordinated boronate species yielding [L_2Pd-Ar^1Ar^2]. Finally, the reductive elimination step (iii) affords the coupling product Ar^1-Ar^2 and subsequent regeneration of the palladium catalyst.[200,204,205].

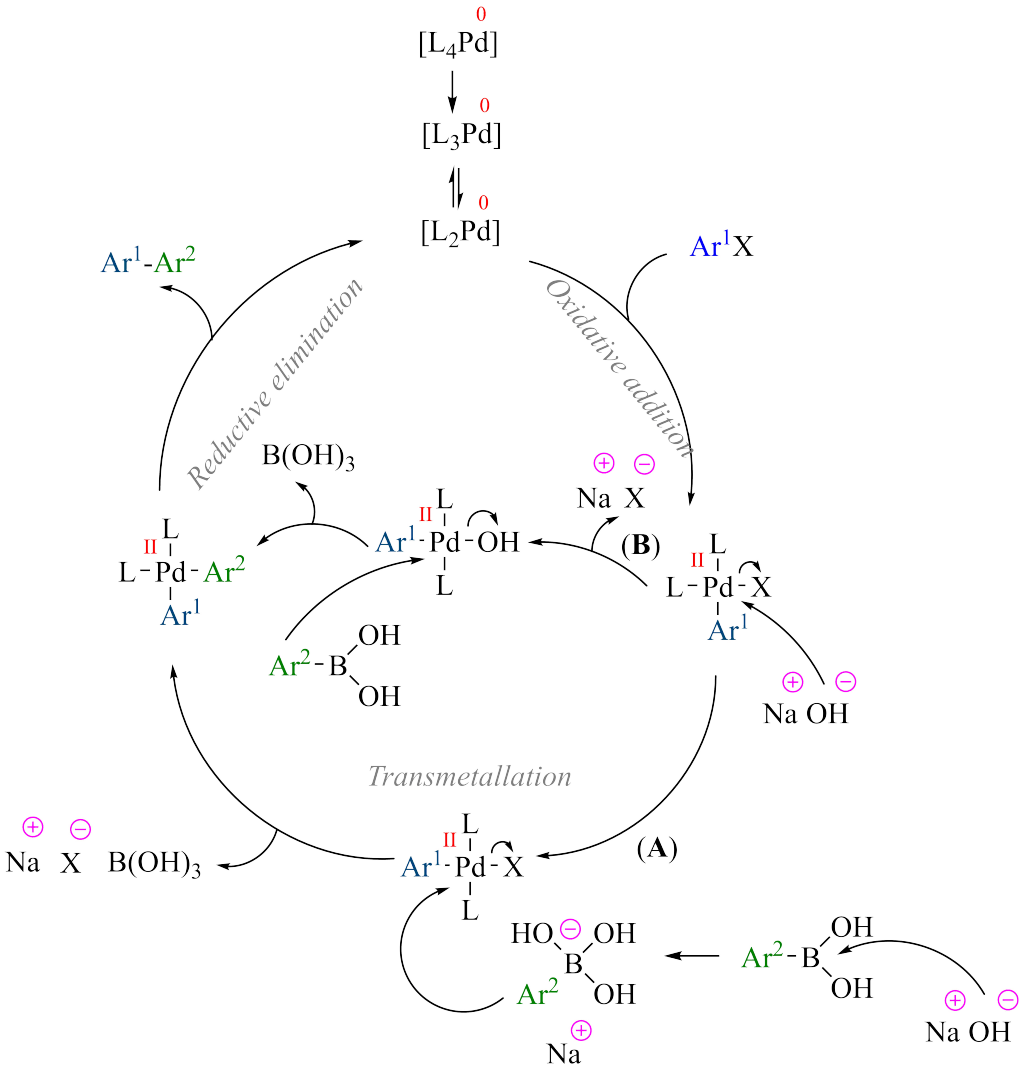

Scheme 11: The general catalytic cycle of the Suzuki-Miyaura cross coupling.[200,204]

1.6 Copper(I)-catalyzed azide-alkyne cycloaddition (CuAAC and the 1,2,3-triazole)

The 1,2,3-triazole heterocycle has shown to possess a number of interesting biological properties. The moiety is chemically inert against reactive conditions such as oxidation, reduction and hydrolysis under both acidic and basic conditions.[206] In addition, it can also participate in hydrogen bond formation, dipole-dipole interactions (about 5 D dipole moment) and π-stacking interactions.[207,208] The hydrogen bonding ability is particularly interesting, as it opens up the possibility of interactions with biomolecules, and in the case of AChE, this interaction has already been established.[135,209,210] In addition, the 1,2,3-triazole has also been reported to be

relatively resistant to metabolic degradation.[211].

The classical uncatalyzed thermal Huisgen cycloaddition was first discovered in 1893.[212] However, the mechanism and potential of the reaction between a terminal alkyne (a dipolarophile) and an organoazide (a 1,3-dipole) was first discovered by Huisgen in the 1960s. The reaction received little attention for decades, in large part due to the reaction requiring elevated temperatures over prolonged periods of time and the reaction yielding a mixture of the 1,4- and 1,5-disubstituted 1,2,3-triazoles regioisomers (Scheme 12).[213,214] However, this quickly changed when the group of Meldal[215] in Denmark and the group of Fokin-Sharpless[216] in the U.S independently and almost simultaneously discovered a copper(I) catalysed variant of the Huisgen azide-alkyne cycloaddition, the CuAAC.

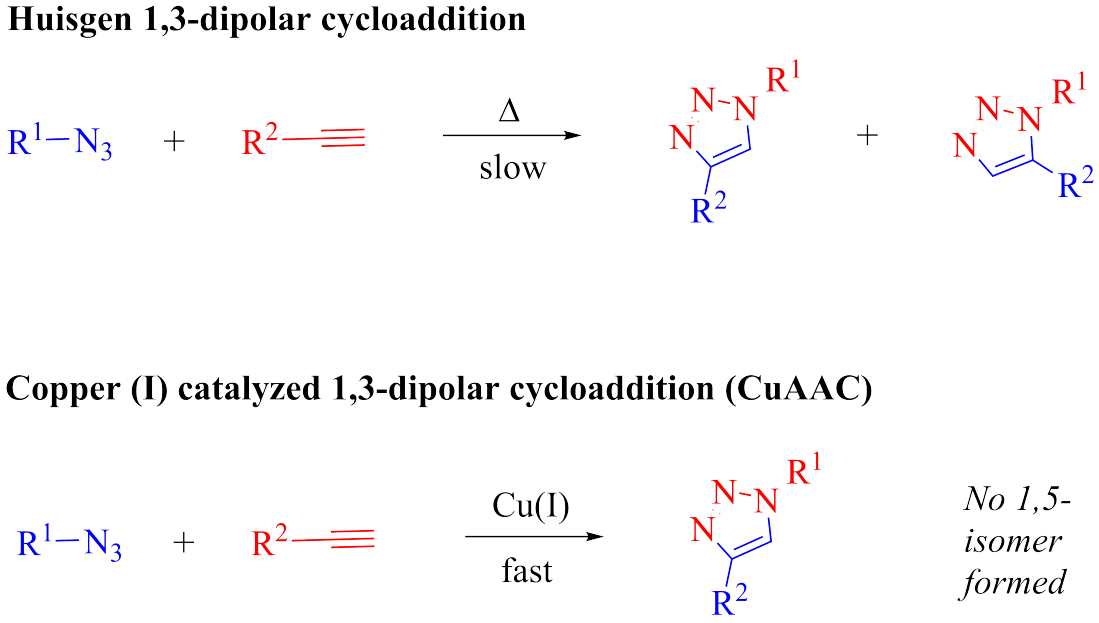

Scheme 12: Overview comparing the classical Huisgen cycloaddition to the Copper(I)-catalyzed cycloaddition (CuAAC).

The CuAAC proved to have several advantages compared to that of the classic non-catalyzed Huisgen cycloaddition. Most importantly it improved the regioselectivity of the reaction solely affording the 1,4-regioisomer (Scheme 12) as well as vastly improving the speed of the reaction (up to 10^7),[217] which allowed the reaction to function over a wide range of temperatures (0–160 °C) as well. In addition, CuAAC works in a variety of solvents (including water), over a wide range of pH (4-12), interference of functional groups are avoided and the reaction is unaffected by steric factors.[215–217]

A CuAAC reaction strictly requires only three components: a terminal alkyne, an azide and some type of Cu(I) (pre)catalyst. Almost any copper source can be used as a catalyst, provided that catalytically active Cu(I) species are formed in the reaction medium.[217,218] One way is the direct use of Cu(I) salts (bromide, chloride, acetate) with an excess of a base (Et_3N, DIPEA), however, the most common source for Cu(I) precatalyst in CuAAC is the use of Cu(II) salts (copper sulfate pentahydrate ($CuSO_4 \cdot 5H_2O$), copper acetate) in the presence of a reducing agent (sodium ascorbate).[217] This ensures the maintenance of significantly high levels of the catalytic Cu(I) species, which is important for the effectiveness of the CuAAC. Ligands are usually not necessary to carry out the CuAAC reaction although they serve a purpose in enhancing the reaction rate and functions as protection of the Cu(I)species from oxidation.[219] Another remarkable feature of the CuAAC reaction is the vast variety of solvents able to be used successfully. The comprehensive review of Meldal[217] list a number of them, including non-coordinating solvents (toluene, dichloromethane), weakly coordinating solvents (tetrahydrofuran, dioxane), polar solvents (DMF, acetone) and aqueous solvents including mixtures of water with an alcohol (tert-butanol, butanol, ethanol).

Despite the wide potential and increasing interest for the CuAAC reaction, many aspects of its mechanism still remains unclear.[220] An early proposal of the mechanism by Fokin, Sharpless and co-workers has served as a surprisingly good starting point for further mechanistic investigations.[216] The group suggested a step wise mechanism with a monomeric copper(I) acetylide complex as the intermediate in the catalytic cycle. However the group of Fokin *et al.* later reported results of experiments that showed monomeric copper(I) acetylide complexes are unreactive towards organic azides and this was postulated as direct evidence of the hypothesis that a dinuclear copper(I) acetylide had to be involved in the catalytic cycle of the reaction (Scheme 13).

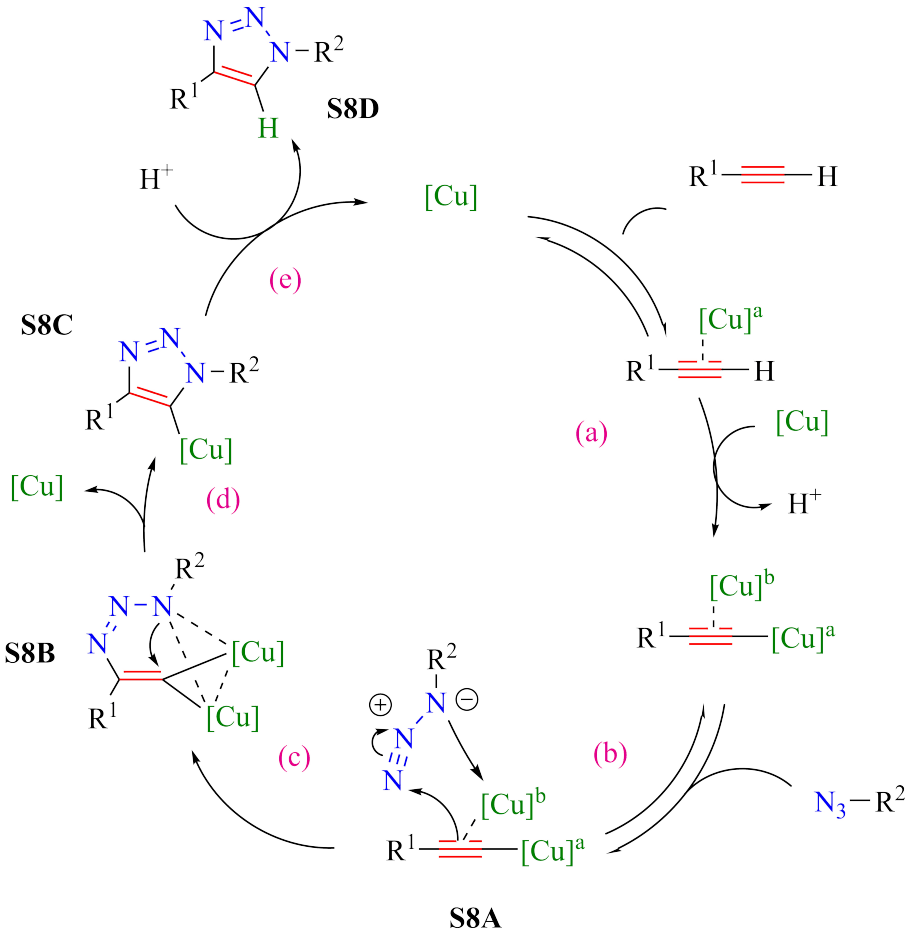

Scheme 13: Proposed catalytic model for the ligand-free CuAAC reaction, with a dinuclear copper intermediate.[221,222]

The formation of the σ, π-di(copper) acetylide initiates the reaction (a). The σ-bound copper acetylide bearing the weak π-bound copper atom proceeds (b) to pick up the organic azide and form an azide-alkyne-copper(I)ternary complex **S8A**. Next, metallacycle formation (c), through a nucleophilic attack at N-3 of the azide by the β-carbon of the acetylide forming the first covalent C–N bond, producing intermediate **S8B**. The introduction of another copper ion to **S8B** could alleviate the ring strain of the intermediate, which could explain the necessity for a dinuclear copper(I) acetylide in the catalytic cycle of the CuAAC. The formation of the second covalent C–N bond (d) is slower, but results in the ring closure yielding the copper(I) triazolide **S8C**.[221,222] Finally, proteolysis (or capture of the intermediate by another electrophile other than proton)[223] of **S8C** releases the triazole product **S8D**, and thereby completing the catalytic cycle. **S8C** deprotonating an alkyne and yielding **S8D** is suggested as an alternative final step of completing the catalytic cycle of the CuAAC[222].

Already in 2002, Sharpless and his group explored the possible use of the 1,2,3-triazole moiety as a linker when designing bivalent ligands functioning as AChEIs by connecting tacrine (**7**) with phenanthridinium (Figure 7.[224] A follow-up study[225] revealed that some of the syn-triazole ligands they synthesized, and in particular the molecule *syn*-TZ2PA6 was discovered to be an excessively strong inhibitor of AChE. In fact, the compound turned out to be the most potent noncovalent AChE inhibitor known at the time, reporting binding affinity (K_d) values (tcAChE) between 77 fM and 410 fM. More recently, Oukoloff and his group[135], inspired by the previous work of Sharpless *et al.*[224,225] assembled two scaffolds, one targeting AChE (tacrine) and one targeting GSK-3 (valmerin) (Figure 7). GSK-3 is a kinase involved in the hyperphosphorylation of the tau protein.[226] The scaffolds, assembled *via* CuAAC, generated MTDLs exhibiting nanomolar affinity for AChE and maybe more interestingly: the incorporation of 1,2,3-triazole moiety preserved, and even increased inhibitory potency toward AChE when compared to that of tacrine (**7**).[135]

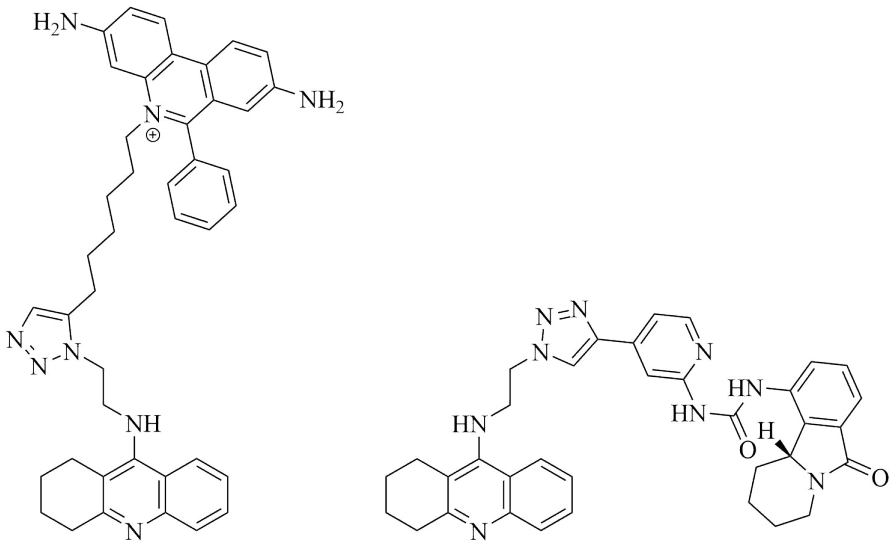

syn-TZ2PA6 (**R**)-**25**

Figure 7: Structures of the bivalent ligands syn-TZ2-PA6[224] and **(R)-25**[135] assembled *via* CuAAC.

2 Objectives

2.1 Synthesis of tacrine-, coumarin- and isocryptolepine scaffolds

In lieu of the recently published work of the group of Wang[125] on tacrine-neocryptolepine hybrids and their remarkably potent ability to inhibit AChE, and furthermore by the early work of the group of Sharpless[224] on potent tacrine-phenanthridinium hybrids as AChEIs linked favourably by a 1,2,3-triazole moiety; the possible synthesis of novel tacrine-isocryptolepine hybrids linked by a 1,2,3 triazole moiety is of interest. Furthermore, the formerly discussed potential of coumarins as multifunctional scaffolds in AD treatment makes synthesis of coumarin-isocryptolepine hybrids an interesting prospect as well. In order to accomplish this, the synthesis of the tacrine, coumarin and isocryptolepine scaffolds and the incorporation of a terminal alkyne and an azide is the first aim of the project (Figure 8).

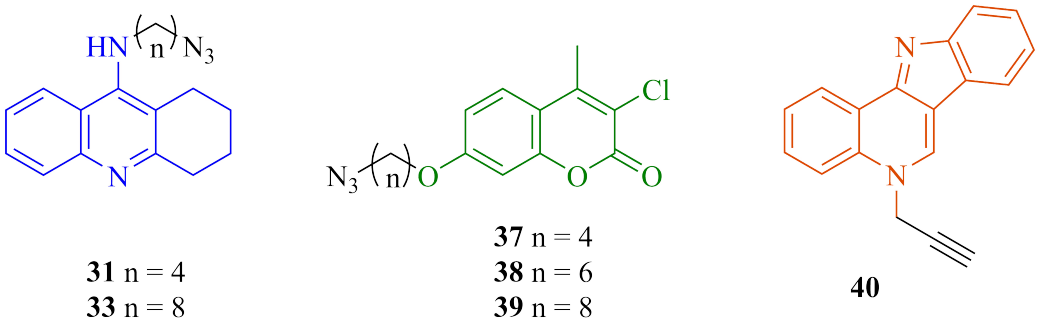

31 n = 4
33 n = 8

37 n = 4
38 n = 6
39 n = 8

40

Figure 8: Structures of the target tacrine, coumarin, and isocryptolepine scaffolds

In order to incorporate a terminal alkyne, the attempted exchange of the *N*-methylation step in the synthetic strategy of isocryptolepine (**25**) (Scheme 8) with a *N*-propargylation step is of the interest. In the case of success, the novel compound, 5-(prop-2-yn-1-yl)-5*H*-indolo[3,2-c]quinoline **40**, would be able to serve as the alkyne moiety in the synthesis of both suggested hybrids.

As for the tacrine scaffold the previously mentioned work of Oukoloff (Scheme 2 will serve as a proposed synthetic strategy for the synthesis of **31**, while the work of Mckenna (Scheme 1) and Wieckowska (Scheme 3) would function as a starting point towards arming tacrine with a longer linker (8C). From here, an azidation reaction similar to the one presented in 2 is suggested to yield **33**.

As for the coumarin scaffold, the previously mentioned work of He[158] on coumarin-dithiocarbamate hybrids (Figure 5), wherein the hybrid **13c** containing the coumarin analog 3-chloro-7-hydroxy-

4-methylcoumarin **19** was reported as both the most poten AChEI, and as a potent MAO-B inhibitor, inspired the choice of **19** as the coumarin analog of interest in this project. A Pechmann condensation (Scheme 5, 6) should yield coumarin analog **19**. From here, the reaction with dibromoalkanes of desired length (Scheme 7) followed by an azidation (Scheme 2) is suggested to yield the coumarin scaffolds **34**, **35** and **36**.

2.2 Synthesis of novel tacrine-isocryptolepine and coumarin-isocryptolepine hybrids

Following the success in synthesizing the target scaffolds, the aim is to assemble the scaffolds utilizing the previously discussed CuAAC reaction to yield the novel tacrine-isocryptolepine-1,2,3-triazoles (**41** and **42**), and the coumarin-isocryptolepine-1,2,3-triazoles (**43**, **44**, **45**) (Figure 9). The objective is to attempt to synthesize the hybrids with varying linker length to allow for the possibility of discovering the optimal length for the design of this project at which a possible AChE inhibition is at its greatest.

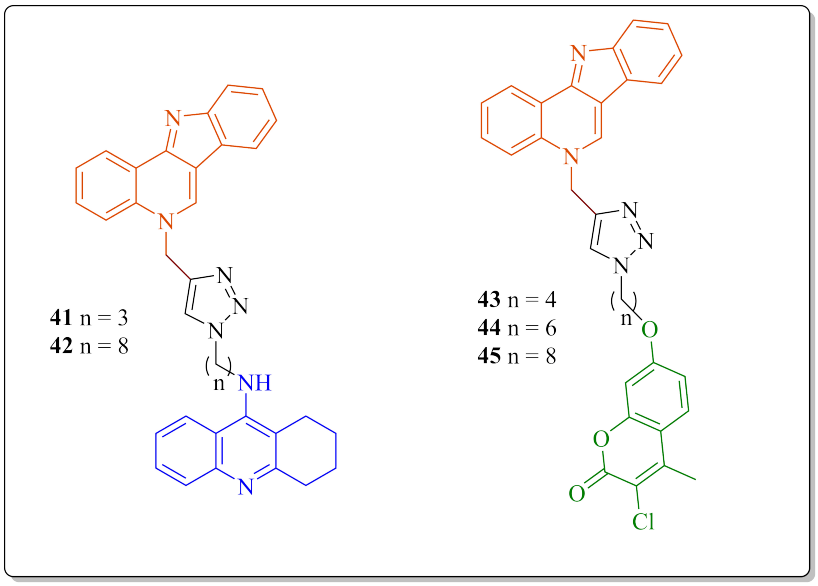

Figure 9: Structures of the suggested novel tacrine-isocryptolepine- and coumarin-isocryptolepine hybrids of which are the main objectives of this project.

Based on research previously discussed, the expectation is for the tacrine-isocryptolepine hybrid to be a strong inhibitor of AChE, establishing binding interactions with both the CAS (tacrine), PAS (isocryptolepine) and gorge (1,2,3-triazole) of AChE. A decrease, or complete elimination of hepatotoxicity relative to that of tacrine as well as potential inhibition of BuChE

is also interesting possibilities.

Regarding the coumarin-isocryptolepine hybrids; coumarins ability to interact with the PAS of AChE has already been discussed and established. It is therefore suggested that the isocryptolepine scaffold will bind to the CAS of AChE, resulting in an inverse orientation compared to that of the expected tacrine-isocryptolepine orientation, which is potentially interesting in itself. Furthermore, potential MAO-B inhibition of this hybrid is also an interesting possibility.

In order to test these assumptions and measure the biological activities of the novel hybrids, pharmacological and docking studies of the novel hybrids was to be conducted in a laboratory in Spain.

3 Results and discussion

3.1 Synthesis of tacrine scaffolds

3.1.1 Synthesis of *N*-(3-azidopropyl)-1,2,3,4-tetrahydroacridin-9-amine (27)

In order to synthesize tacrine scaffold **27**, the Niementowski reaction of anthranilic acid (**8**) and cyclohexanone (**6**) in tandem with a simultaneous POCl3-mediated chlorination of the aromatic OH-group, as suggested by[135], worked as an intended starting point. The reaction easily yielded chloro-1,2,3,4-tetrahydroacridine (**9**) (Scheme 14), in an even greater yield (73%) than reported by others[135] recently (52%), which was a pleasant surprise for a starting experiment. Spectroscopic and spectrometric data were in accordance with previously reported data and will therefore not be further discussed.[135]

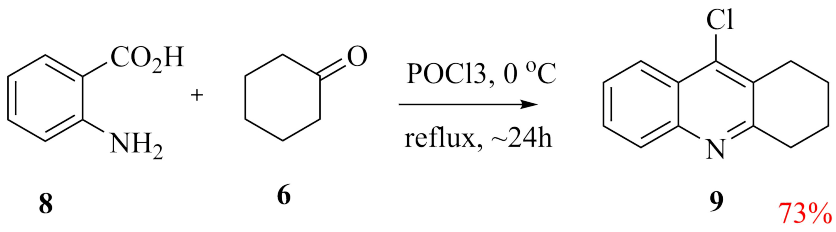

8 **6** **9** 73%

Scheme 14: Preparation of chloro-1,2,3,4-tetrahydroacridine (**9**) by a Niementowski reaction followed by a simultaneous POCl3 mediated chlorination.

Having prepared an excess (4.63g) of compound **9** the next step towards the completion of the desired tacrine scaffold was the arming of **9** with a 3 methylene long linker. The synthetic strategy of Oukoloff et al. (Scheme 2)[135] towards a 2-methylene long linker using **9** as a starting material proved useful in this regard. 3-((1,2,3,4-tetrahydroacridin-9-yl)amino)propan-1-ol (**26**) (Scheme 15) was easily prepared, and in great yield after re-crystallization (1.81g, 77%) from the S_NAr reaction between 9-chloro-1,2,3,4-tetrahydroacridine (**9**) and 3-amino-1-propanol. Since primary amines are considered good nucleophiles and halides are considered great electrophiles, this was as expected.

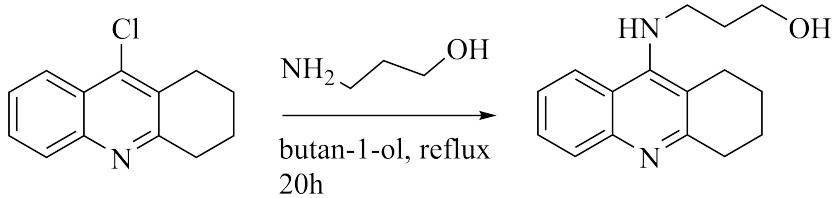

9 **30** 77%

Scheme 15: The S_NAr reaction of 9-chloro-1,2,3,4-tetrahydroacridine (**9** and 3-amino-1-propanol to yield 3-((1,2,3,4-tetrahydroacridin-9-yl)amino)propan-1-ol (**30**).

^{1}H-NMR confirmed the presence of 4 aromatic proton signals around δ 7.98-7.29 ppm as doublet and triplet signals. Furthermore, 6 protons belonging to the three methylene groups was registered at δ 1.96-1.80 ppm as a multiplet signal, placing the remainding 8 proton signals to the aliphatic ringsystem. Finally, the presence of broad singlet proton signals belonging to the NH-group (δ 4.70 ppm) and to the OH-group (δ 3.38 ppm) confirmed the identification of **30** (Figure 10). ^{13}C-NMR further confirmed the presence of 9 aromatic and 7 aliphatic carbon signals.

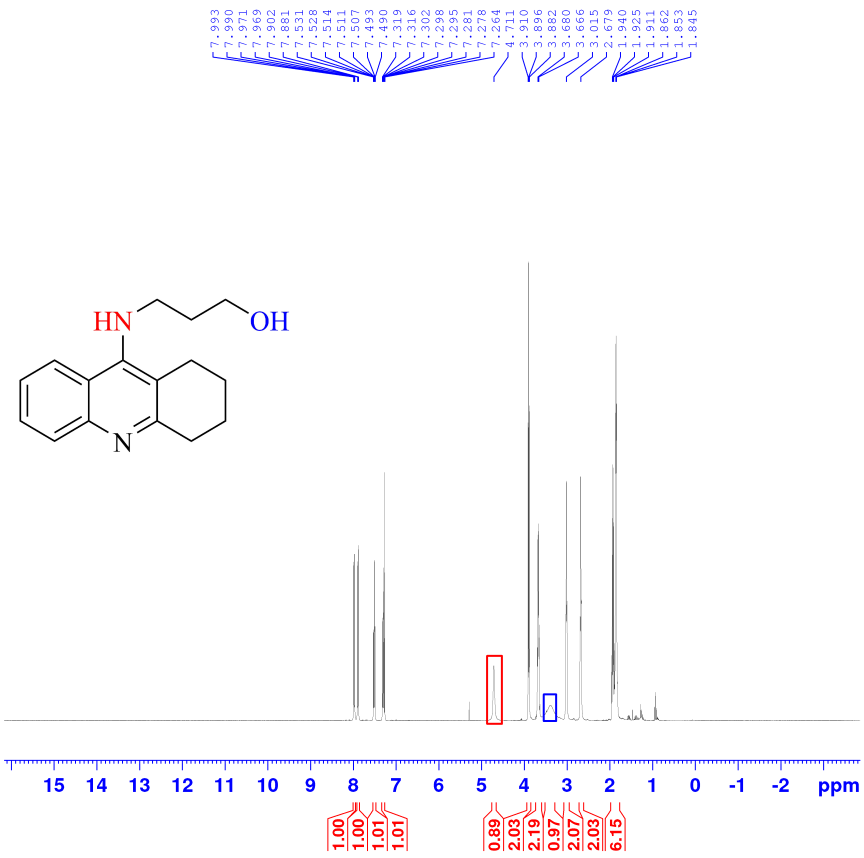

Figure 10: ^{1}H-NMR of **30** confirming the presence of a NH-group (red) and an OH-group (blue).

As opposed to Oukoloff[135] who applied the halogenating agent ($SOCl_2$) followed by an azidation of the halide (Figure 2), a slightly different approach was applied in this project for the synthesis of **31** (Scheme 16).

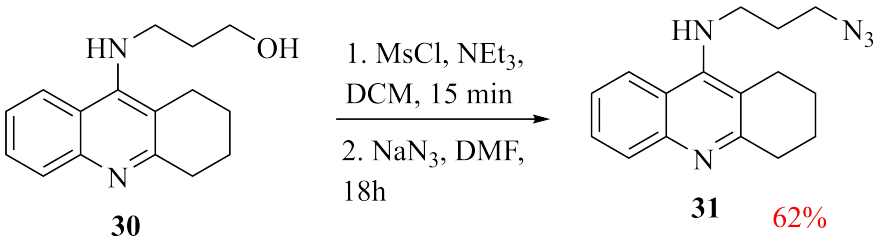

Scheme 16: The two-step synthesis of *N*-(3-azidopropyl)-1,2,3,4-tetrahydroacridin-9-amine (**31**).

The formation of the desired tacrine scaffold *N*-(3-azidopropyl)-1,2,3,4-tetrahydroacridin-9-amine (**31**) follows a two-step synthesis: Compound **30** was treated with methanesulfonyl chloride (MsCl) in the presence of the weak base triethylamine (Et_3N) substituting the alcohol-group with a mesylate group (OMs), a much better leaving group. The reaction progress was monitored by TLC. This conversion allowed for the second step of the reaction wherein the addition of NaN_3 yielded the desired *N*-(3-azidopropyl)-1,2,3,4-tetrahydroacridin-9-amine (**31**) in good yield after purification (0.78g, 62%) compared to that of the similar tacrine scaffold of Oukoloff[135] et al. (46%). However, as the NMR-results would show, this was a truth with slight modifications. The ^{1}H-NMR indicated contamination at δ 7.99, 5.27, 3.06 and 2.71 ppm. A review of the literature[227] confirmed the suspicion that this was a clear indication of DCM and DMF contamination (Figure 11). This would lower the value of the actual yield from that of the reported.

A direct comparison to the the ^{1}H-NMR of **30** confirmed the suspected loss of the OH-signal as the only difference, and therefore suggested the formation of **31** (Figure 11). The shift downfield is a result of deshielding by the azide. In addition IR also confirmed the presence of an azide (Figure 12)

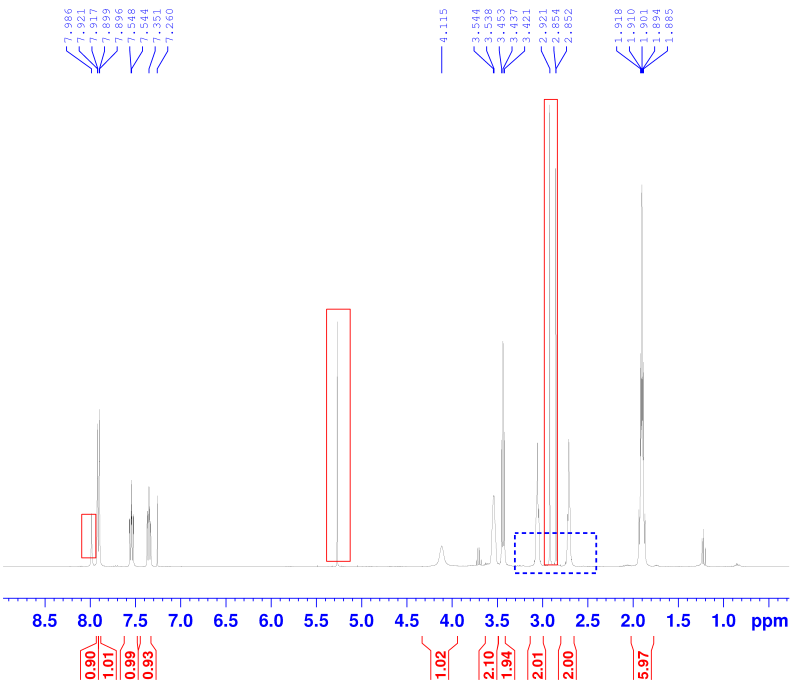

Figure 11: Solvent contamination (red) by DCM and DMF, and the lack of an OH-signal (blue) when compared to **30** (Figure 10), suggesting the formation of an azide.

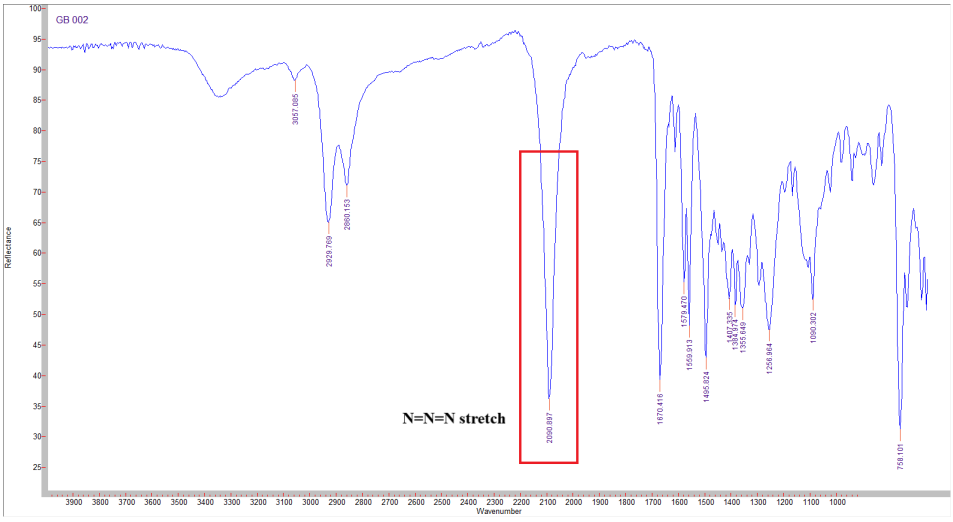

Figure 12: IR of **31** confirming the introduction of an azide.

3.1.2 Synthesis of *N*-(8-azidooctyl)-1,2,3,4-tetrahydroacridin-9-amine (33)

The first step towards the synthesis of **33** was the synthesis of tacrine **7** (Scheme 17. The Friedländer type condensation of 2-aminobenzonitrile (**5**) and cyclohexanone (**6**), mediated by BF_3OEt_2) produced tacrine (**7**) in great yield after basic work-up and purification (8.38g, 88%). Spectroscopic and spectrometric data were in accordance with previously reported data.[131]

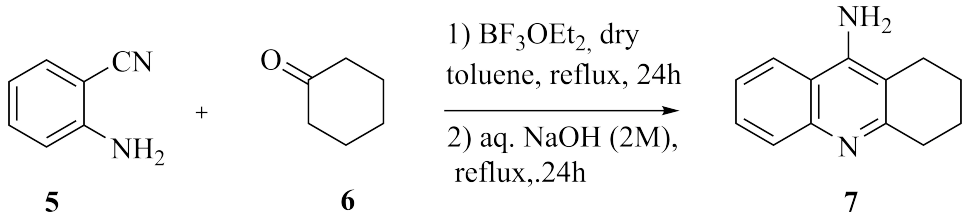

5 **6** **7**

Scheme 17: A Friedländer type condensation of 2-aminobenzonitrile (**5**) and cyclohexanone (**6**) yielding tacrine (**7**).[131]

For the arming of the longer linker, the previously mentioned synthetic strategy of the group of Wieckowska (Scheme 3) was the strategy of choice. Whereas some report the use of acetonitrile as a solvent, the synthetic strategy the group of Wieckowska[136] used dry DMSO as the solvent of choice. This strategy, and several similar strategies for the arming of a linker to tacrine[136,228,229], almost exclusively report the use of potassium hydroxide (KOH) as the strong base. However at the time of first working with this reaction, due to a lack of KOH, sodium hydroxide (NaOH) was used in its stead (Scheme 18). It was therefore a surprise when monitoring the reaction by TLC revealed a much slower reaction time (48h) than what had been described in the literature using KOH (24h).[136] An attempt at reviewing the literature gave no real good answer. A suggestion to an explanation could be the difference in water-content between the two bases. Whereas NaOH is acquired virtually anhydrous, KOH has a 15% water content, which could influence solubility and in turn influence the reaction rate.

At a later point, a new attempt at this reaction was attempted, this time using KOH as the base, and this time the reaction time was as described (24h).[136] The reaction between tacrine **7** and 1,8-dibromooctane in the presence of a strong base (KOH/NaOH) yielded compound **32** after purification in varying yield (16% and 72% respectively) (Scheme 18).

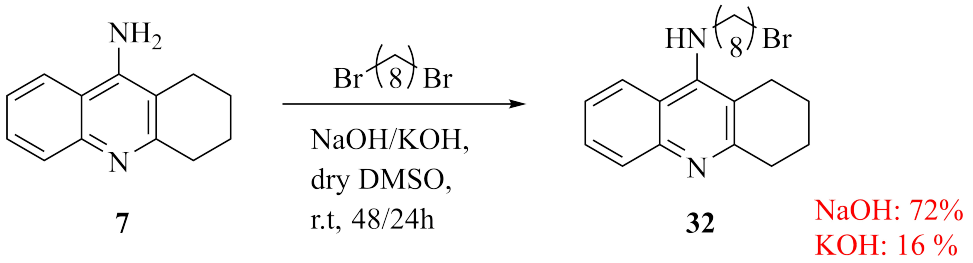

Scheme 18: S_NAr reaction between tacrine **7** and 1,8-dibromooctane mediated by a strong base, yielding **32**.[136]

Some of the reason for the low yield of the KOH-mediated version can be attributed to extensive attempts at purification, as well as to the difficult chromatography this reaction presented. Interestingly, in the case of the KOH-mediated reaction, TLC showed the formation of another product with a slightly higher R_f-value compared to the starting material **7**, further explaining the loss of yield. However, the side product was not able to be identified.

Even though **32** has previously been reported in the literature[228], the differences between the reported data and the ones obtained in this project were significant enough to warrant a little discussion. The ^{1}H-NMR of both acquired samples (NaOH/KOH) were of similar quality and only one of them will be presented here (Figure 19). All 16 methylene bridge protons are found in two separate multiplets (δ 1.95-1.60 ppm, 8H and δ 1.45-1.24 pp, 8H). The proton from the NH-group is present as a broad singlet at 4.03 ppm, the 4 aromatic protons in the range of δ 7.95-7.33 ppm and the 8 aliphatic ring protons in the range of δ 3.48-2.69 ppm confirm the synthesis of compound **32**.

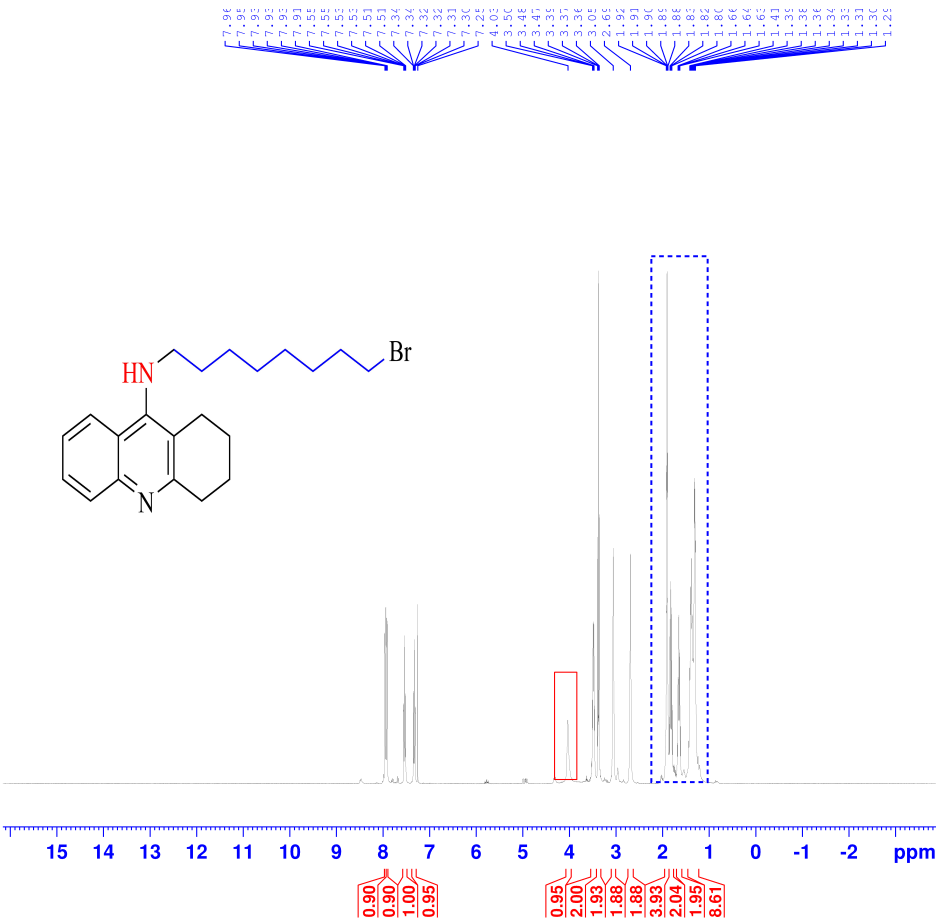

Scheme 19: ^{1}H-NMR spectra of compound **32**, showing the protons of the methylene bridge (blue) and the proton of the NH-group (red). Downfield are the 4 aromatic protons, and upfield the 8 aliphatic ring protons.

Having obtained **32** in good enough yield (1.42 g), the final step in synthesizing the target scaffold **33** was the azidation of **32** by NaN_3 (Scheme 20). For this step the same reaction conditions previously described by Oukoloff (Scheme 2)[135] was suggested to work for this reaction as well. Prior to purification, and in order to check if the reaction conditions indeed were transferable, LRMS confirmed the formation of **33** (Figure 13) The result was the successful formation of **33** in great yield after purification (80%).

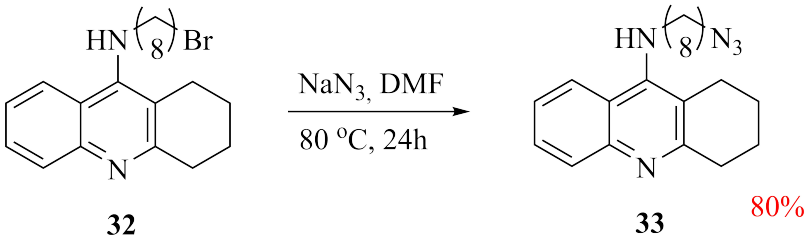

32 **33**

Scheme 20: Azidation of **32** yielding target tacrine scaffold **33**.

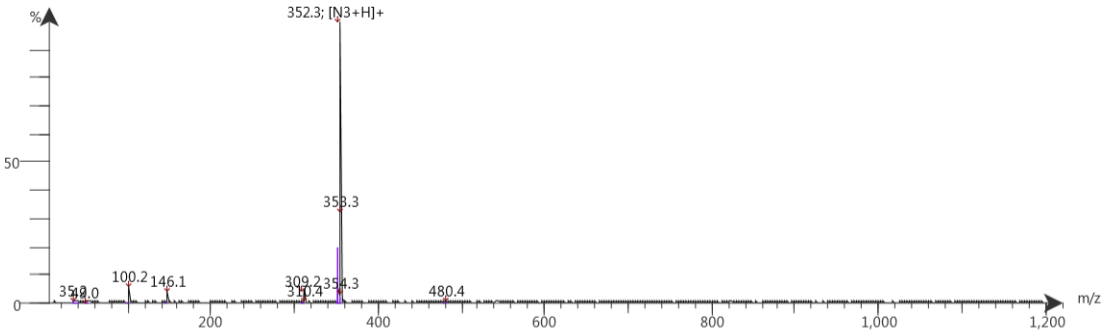

Figure 13: LRMS spectrum of the azidation (Scheme 20) reaction mixture confirming the formation of **33**.

As the final reaction step only involved the substitution of a halide with an azide, it was expected that a direct comparison of the ^{1}H-NMR spectra of **32** and **33** should result in little difference besides some possible downshift of some of the methylene protons due to the incorporation of the azide (Figure 14). As expected, a comparison of the two confirmed this. Furthermore, the IR-spectra of **33** confirmed the presence of an azide (Figure 15) further supporting the successful addition of an azide and the formation of **33**.

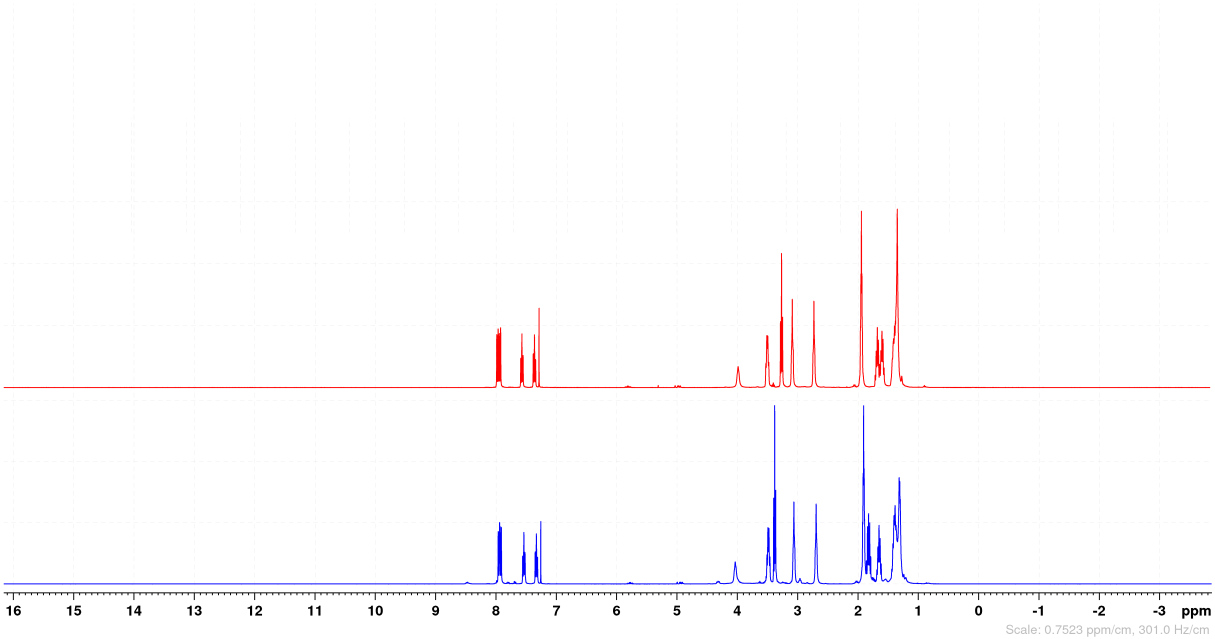

Figure 14: Comparison of the ^{1}H-NMR spectra of **33** (red) and **32** (blue).

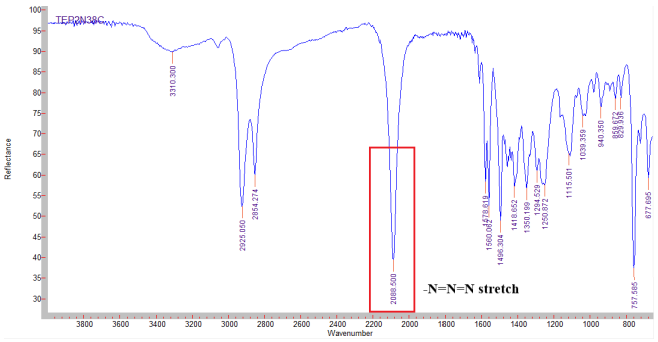

Figure 15: IR-spectra of compund **33** confirming the presence of an azide.

3.2 Synthesis of coumarin scaffolds

3.2.1 Synthesis of 3-chloro-7-hydroxy-4-methyl-2H-chromen-2-one (19)

The synthesis of all three coumarin scaffolds (**37**, **38** and **39**) follow the same reaction conditions and utilize the same reaction strategies, and as such will be discussed grouped together. The first step towards the synthesis of the coumarin scaffolds was the synthesis of the coumarin analog **19**. After a review of the literature the use of standard Pechmann condensation, as described by He et al.[158] seemed like a good approach to synthesizing **19** (Method A, Scheme 21).

Method A:

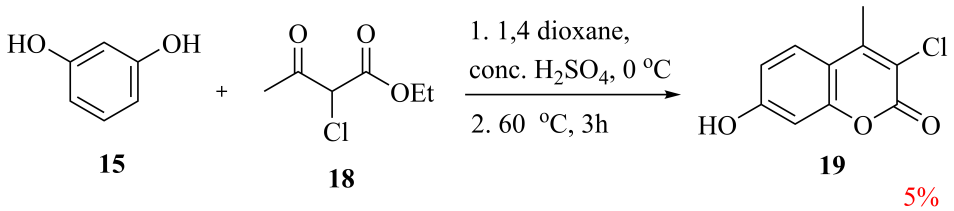

Method B:

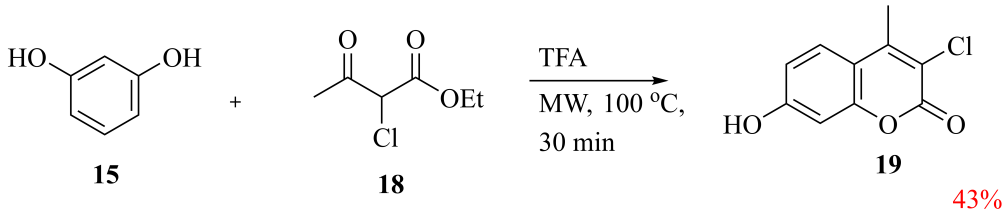

Scheme 21: Overview of the two methods used in this project to synthesize **19**.

However, after following the reaction procedures as presented, testing of the reaction mixture aided by TLC resulted in seven different visible spots. Although the method of He[158] was reported in the synthesis of mono-substituted 7-hydroxycoumarins, standard Pechmann condensation reaction conditions should allow for a wide array of substitutions, making this a surprise. However, the reaction conditions of the Pechmann condition are relatively harsh (heat, acid). An attempt at isolating all 7 spots by silica gel column chromatography was made. The resulting NMR-data confirmed a weak presence of **19** in 2 of the fractions (Figure 16).

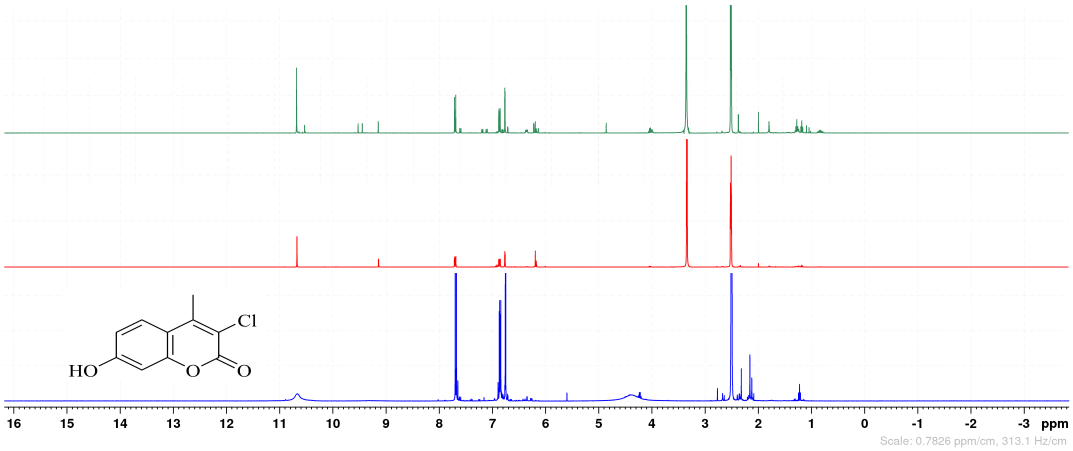

Figure 16: ^{1}H-NMR spectra comparing 2 out of 7 spots from the TLC after attempting Method A to the spectra obtained after using Method B (blue). Indication of **19** in both spots.

However, the attempt at isolating the spots was unsuccessful, maybe best represented by the ^{1}H-NMR data from the two spots presented (Figure **??**), as these samples were contaminated. The yield after isolation was low as well (5%). This was the norm for all of the attempted isolated spots, and isolation and identification of the sideproducts created by Method A were therefore, regretfully, not successful. A couple of suggestions might however still be briefly presented (Scheme 22). Suggestion a) indicates the actions of acid hydrolysis, cleaving the ester group of the finished product **19**. Suggestion b) indicates time constraint, suggesting the reaction not reaching further than the transesterfication step of the Pechmann reaction[230] and prior to ring closure.

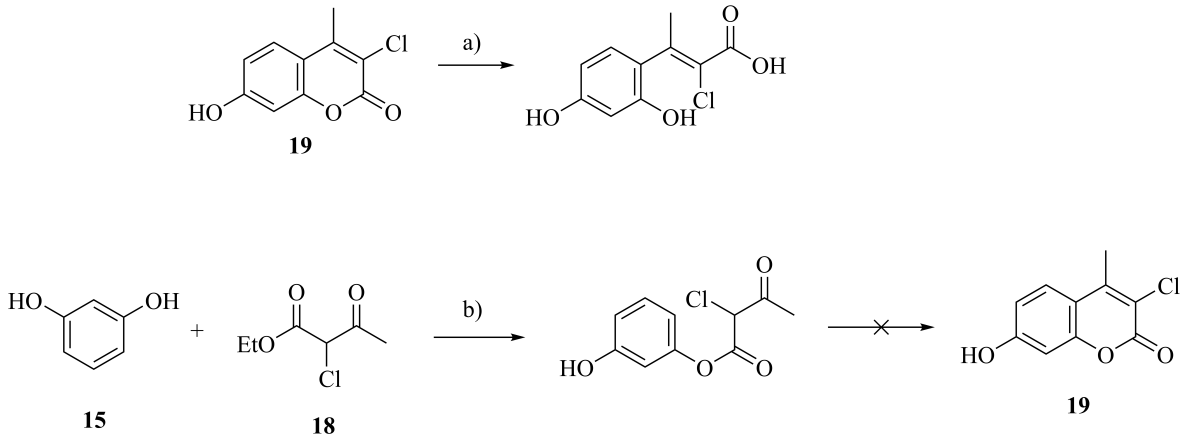

Scheme 22: Two suggested explanations for the failure of Method A in the synthesis of **19**.

Method B[170] (Scheme 21), utilizing the strategy of microwave chemistry, yielded compound **19** in both better yield (43%), better purity (Figure 11), at a faster pace, and with easier means of purification (no chromatography). Probably as a result of the milder reaction conditions and faster reaction rate provided by the MW-assistance, and by the use of a weaker acid (TFA).

3.2.2 Synthesis of coumarin analogs armed with methylene bridge, compounds 34-36.

For the arming of **19** with a desired linker, the strategy proposed by the group of Jiang[173] utilizing Williamson ether synthesis to arm the linker to the alchohol group in position 7 was the strategy of choice.

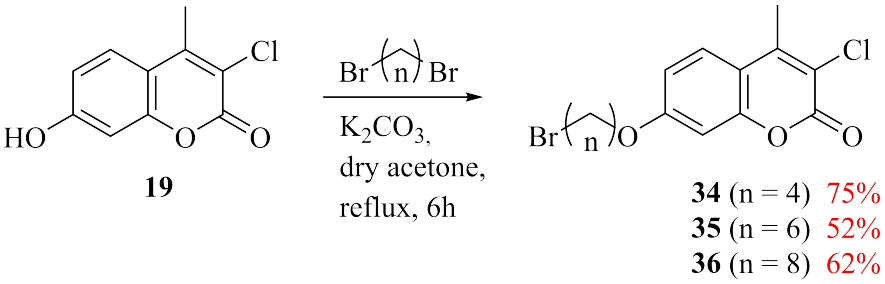

Scheme 23: Utilization of Williamson ether synthesis towards arming coumarin analog **19** with a methylene bridge of desired length.[173]

The synthetic strategy was a success, providing good yields (Scheme 23) and good purity. The ^{1}H-NMR spectra for compound **34** (Figure 17) confirmed the formation of **34**. The presence of 3 aromatic protons in the range of δ 7.48-6.73 ppm (surrounding the $CDCl_3$ peak), protons of the CH_3 at position 4 as a singlet at δ 2.50 ppm, with the remainding 8 aliphatic protons in the region of δ 4.03-2.01 ppm. The two triplets downfield represent the methylene groups in the nearest vicinity to the ether-oxygen and the halide.

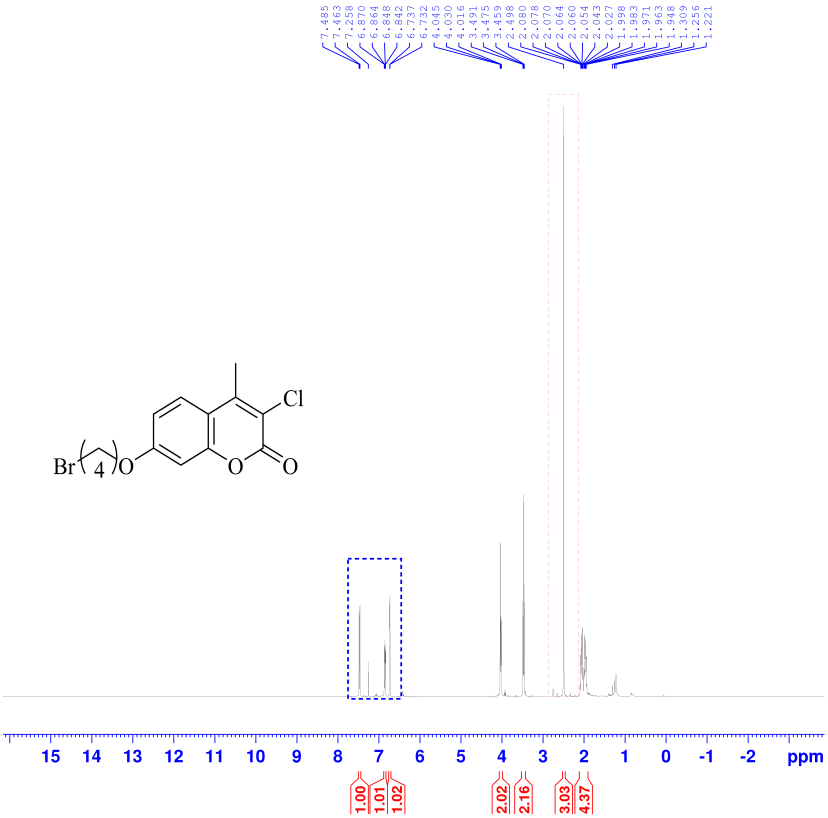

Figure 17: ^{1}H-NMR spectra of compound **34**. Indicated by color are the presence of the three aromatic protons (blue) and the protons of CH_3 substituted in position 4.

With the formation of **34** confirmed, the easiest way to confirm the formation of the coumarin analogs with a longer linker is by comparing the ^{1}H-NMR of the three compounds (Figure **??**). As expected, for each 2 methylene group elongation, the number of aliphatic protons in the δ 1.90-1.32 ppm area increases by 4. The remaining protons of the ^{1}H-NMR spectra are nearly identical, confirming the formation of compound **35** and **36** as well.

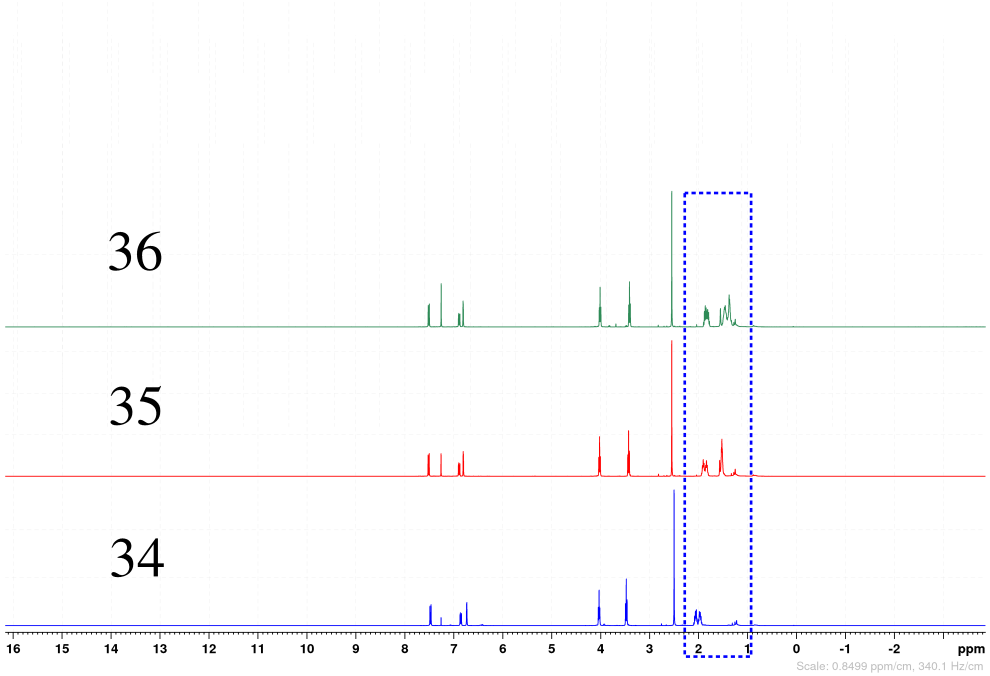

Figure 18: ^{1}H-NMR spectra of compound **34**, **35** and **36**. Indicated by color (blue) is the aliphatic methylene bridge area, increasing with 4 protons for each 2 methylene group addition to the linker.

3.2.3 Azidation of coumarin analogs 34-36

Similar to the reaction conditions of Oukoloff et al.[135] and work by the group of Tian[231] on similar substituted 7-hydroxy-coumarins, the choice of synthetic strategy for the azidation of compounds **34-36** to form the coumarin scaffolds **37-39** (Scheme 24) exploited the use of NaN_3 and the substitution reaction it engages in with the halide attached to the respective linker.

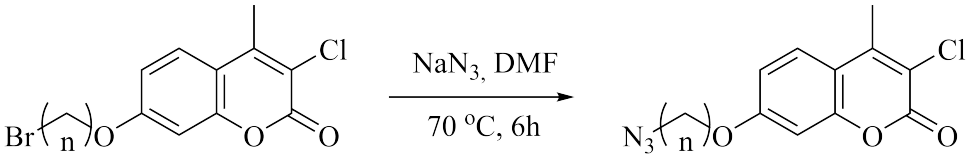

34 (n = 4)
35 (n = 6)
36 (n = 8)

37 (n = 4) 96%
38 (n = 6) 44%
39 (n = 8) 96%

Scheme 24: The synthetic strategy towards azidation of coumarin analogs **34-36**.

Regrettably, the identification of compounds **37-39** have not yet been confirmed by NMR, as unforeseen problems with the NMR-machinery occurred towards the end of this project, and have yet to be resolved as of the due date. Samples of all three compounds have been prepared and are ready to be analyzed. However, as reported by others[231,232], the azidation step of similiar coumarin analogs require no further purification for the use in CuAAC-reactions. This, in combination with IR-spectra confirming the addition (Figure 19) of an azide, leaves us to conclude with a certain degree of confidence that the suggested azidated coumarin analogs have been prepared.

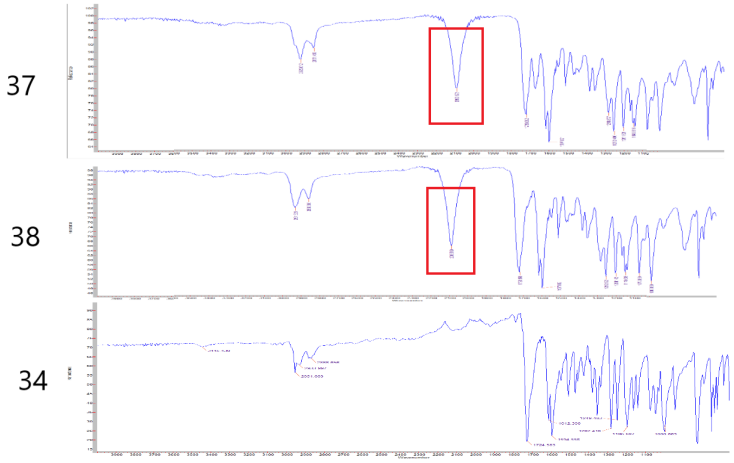

Figure 19: IR spectra of compound **37** and **38**, compared to the IR spectra of **34**, confirming the addition of an azide (red).

The reason for the lower yield reported for **38** is that an attempt at further purification was performed regardless of former reports, out of curiosity and with the idea of testing the effect purification would have by comparing potential differences in NMR-spectra.

3.3 Synthesis of the isocryptolepine scaffold

3.3.1 Synthesis of 2-(quinolin-3-yl)aniline (23)

The first step towards the synthesis of the isocryptolepine scaffold, 5-(prop-2-yn-1-yl)-5*H*-indolo[3,2-c] **40** was the synthesis of 2-(quinolin-3-yl)aniline (**23**) (Scheme 25).

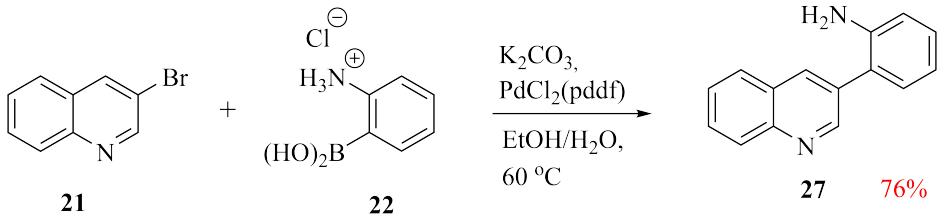

Scheme 25: Suzuki-coupling of **21** and **22** to yield the biaryl **23** as described by Helgeland and Sydnes.[188]

The synthetic strategy provided great yield (76%) and great excess (1.22 g). As spectroscopic and spectrometric data were in accordance with previously reported data it will therefore not be further discussed.[188]

3.3.2 Synthesis of 11*H*-indolo[3,2-c]quinoline 29

Following the synthesis of **23**, the strategy formerly reported by Timari[190] functioned as the chosen strategy towards the synthesis of the isocryptolepine precursor **29** (Scheme 26).

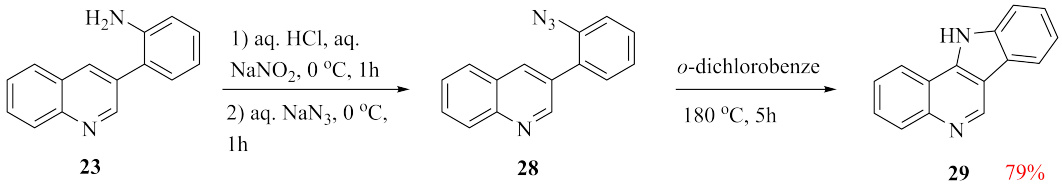

Scheme 26: Synthetic strategy towards the synthesis of the isocryptolepine precursor **29** as described by the group of Timari.[190]

The reaction provided great yield (79%) when compared to the reported (75%). As spectroscopic and spectrometric data were in accordance with previously reported data it will therefore not be further discussed.[233]

3.3.3 Synthesis of 5-(prop-2-yn-1-yl)-5*H*-indolo[3,2-c] 40

The synthetic strategy for the synthesis of the novel compound 5-(prop-2-yn-1-yl)-5*H*-indolo[3,2-c] **40** (Scheme 27) is modified based on the *N*-methylation described by Helgeland and Sydnes[188] which have previously been discussed. Our suggestion was a *N*-propargylation.

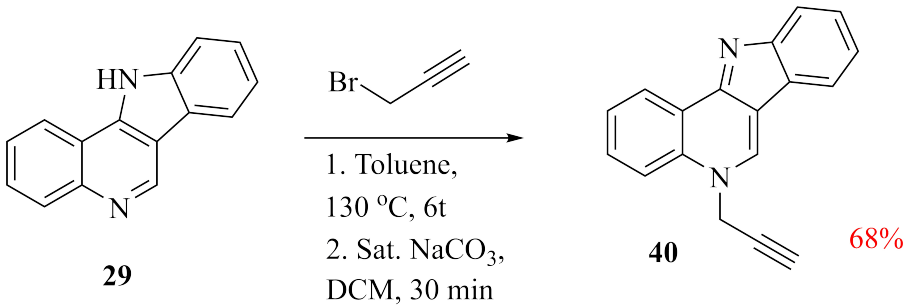

Scheme 27: Synthetic strategy towards the synthesis of the isocryptolepine scaffold **40**.

The addition of propargylbromide to the reaction, mediated by heat and under pressure yields **40** after basic work-up and in good yield (68%). However, getting good NMR-spectra for this compound would turned out harder than expected. Although previous attempts proved to contain slight contamination, the stability of the CuAAC reaction towards other functional groups still allowed for attempts at the target molecules. After multiple attempts however, identification of compound **40** by NMR was finally obtained (Figure 20). The blue color of the figure represents the identification of the aliphatic methylene group at δ 4.98 ppm, binding the alkyne to isocryptolepine, whereas red represents the identification of the acetylenic proton δ 2.55 ppm, confirming the presence of the terminal alkyne. Interestingly, a coupling constant of about 2.2 Hz was observed as well from the acetylenic proton to the methylene bridge.

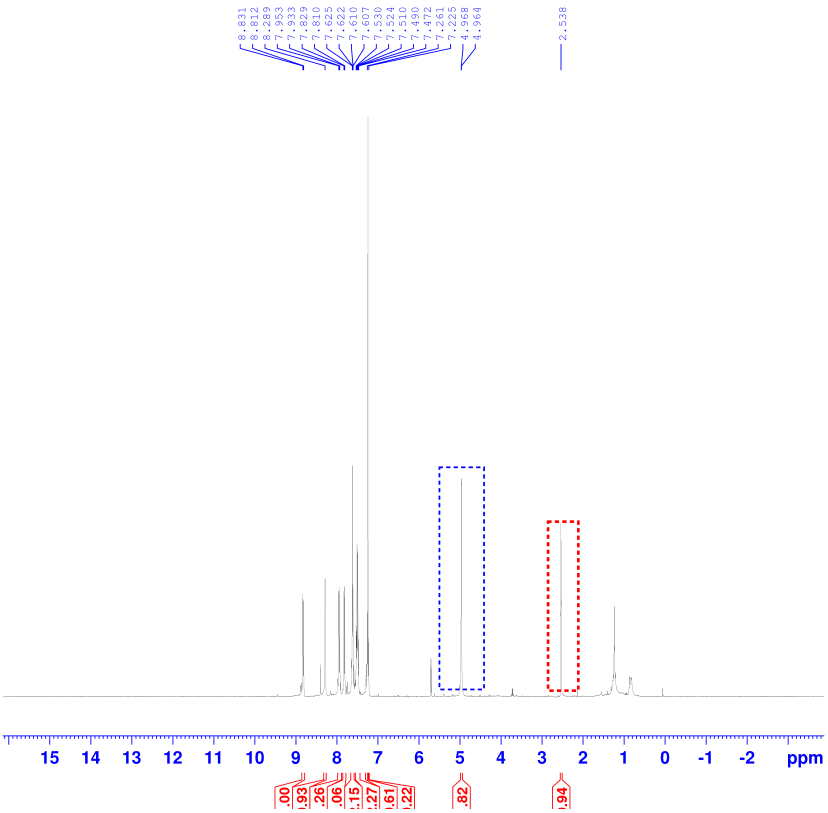

Figure 20: ^{1}H-NMR spectra of compound **40** proving the formation of the targeted isocryptolepine scaffold. Blue represents the 2 aliphatic protons of the methylene group connecting the alkyne functionality to isocryptolepine, while red is conformation of the acetylenic proton.

3.4 Synthesis of novel tacrine-isocryptolepine and coumarin-isocryptolepine hybrids

After acquiring all of the needed scaffolds (compound **40**, **31** and **33**), the final step, and main objective of this project was the attempted synthesis of the tacrine- and coumarin-isocryptolepine hybrids. The synthesis of both **41** and **42** used the same reaction conditions, only variance being the reaction time, monitored by TLC (Scheme 28).)

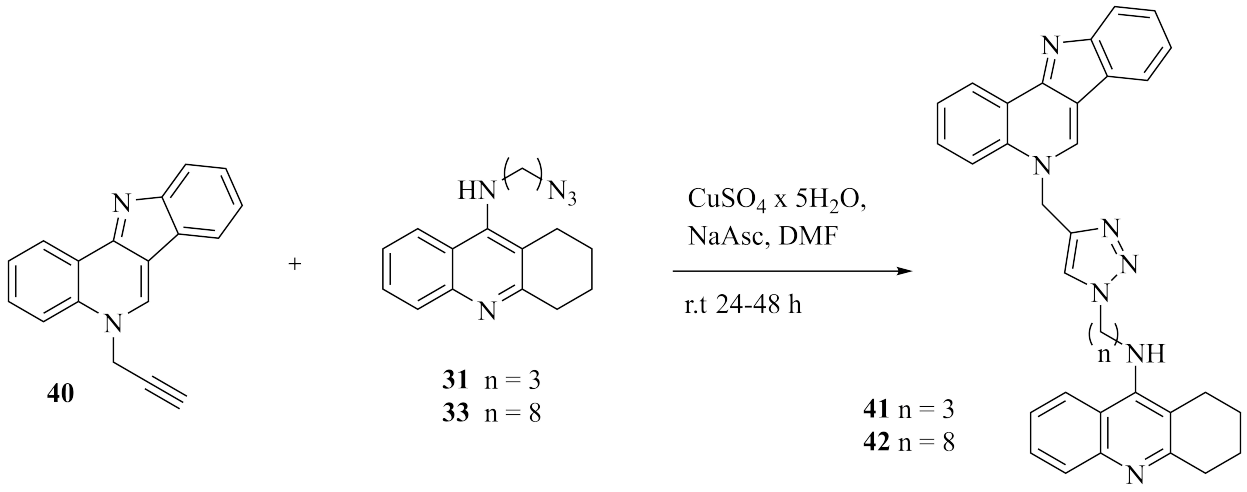

Scheme 28: Synthetic strategy towards the synthesis of target novel tacrine-isocryptolepine hybrids.

As for the coumarin-isocryptolepine hybrids, the reaction conditions was transferred over and attempted used for these hybrids as well.

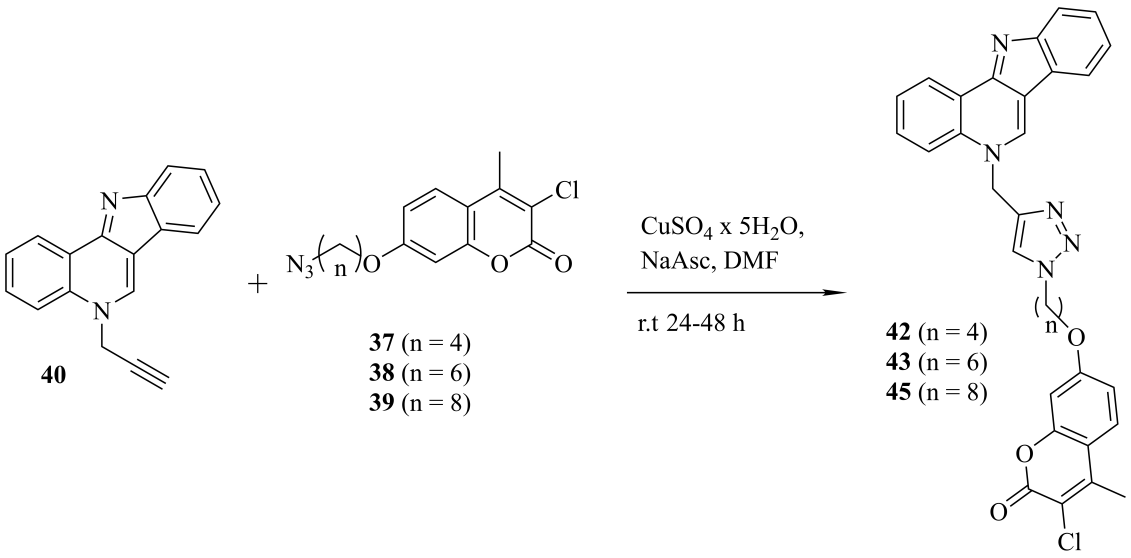

Scheme 29: Synthetic strategy towards the synthesis of target novel coumarin-isocryptolepine hybrids.

3.4.1 Synthesis of *N*-(3-(4-((5*H*-indolo[3,2-c]quinolin-5-yl)methyl)-1*H*-1,2,3-triazol-1-yl)propyl)-1,2,3,4-tetrahydroacridin-9-amine (41)

The synthesis of the tacrine-isocryptolepine hybrid **41** was the first attempt at synthesizing and isolating one of the target hybrids of this project. However, it would not be a quick attempt. Seven seperate attempts at chromatography with seven different eluents were tried and tested,

as well as an attempt at recrystallization ($CHCl_3$), but to no prevail. Especially eluent mixtures containing Et_3N were disappointing. Although seeming promising on TLC, the same result did not transfer to the column. However, in the end, the struggle was not for naught as **41** was isolated (68% yield) and confirmed by NMR (Figure 21).

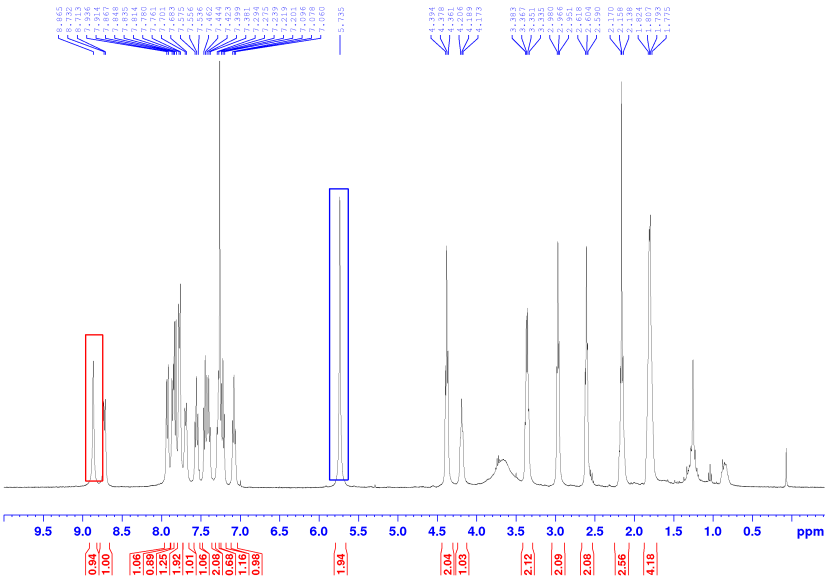

Figure 21: ^{1}H-NMR spectra of tacrine-isocryptolepine hybrid **41** showing triazole proton (red) and the methylene bridge protons ((blue)) between isocryptolepine and the triazole.

As seen in Figure 21 the presence of a triazole proton at δ 8.87 ppm and the methylene bridge proton at δ 5.74 ppm, between the isocryptolepine scaffold and the triazole. We also observed the triazole methine carbon by HSQC NMR and HMBC coupling from the methylene bridge to the triazole (Figure 22)

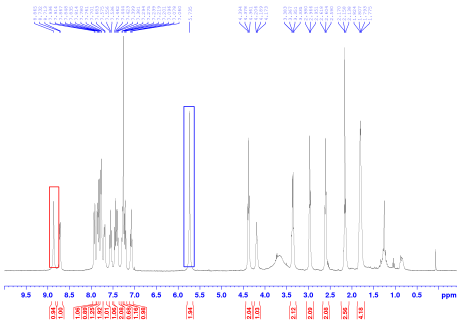

Figure 22: HMBC spectra showing coupling from isocryptolepine methylene bridge to the triazole methine carbon.

3.4.2 Attempted synthesis of *N*-(8-(4-((5*H*-indolo[3,2-c]quinolin-5-yl)methyl)-1*H*-1,2,3-triazol-1-yl)octyl)-1,2,3,4-tetrahydroacridin-9-amine (42)

After the success of isolating hybrid *41*, an attempt was made towards the synthesis of hybrid *42* using the same reaction conditions, and with even more starting material. However, the attempted purification and isolation of compound **42** was unsuccessful. The result was a complex mixture on NMR, which turned out to be impossible to interpret. After this attempt, the decision was made to change focus over to the coumarin-isocryptolepine hybrids. However, LRMS confirmed that the product had been produced, the isolation process was at fault (Figure 23).

Figure 23: LRMS of the reaction mixture strongly suggested the formation of hybrid **42**.

3.4.3 Synthesis of 7-(4-(4-((5*H*-indolo[3,2-c]quinolin-5-yl)methyl)-1H-1,2,3-triazol-1-yl)butoxy)-3-chloro-4-methyl-2*H*-chromen-2-one (43)

As depicted in (Scheme 29), the same reaction conditions were used for the coumarin-isocryptolepine hybrids as well. The first attempt on these hybrids were of compound **43**. The compound was actually isolated fairly easily, at least compared to that of the tacrine-isocryptolepine hybrids and in decent yield (30%). The ^{1}H-NMR (Figure 24)

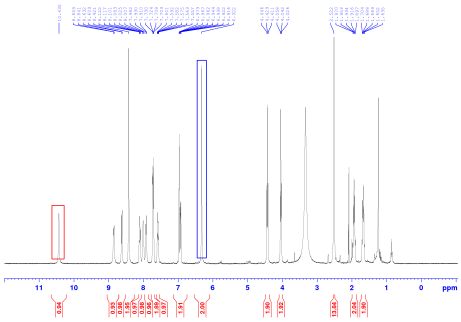

Figure 24: ^{1}H-NMR spectra of hybrid **43**. The spectra confirmed the same as for compound **41**, with slighly chemical shift vaules. Triazole proton is marked by red, and methylene bridge is in blue.

The ^{1}H-NMR spectra confirmed the the presence of a triazole proton at δ 10.43 ppm and the methylene bridge proton at δ 6.32 ppm, between the isocryptolepine scaffold and the triazole. As for **41** the observations was backed by the use of HSQC and HMBC NMR.

3.4.4 Attempted synthesis of 7-((6-(4-((5*H*-indolo[3,2-c]quinolin-5-yl)methyl)-1*H*-1,2,3-triazol-1-yl)hexyl)oxy)-3-chloro-4-methyl-2*H*-chromen-2-one (44)

For both compound **44** and **45**, COVID-19 intervened. At the return, atleast one of the precursor coumarin scaffolds (6C-linker) was suggested to have decomposed by TLC. This was not confirmed by NMR, because of problems with the NMR-machinery (probe). An attempt at CuAAC-reaction was therefore made using both, with poor results. The worst NMR-spectra was attributed to the coumarin scaffold which had seemed to decompose (6C-linker)

3.4.5 Attempted synthesis of 7-((8-(4-((5*H*-indolo[3,2-c]quinolin-5-yl)methyl)-1*H*-1,2,3-triazol-1-yl)octyl)oxy)-3-chloro-4-methyl-2-textitH-chromen-2-one (45)

See section above.

3.5 Conclusion and future work

In summary, the synthesis of the isocryptolepine scaffold **40**, the tacrine scaffolds **31** and **33**, and the coumarin scaffolds **37-39** was a success with varying degree of spectroscopic evidence. In addition, the synthesis of the novel tacrine-isocryptolepine compound **41** (68% yield) and the novel coumarin-isocryptolepine compound **43%** was a success. Regrettably the attempts at compound **42, 44, 45** was unsuccessful .

For future, the first recommended point on the agenda would be to get the novel isolated bivalent ligands of **41** and **43** evaluated by pharmacological and docking studies, as to evaluate their potential as dual binding site acetylcholinesterase inhibitors. These results would also be able to direct future work easier.

Would also recommend the attempts at different reaction conditions for the CuAAC**??**, as only one set of reaction conditions was tested during this project. This could have a positive effect towards the purification process (higher yield), and especially the potential of adding a ligand could be of interest.

Of course, the synthesis of more of these novel bivalent hybrids with different length of the linker is also desired, as it would make it possible to determine optimal length.

Finally, based on the interactions of the different scaffolds with the aromatic residues of AChE, it could also be of potential interest to attempt more hybrids containing the, in regards to AD research, isocryptolepine scaffold. An example is the potential use of imino-sugars **??**

4 Experimental

4.1 General

4.1.1 Solvents and reagents

All chemicals were obtained from Sigma Aldrich, Merck or VWR and used without further purification. When specified, acetone, DCM and toluene were dried by storing over 4 Å molecular sieves.

4.1.2 Spectroscopic and spectrometric analysis

Nuclear magnetic resonance (NMR) spectra were recorded on a Bruker Ascend^{TM} 400 series, operating at 400 MHz for ^{1}H and 100 MHz for ^{13}C. The chemical shifts (δ) are expressed in ppm relative to residual chloroform-d (^{1}H, 7.26 ppm; ^{13}C, 77.16 ppm), DMSO-d_6 (^{1}H, 2.50 ppm; ^{13}C, 39.52 ppm) and methanol-d_4 (^{1}H, 3.31 ppm; ^{13}C, 49.00 ppm).[234] Coupling constants (J) are given in Hertz (Hz) and the multiplicity is reported as: singlet (s), doublet (d), triplet (t), doublet of doublets (dd), doublet of doublet of doublets (ddd), multiplet (m) and broad singlet (bs). The assignments of signals in various NMR spectra was often assisted by conducting heteronuclear single-quantum correlation spectroscopy (HSQC) and/or heteronuclear multiple bond correlation spectroscopy (HMBC).

Infrared (IR) spectra were recorded on an Agilent Cary 630 FTIR spectrophotometer. Samples were analyzed by placing the sample directly onto the crystal of an attenuated total reflectance (ATR) module.

Melting points (mp) were determined on a Stuart SMP20 melting point apparatus and are uncorrected.

The microwave (MW) assisted experiments were performed in a CEM Focused Microwave^{TM} Synthesis System, model type Discover that operated at 0-300 W at a temperature of 100 °C, a pressure range of 0-290 psi, with reactor vial volumes of 10 mL.

Low resolution mass spectra were obtained on an Advion expression^{s} CMS mass spectrometer operating at 3.5 kV in electrospray ionization (ESI) mode.

4.1.3 Chromatography

Thin-layer chromatography (TLC) was carried out using aluminium backed 0.2 mm thick silica gel plates from Merck (type: 60 F_{254}). The spots were detected with ultraviolet (UV) (extinction at λ = 254 nm or fluorescent at λ = 366 nm). Flash chromatography (FC) was carried out with silica gel (particle size 40-63 μm), with solvent gradients as indicated in the experimental procedures.

4.2 Methods

9-Chloro-1,2,3,4-tetrahydroacridine (9)[135]

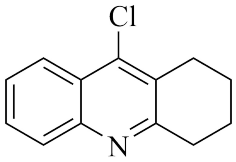

To a mixture of 2-aminobenzoic acid (**8**) (4.0 g, 29.2 mmol) and cyclohexanone (**6**) (3.63 mL, 35 mmol) was added slowly $POCl_3$ (26.7 mL, 292 mmol) at 0 °C. The mixture was refluxed (116 °C) for ∼24 h and cooled to 0 °C. The reaction mixture was added ice-cooled saturated $NaCO_3$ and the aqueous solution was extracted with EtOAc (x3) and dried over $MgSO_4$, filtered and concentrated under reduced pressure. The crude product was purified by recrystallization in acetone and washed in petroleum ether to give the title compound **9** as a brown solid (4.63 g, 73%). [R_f = 0.67 (PE/EtOAc, 9.5/0.5 v/v)].

mp: 74-76 °C.
IR (ATR): ν_{max} 3050, 2935, 2867, 1578, 1553, 1481, 1426, 1394, 1365, 1308, 916, 741 cm^{-1}.
^{1}**H-NMR** (400 MHz, $CDCl_3$): δ 8.14 (d, J = 8.5 Hz, 1H), 7.96 (d, J = 8.4 Hz, 1H), 7.64 (ddd, J = 8.4, 6.9, 1.2 Hz, 1H), 7.51 (ddd, J = 8.2, 6.9, 1.0 Hz, 1H), 3.11 (t, J = 6.1 Hz, 2H), 2.99 (t, J = 6.1 Hz, 2H), 1.98-1.88 (m, 4H).
^{13}**C-NMR** (100 MHz, $CDCl_3$): δ 159.6, 146.8, 141.6, 129.4, 129.0, 128.8, 126.6, 125.5, 123.8, 34.3, 27.6, 22.8 (2×C).
Spectroscopic and spectrometric data are in accordance with previously reported data.[135]

3-((1,2,3,4-Tetrahydroacridin-9-yl)amino)propan-1-ol (26)

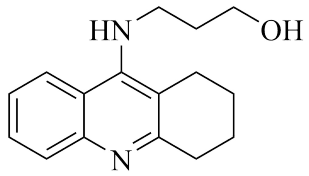

A mixture of 9-chloro-1,2,3,4-tetrahydroacridine **9** (2.0 g, 9.18 mmol) and 3-aminopropan-1-ol (2.07 g, 27.6 mmol) in butan-1-ol (10 mL) was heated under reflux for 20 h. After cooling to ambient temperature, the mixture was diluted with DCM (40 mL) and the organic layer was washed with brine (x4). The organic layer was concentrated under reduced pressure evaporated onto celite and purified by chromatography on silica gel (DCM/MeOH, 9/1 v/v) to afford the title compound **26** as a light-brown solid (1.81g, 77%).[R_f = 0.50 (DCM/MeOH/NH4OH), 8.5/1.5/0.1 v/v)].

mp: 135-138 °C.
IR (ATR): ν_{max} 3057, 2928, 2859, 1577, 1562, 1500, 1420, 1326, 1070, 757, 732 cm^{-1}.
^{1}**H-NMR** (400 MHz, $CDCl_3$): δ 7.98 (dd, J = 8.5, 0.9 Hz, 1H), 7.89 (d, J = 8.5 Hz, 1H), 7.51 (ddd, J = 8.2, 6.9, 1.3, 1H), 7.29 (ddd, J = 8.3, 6.9, 1.1 Hz, 1H), 4.70 (bs, 1H), 3.89 (t, J = 5.7 Hz, 2H), 3.70-3.62 (m, 2H), 3.38 (bs, 1H), 3.01 (t, J = 5.5 Hz, 2H), 2.67 (t, J = 5.5 Hz, 2H), 1.96-1.80 (m, 6H).
^{13}**C-NMR** (100 MHz, $CDCl_3$): δ 158.3, 151.2, 147.2, 128.6, 128.3, 123.8, 123.1, 120.1, 115.9, 61.5, 47.9, 33.8, 33.5, 25.0, 23.1, 22.8.

***N*-(3-azidopropyl)-1,2,3,4-tetrahydroacridin-9-amine (27)**

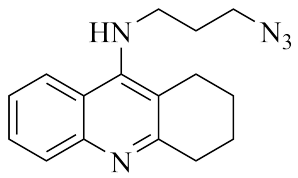

A suspension of 3-((1,2,3,4-tetrahydroacridin-9-yl)amino)propan-1-ol (**26**) (1.81g, 7.08 mmol) and anhydrous triethylamine (1.13 mL, 8.14 mmol) in anhydrous DCM (45 mL) at 0 °C was slowly added MsCl (0.59 mL, 7.57 mmol) and the mixture was stirred for 15 minutes. Saturated aqueous $NaHCO_3$ (55 mL) and DCM (55 mL) were added to the reaction mixture, the phases were separated, and the aqueous layer was extracted with DCM (x2). The collected organic extract were concentrated under reduced pressure and the obtained crude was dissolved in DMF

(14.5 mL), added NaN_3 (1.84 g, 28.3 mmol) and kept stirring at 45 °C overnight. The reaction mixture was added EtOAc (15 mL) and saturated aq. NaCl (15 mL). The organic layer was separated and the aqueous layer was extracted with EtOAc (10 mL x 3). The organic layers was concentrated under reduced pressure, evaporated onto celite and purified by silica gel column chromatography (DCM/MeOH, 9.5/0.5 → 9/1 v/v) and concentrated under reduced pressure to give the title compound **27** as a yellow oil (1.22 g, 62%). [R_f = 0.78 (DCM/MeOH/NH_4OH, 8.5/1.5/0.1 v/v)].

IR (ATR): ν_{max} 2930, 2860, 2091, 1670, 1560, 1496, 1256, 1090, 758 cm^{-1}.
^{1}**H-NMR** (400 MHz, $CDCl_3$): δ 7.92 (d, J = 1.38 Hz, 1H), 7.90 (d, J = 1.31 Hz, 1H) 7.54 (t, J = 7.9 Hz, 1H), 7.35 (t, J = 7.6 Hz, 1H) 4.11 (bs, 1H), 3.54 (bs, 2H) 3.44 (t, J = 6.4 Hz, 2H), 3.06 (t, J = 6.22 Hz, 2H), 2.71 (t, J = 6.29, 2H) 1.93-1.87 (m, 6H)
^{13}**C-NMR** (100 MHz, $CDCl_3$): δ 158.5, 150.3, 147.2, 128.7, 128.5, 124.0, 122.4, 120.4, 116.8, 49.4, 46.6, 33.9, 30.5, 24.9, 23.0, 22.7

1,2,3,4-tetrahydro-9-acridinamine (7)[132]

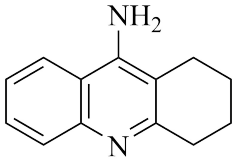

To a solution of anhydrous toluene (110 mL), cyclohexanone (**6**) (4.9 mL, 47.40 mmol) and 2-aminobenzonitrile (**5**) (5.00 g, 42.32 mmol) was added. The mixture was added boron trifluoride diethyl etherate (6.2 mL, 50.36 mmol) slowly and was stirred at reflux under an argon atmosphere for 24 h. On cooling, the toluene was decanted and 2M NaOH (120 mL) was added. The mixture was refluxed under an argon atmosphere for 24 h before being cooled to ambient temperature. The organic components was extracted with DCM (3 x 50 mL), dried ($MgSO_4$), filtered and concentrated under reduced pressure to afford the title compound **7** as a yellow solid (7.40g, 88%). [R_f = 0.25 (DCM/MeOH/NH_4OH, 9/1/0.1 v/v)].

mp: 177-179 °C (lit.[131] 178-180 °C).
IR (ATR): ν_{max} 3049, 2930, 2847, 1641, 1561, 1495, 1426, 1373, 746 cm^{-1}.
^{1}**H-NMR** (400 MHz, $CDCl_3$): δ 7.90 (d, J = 8.5 Hz, 1H), 7.70 (dd, J = 8.5, 0.8 Hz, 1H), 7.57 (t, J = 7.6 Hz, 1H), 7.37 (t, J = 7.6 Hz, 1H), 4.68 (bs, 2H), 3.04 (t, J = 6.32 Hz, 2H), 2.62 (t, J = 6.1 Hz, 2H), 1.99-1.89 (m, 4H).
^{13}**C-NMR** (100 MHz, $CDCl_3$): δ 158.5, 146.5, 146.4, 128.8, 128.5, 123.9, 119.6, 117.1, 110.4,

34.0, 23.8, 22.9, 22.8.

Spectroscopic and spectrometric data are in accordance with previously reported data.[131]

***N*-(8-bromooctyl)-1,2,3,4-tetrahydroacridin-9-amine (28)**

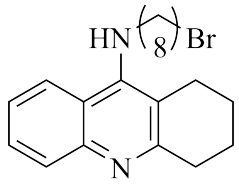

To a solution of 1,2,3,4-tetrahydroacridin-9-amine (**7**) (1.0 g, 5.04 mmol) and dimethyl sulfoxide (DMSO) (10 mL), NaOH (0.61 g, 15.13 mmol) was added slowly and stirred for 1 h before 1,8-dibromooctane (1.9 mL, 10.09 mmol) was added and the mixture was stirred under an argon atmosphere at room temperature for 44 h. The reaction mixture was added dest. H_2O (50 mL), the organic layer was separated and the aqueous layer was extracted with DCM (50 mL x 3). The organic layers were washed with saturated NaCl-solution (50 mL x 3), dried ($MgSO_4$) and concentrated under reduced pressure. The concentrate was evaporated onto celite and purified by silica gel column chromatography (DCM/MeOH/NH_4OH, 9.5/0.5/0.1 $\rightarrow$ 9/1/0.2). Concentration of the relevant fractions yielded title compound **28** as an orange oil (1.42 g, 72%). [R_f = 0.51 (DCM/MeOH/NH_4OH, 9:2:0.2 v/v)]

IR (ATR): ν_{max} 2920, 2851, 1572, 1498, 1350, 1293, 1253 cm^{-1}.
^{1}**H-NMR** (400 MHz, $CDCl_3$): δ 7.95 (d, J = 8.7 Hz, 1H), 7.92 (d, J = 8.3 Hz, 1H), 7.54 (t, J = 7.8 Hz, 1H), 7.33 (t, J = 7.7 Hz, 1H), 4.03 (bs, 1H), 3.48 (dd, J = 12.9 Hz, 6.3 Hz, 2H), 3.38 (t, J = 6.4 Hz, 2H) 3.06 (bs, 2H), 2.69 (bs, 2H), 1.95-1.60 (m, 8H), 1.45-1.24 (m, 8H).
^{13}**C-NMR** (100 MHz, $CDCl_3$): δ 158.3, 151.1, 147.2, 139.0, 128.6, 123.8, 123.0, 120.2, 115.8, 49.6, 34.1, 34.0, 32.8, 31.8, 29.3, 28.7, 28.1, 26.9, 24.9, 23.2, 22.8.

Spectroscopic and spectrometric data are in accordance with previously reported data.[235]
***N*-(8-azidooctyl)-1,2,3,4-tetrahydroacridin-9-amine (29)**

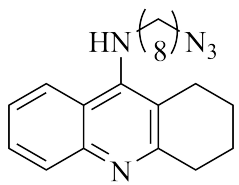

To a solution of *N*-(8-bromooctyl)-1,2,3,4-tetrahydroacridin-9-amine (**28**) (1.37 g, 3.52 mmol) and DMF (10 mL), NaN_3 (0.92 g, 14.09 mmol) was added slowly and the reaction mixture was stirred at reflux under an argon atmosphere for 24 h. The mixture was cooled to ambient temperature and added dest. H_2O (50 mL). The organic layer was separated and the aqueous layers were extracted with EtOAc (30 mL x 3). The combined organic layers were dried ($MgSO_4$), filtered and concentrated under reduced pressure. The concentrate was evaporated onto celite and purified by silica gel column chromatography (DCM/MeOH/NH_4OH, 9/1/0.1) to afford the title compound **29** as a brown oil (1.0 g, 80%). [R_f = 0.46 (DCM/MeOH/NH_4OH, 9/1/0.1 v/v)].

IR (ATR): ν_{max} 2925, 2854, 2088, 1579, 1560, 1496, 1419, 1350. 1116, 758 cm^{-1}.
^{1}**H-NMR** (400 MHz, $CDCl_3$): δ 7.98 (d, *J* = 8.4 Hz, 1H), 7.93 (d, *J* = 8.4 Hz, 1H), 7.57 (t, *J* = 7.6 Hz, 1H), 7.36 (t, *J* = 7.6 Hz, 1H), 3.98 (bs, 1H), 3.50 (dd, *J* = 12.4 Hz, 6.9 Hz, 2H), 3.27 (t, *J* = 6.6 Hz 2H), 3.09 (bs, 2H), 2.73 (bs, 2H), 1.97-1.91 (m, 4H), 1.73-1.54 (m, 4H), 1.46-1.26 (m, 8H).
^{13}**C-NMR** (100 MHz, $CDCl_3$): δ 158.5, 150.9, 147.6, 128.9, 128.5, 123.7, 123.0, 120.4, 51.6, 49.6, 34.2, 31.9, 29.4, 29.2, 28.9, 27.0, 26.7, 24.9, 23.2, 22.9.

3-chloro-7-hydroxy-4-methyl-2H-chromen-2-one (19)[158]

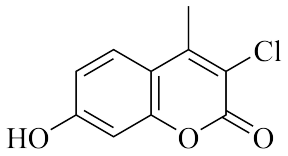

Method A

A mixture of resorcinol **12** (1.50g, 13.62 mmol) dissolved in 1,4-dioxane (5 mL) was cooled with a surrounding ice bath. Concentrated (95-97%) sulfuric acid (0.60 ml) was added slowly while stirring to keep the temperature of the mixture below 10 °C. The reaction mixture was added ethyl 2-chloroacetoacetate **15** (2.1 ml, 15.18 mmol) and the ice bath was removed. The reaction flask was stirred at 60 °C for 3h before the mixture was quenched by the addition of crushed ice ($\sim$150 ml) cautiously. The reaction mixture was extracted with EtOAc (50 mL x3). The organic layers were concentrated under reduced pressure, evaporated onto celite and purified by silica gel column chromatography (PE/EtOAc, 5/1 $\rightarrow$ 3/1 v/v) to yield a contaminated white solid (135.6 mg, 5%). [R_f = 0.12 (PE/EtOAC, 6:1 v/v)]

3-chloro-7-hydroxy-4-methyl-2H-chromen-2-one (19)[170]

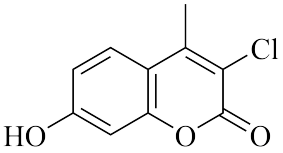

Method B

Resorcinol **12** (1.10 g, 10 mmol) and ethyl 2-chloroacetoacetate **15** (1.5 mL, 10.47 mmol) were mixed at ambient temperature and added TFA (2.5 mL) slowly while stirring. The combined reaction mixture was subjected to microwave irradiation at 100 °C for 30 min. The reaction was cooled at room temperature for 30 min. and the resulting precipitate was filtered, washed with hexane (10 ml x 5) and concentrated under reduced pressure yielding the title compound **16** as a brown-black solid (907.4 mg, 43%). [R_f = (PE/EtOAC, 3:1 v/v)] XXX,

mp: 235-238 °C (lit.[170] 237-240 °C).
IR (ATR): ν_{max} 3388, 1691, 1607, 1551, 1310, 1144, 1075, 1011 cm^{-1}.
^{1}**H-NMR** (400 MHz, DMSO-d_6): δ 10.67 (bs, 1H), 7.69 (d, J = 8.9 Hz, 2H), 6.87 (d, J = 2.5 Hz, 1H), 6.84 (d, J = 2.5 Hz, 1H), 6.75 (d, J = 2.5 Hz, 2H).
^{13}**C-NMR** (100 MHz, DMSO-d_6): δ 161.1, 156.5, 152.7, 149.0, 127.2, 115.2, 113.5, 111.6, 102.1, 16.0.

Spectroscopic and spectrometric data are in accordance with previously reported data.[170]

7-(4-bromobutoxy)-3-chloro-4-methyl-2H-chromen-2-one (30)

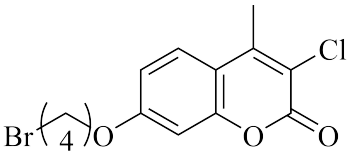

3-chloro-7-hydroxy-4-methyl-2H-chromen-2-one (**16**) (131.5 mg, 0.624 mmol) and K_2CO_3 (129.4 mg, 0.94 mmol) was suspended in anhydrous acetone (4 ml). 1,4-Dibromobutane (1.50 mL, 12.49 mmol) was added and the mixture was refluxed for 6 h. After cooling to ambient temperature the solid was filtered and washed with acetone and the filtrate was concentrated under reduced pressure. The concentrate was evaporated onto celite and purified by silica gel column chromatography (PE/EtOAc, 8/1 v/v) to yield the title compound **30** as a white solid (161.9 mg, 75%). [R_f = 0.26 (PE/EtOAC, 6/1 v/v)].

mp: 117-119 °C
IR (ATR): ν_{max} 2952, 1725, 1595, 1282, 1196, 1001 cm^{-1}.
^{1}**H-NMR** (400 MHz, $CDCl_3$): δ 7.48 (d, *J* = 8.7 Hz, 1H), 6.86 (d, *J* = 8.9 Hz, 1H), 6.74 (d, *J* = 2.2 Hz, 1H), 4.03 (t, *J* = 6.0 Hz, 2H), 3.48 (t, *J* = 6.2 Hz, 2H), 2.50 (s, 3H), 2.10-1.94 (m, 4H).
^{13}**C-NMR** (100 MHz, $CDCl_3$): δ 161.9, 157.4, 153.1, 148.1, 126.0, 117.7, 113.3, 113.2, 101.3, 67.7, 33.3, 29.4, 27.7, 16.3.

7-((6-bromohexyl)oxy)-3-chloro-4-methyl-2H-chromen-2-one (31)

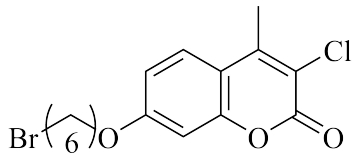

3-chloro-7-hydroxy-4-methyl-2H-chromen-2-one (**16**) (150 mg, 0.71 mmol) and K_2CO_3 (147.6 mg, 1.07 mmol) was suspended in anhydrous acetone (4.5 ml). 1,6-Dibromohexane (2.20 mL, 14.30 mmol) was added and the mixture was refluxed for 5 h. After cooling to ambient temperature the solid was filtered and washed with acetone and the filtrate was concentrated under reduced pressure. The concentrate was evaporated onto celite and purified by silica gel column chromatography (PE/EtOAc, 9/1 v/v) to yield the title compound **31** as a white solid (137.5 mg, 52%). [R_f = 0.31 (PE/EtOAC, 6/1 v/v)].
mp: 92-94 °C
IR (ATR): ν_{max} 2938, 2864, 1733, 1598, 1355, 1255, 1207, 1014 cm^{-1}.
^{1}**H-NMR** (400 MHz, $CDCl_3$): δ 7.51 (d, *J* = 8.9 Hz, 1H), 6.89 (dd, *J* = 8.9 Hz, 2.4 Hz, 1H), 6.80 (d, *J* = 2.4 Hz, 1H), 4.02 (t, *J* = 5.8 Hz, 2H), 3.43 (t, *J* = 6.3 Hz, 2H), 2.54 (s, 3H), 1.94-1.80 (m, 4H), 1.52 (t, *J* = 3.7 Hz, 4H)
^{13}**C-NMR** (100 MHz, $CDCl_3$): δ 162.2, 157.6, 153.3, 148.1, 126.0, 117.9, 113.5, 113.3, 101.4, 68.6, 33.9, 32.8, 29.0, 28.0, 25.4, 16.3.

7-((8-bromooctyl)oxy)-3-chloro-4-methyl-2H-chromen-2-one (32)

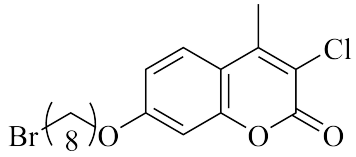

3-chloro-7-hydroxy-4-methyl-2H-chromen-2-one (**16**) (150 mg, 0.71 mmol) and K_2CO_3 (197 mg, 1,42 mmol) was suspended in anhydrous acetone (4.5 ml). 1,8-Dibromooctane (2.00 mL,

10.79 mmol) was added and the mixture was refluxed for 6 h. After cooling to ambient temperature the solid was filtered and washed with acetone and the filtrate was concentrated under reduced pressure. The concentrate was evaporated onto celite and purified by silica gel column chromatography (PE/EtOAc, 10/1 v/v) to yield the title compound **32** as a white solid (176.0 mg, 62%). [R_f = 0.38 (PE/EtOAC, 6/1 v/v)].
mp: 99-101 °C
IR (ATR): ν_{max} 2936, 2854, 1721, 1598, 1470, 1287, 1205, 1151 cm^{-1}.
^{1}**H-NMR** (400 MHz, $CDCl_3$): δ 7.51 (d, J = 9.1 Hz, 1H), 6.89 (dd, J = 8.9 Hz, 2.3 Hz, 1H), 6.81 (d, J = 2.4 Hz, 1H), 4.01 (t, J = 6.8 Hz, 2H), 3.41 (t, J = 6.8 Hz, 2H), 2.55 (s, 3H), 1.90-1.78 (m, 4H), 1.47-1.33 (m, 8H)
^{13}**C-NMR** (100 MHz, $CDCl_3$): δ 162.3, 157.7, 153.4, 148.2, 126.0, 117.9, 113.6, 113.3, 101.4, 68.8, 34.1, 32.9, 29.3, 29.1, 28.8, 28.2, 26.0, 16.4.

7-(4-azidobutoxy)-3-chloro-4-methyl-2H-chromen-2-one (33)

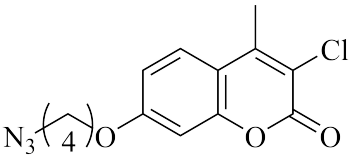

To a solution of 7-(4-bromobutoxy)-3-chloro-4-methyl-2H-chromen-2-one (**30**) (161.1 mg, 0.47 mmol) and DMF (2 ml), NaN_3 (121.2 mg, 1.86 mmol) was added. The solution was heated at 70 °C for 6 h. The solution was cooled to ambient temperature and added dest. H_2O (20 mL) and EtoAc (15 mL). The organic layer was separated and the aqueous layer was extracted with EtoAc (10 mL x 3). The organic layers were dried ($MgSO_4$), filtered and concentrated under reduced pressure to yield title compound **33** without further purification as a yellow-brown dense oil (138.1 mg, 96%). [R_f = 0.28 (PE/EtOAC, 6/1 v/v)]

IR (ATR): ν_{max} 2922, 2851, 2091, 1720, 1597, 1252, 1201, 1150 cm^{-1}.
Due to unfortunate circumstances regarding the NMR-apparatus, NMR-data is lacking for this compound. Prepared sample is ready for analysis.

7-((6-azidohexyl)oxy)-3-chloro-4-methyl-2H-chromen-2-one (34)

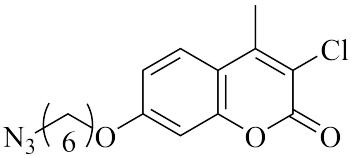

To a solution of 7-((6-bromohexyl)oxy)-3-chloro-4-methyl-2H-chromen-2-one (**31**) (137.5 mg, 0.37 mmol) and DMF (2 ml), NaN_3 (95.7 mg, 1.47 mmol) was added. The solution was heated at 70 °C for 6 h. The solution was cooled to ambient temperature and added dest. H_2O (20 mL) and EtoAc (15 mL). The organic layer was separated and the aqueous layer was extracted with EtoAc (10 mL x 3). The organic layers were dried ($MgSO_4$), filtered and concentrated under reduced pressure. The concentrate was evaporated onto celite and purified by silica gel column chromatography (PE/EtOAc, 10/1 → 1/1 → 0/1) to yield title compound **34** as a brown oil (53.9 mg, 44%). [R_f = 0.22 (PE/EtOAc, 6/1 v/v)].

IR (ATR): ν_{max} 2931, 2860, 2089, 1720, 1597, 1253, 1201, 1150, 1073, 1008 cm^{-1}.

Due to unfortunate circumstances regarding the NMR-apparatus, NMR-data is lacking for this compound. Prepared sample is ready for analysis.

7-((8-azidooctyl)oxy)-3-chloro-4-methyl-2H-chromen-2-one (35)

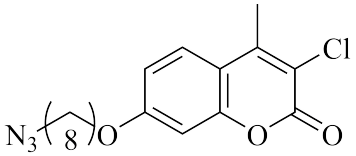

To a solution of 7-((8-bromooctyl)oxy)-3-chloro-4-methyl-2H-chromen-2-one (**32**) 176 mg, 0.44 mmol) and DMF (2.5 mL), NaN_3 (113.9 mg, 1.75 mmol) was added. The solution was heated at 70 °C for 6 h. The solution was cooled to ambient temperature and added dest. H_2O (20 mL) and EtoAc (15 mL). The organic layer was separated and the aqueous layer was extracted with EtOAc (10 mL x 3). The organic layers were dried ($MgSO_4$), filtered and concentrated under reduced pressure to yield title compound **35** without further purification as a yellow-brown dense oil (153.4 mg, 96%). [R_f = 0.38 (PE/EtOAc, 6/1 v/v)].

IR (ATR): ν_{max} 2925, 2854, 2091 (-N3), 1726, 1600, 1254, 1150, 1008. cm^{-1}.

Due to unfortunate circumstances regarding the NMR-apparatus, NMR-data is lacking for this compound. Prepared sample is ready for analysis.

2-(Quinolin-3-yl)aniline (23)[188]

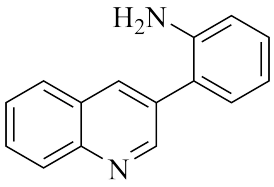

3-Bromoquinoline **21** (500 mg, 2.40 mmol) was dissolved in EtOH (10 mL) and added 2-aminophenylboronic acid **22** (500 mg, 2.88 mmol) and K_2CO_3 (995 mg, 7.2 mmol) in H_2O (2 mL). The reaction mixture was added $PdCl_2$(pddf) (98 mg, 0.12 mmol) and the reaction was stirred at 60 °C under a a nitrogen atmosphere for 24 h. The reaction mixture was cooled to ambient temperature and the volatiles were removed under reduced pressure, evaporated onto celite and purified by silica gel column chromatography (PE/EtoAc, 95/5 $\rightarrow$ 55/45 v/v) yielding compound **23** as yellow crystals (404 mg, 77%). [R_f = 0.26 (PE/EtOAc, 7/3 v/v)].

mp: 131-134 °C.
IR (ATR): ν_{max} 3416, 3318, 3217, 3024, 1633, 1566, 1490, 1306, 1140, 915, 782, 737 cm^{-1}.
^{1}**H-NMR** (400 MHz, $CDCl_3$): δ 9.03 (d, J = 2.2 Hz, 1H), 8.28 (d, J = 1.9 Hz, 1H), 8.17 (d, J = 8.4 Hz, 1H), 7.87-7.85 (m, 1H), 7.77-7.74 (m, 1H), 7.62-7.58 (m, 1H), 7.25-7.21 (m, 2H), 6.93-6.89 (m, 1H), 6.85-6.83 (m, 1H), 3.79 (bs, 2H).
^{13}**C-NMR** (100 MHz, $CDCl_3$): δ 151.4, 147.0, 144.0, 135.7, 132.5, 130.9, 129.7, 129.5, 129.2, 128.0, 127.9, 127.1, 123.7, 119.1, 116.0.

Spectroscopic and spectrometric data are in accordance with previously reported data.[188]
11*H*-indolo[3,2-c]quinoline (29)[190]

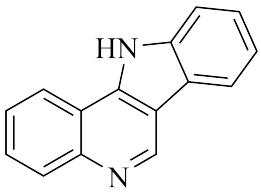

A solution of 2-(quinolin-3-yl)aniline **23** (398 mg, 1.81 mmol) dissolved in HCl (37%) (12 mL) was cooled to 0 °C. Ice cooled $NaNO_2$ (0.4M) (12 mL, 4.78 mmol) was slowly added and the solution was stirred at 0 °C for 1.5h. An ice cooled mix of NaN_3 (247 mg, 3.80 mmol) and NaOAc (20 mL) was added slowly and the solution was stirred at 0 °C for 1h. The reaction mixture was slowly quenched using aq. Na_2CO_3 (40mL) cooled to 0 °C. The reaction mixture was added EtOAc (20 mL), the organic layer was separated and the aqueous layer was extracted

with EtOAc (4 x 10 mL). The combined organic layers were dried ($MgSO_4$) concentrated under reduced pressure. The residue was dissolved in 1,2-dichlorobenzene (10 mL) and stirred for 3h at 180 °C under a nitrogen atmosphere. The reaction mixture was concenrated under reduced pressure, the concentrate was evaporated onto celite and purified by silica gel column chromatography (PE/EtOAc, 7/3 → 6/4 to yield the title compound **29** as a light brown solid (314 mg, 79%). [R_f = 0.68 (DCM/MeOH, 5/1 v/v)].

mp: 330-332 °C (lit.[233] 329-331 °C)
IR (ATR): ν_{max} 3037, 2714, 2653, 1735, 1595, 1566, 1509, 1458, 1364, 1337, 1234, 930, 732 cm^{-1}.
^{1}**H-NMR** (400 MHz, MeOD): δ 9.46 (s, 1H), 8.28 (dd, *J* = 8.3 Hz, 1.0 Hz, 1H), 8.25 (d, *J* = 7.9 Hz, 1H), 8.14 (d, *J* = 8.20, 1H), 7.75 (ddd, *J* = 15.4 Hz, 8.3 Hz, 1.5 Hz 1H), 7.70-7.65 (m, 2H), 7.50 (ddd, *J* = 15.3 Hz, 9.2 Hz, 1.1 Hz, 1H) 7.36 (ddd, *J* = 15.0 Hz, 8.9 Hz, 1.0 Hz, 1H).
^{1}**H-NMR** (400 MHz, DMSO-d_6): δ 12.80 (bs, 1H)
^{13}**C-NMR** (100 MHz, $MeOD_3$): δ 151.4, 147.0, 144.0, 135.7, 132.5, 130.9, 129.7, 129.5, 129.2, 128.0, 127.9, 127.1, 123.7, 119.1, 116.0.

Spectroscopic and spectrometric data are in accordance with previously reported data.[233]

5-(Prop-2-yn-1-yl)-5*H*-indolo[3,2-c] (40)

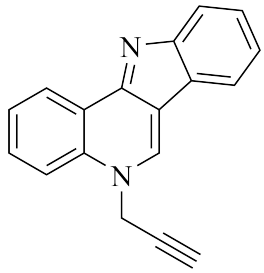

To a mixture of 11*H*-indolo[3,2-c]quinoline (**29**) (161 mg, 0.74 mmol) and anhydrous toluene (5.8 mL) in a pressure tube, propargyl bromide (80 % in toluene) (1.23 mL, 11.04 mmol) was added. The solution was stirred at 130 °C for 5 h. The reaction mixture was concentrated under reduced pressure to remove volatiles. The crude was added DCM (35 mL) and sat. aq. Na_2CO_3 (30 mL) and was stirred at ambient temperature for 30 min. The organic layer was separated and the aqueous layer was extracted with DCM (25 mL x 4). The organic layers were concentrated under reduced pressure and the concentrate was evaporated onto celite and attempted purified by silica gel column chromatography (DCM/MeOH, 1/0 → 9.5/0.5 → 9.0/1

v/v). [R_f = 0.33 (DCM/MeOH/NH_4OH, 9/1/0.1 v/v)].

IR (ATR): ν_{max} 3188, 2920, 2850, 2777, 2116, 1607, 1347, 1212. cm^{-1}.
^{1}**H-NMR** (400 MHz, $CDCl_3$): δ 8.84 (d, J = 7.7 Hz, 1H), 8.31 (s, 1H), 7.96 (d, J = 8.1 Hz, 1H), 7.84 (d, J = 7.7 Hz, 1H), 7.64-7.62 (m, 2H), 7.55-7.49 (m, 2H), 7.28-7.24 (m, 1H, overlaps with solvent residual signal), 4.98 (d, J = 2.2 Hz, 2H), 2.55 (t, J = 2.2 Hz, 1H).

IR is scuffed due to impurities/solvent.
***N*-(3-(4-((5*H*-indolo[3,2-c]quinolin-5-yl)methyl)-1*H*-1,2,3-triazol-1-yl)propyl)-1,2,3,4-tetrahydroacridin**
9-amine (37)

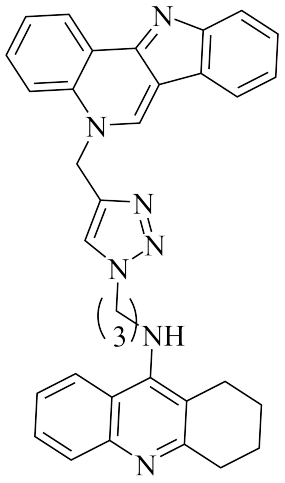

To a solution of 5-(prop-2-yn-1-yl)-5*H*-indolo[3,2-c]quinoline (**36**) (47.8 mg, 0.19 mmol) and *N*-(3-azidopropyl)-1,2,3,4-tetrahydroacridin-9-amine **(27)** (52.5 mg, 0.19 mmol) in DMF (1.2 mL), $CuSO_4$ x H2O (14 mg, 0.056 mmol) and (+)-sodium L-ascorbate (NaAsc) (22.2 mg, 0.11 mmol) was added. The reaction mixture was stirred at ambient temperature for 44 h. The mixture was concentrated under reduced pressure, evaporated onto celite and purified by silica gel column chromatography (DCM/MeOH/NH_4OH, 8.5/1.5/0.15 v/v) to yield target compound **37** as a yellow solid (67.9 mg, 68%). [R_f = 0.12 (DCM/MeOH/NH_4OH, 8.5/1.5/0.07 v/v].
mp: 112-114 °C.
IR (ATR): ν_{max} 3334 (-NH), 2933, 2855, 1721, 1597, 1347, 1205, 1139. cm^{-1}.
^{1}**H-NMR** (400 MHz, $CDCl_3$): δ 8.86 (s, 1H), 8.72 (d, J = 7.6, 1H), 7,92 (d, J = 8.7 Hz, 1H), 7.86 (d, J = 7.6 Hz, 1H), 7.82 (d, J = 8.6 Hz, 1H), 7.77 (d, J = 7.6 Hz, 2H), 7.69 (d, J = 7.6 Hz, 1H), 7.57-7.54 (m, 1H), 7.46-7.38 (m, 2H), 7.29-7.20 (m, 2H), 7.10-7.06 (m, 1H), 5.73 (s, 2H), 4.38 (t, J = 6.5 Hz, 2H),4.19 (t, J = 6.5 Hz, NH), 3.36 (q, J = 6.5 Hz, 2H), 2.97 (t, J = 5.8 Hz, 2H), 2.60 (t, J = 5.8 Hz, 2H),2.17-2.14 (m, 2H), 1.82-1.78 (m, 4H).
^{13}**C-NMR** (100 MHz, $CDCl_3$): δ 158.8, 151.0, 149.8, 147.2, 142.3, 136.6, 134.7, 130.3, 128.8,

128.5, 127.1, 125.9, 125.5, 124.3, 124.2, 123.6, 122.2, 121.6, 120.5, 120.0, 119.8, 117.4, 117.3, 117.0, 117.0, 50.5, 48.1, 45.4, 34.0, 31.5, 25.1, 23.0, 22.7. One quaternary carbon signal missing.

***N*-(8-(4-((5*H*-indolo[3,2-c]quinolin-5-yl)methyl)-1*H*-1,2,3-triazol-1-yl)octyl)-1,2,3,4-tetrahydroacridin-9-amine (38)**

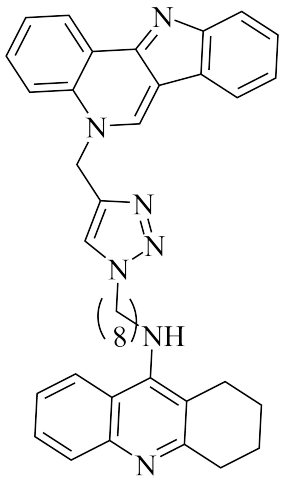

To a solution of 5-(prop-2-yn-1-yl)-5*H*-indolo[3,2-c]quinoline (**36**) (47.8 mg, 0.19 mmol) and *N*-(8-azidooctyl)-1,2,3,4-tetrahydroacridin-9-amine (**29**) (52.5 mg, 0.19 mmol) in DMF (1.2 mL), $CuSO_4$ x H2O (14 mg, 0.056 mmol) and (+)-sodium L-ascorbate (NaAsc) (22.2 mg, 0.11 mmol) was added. The reaction mixture was stirred at ambient temperature for 43 h. The mixture was concentrated under reduced pressure, evaporated onto celite and attempted purified by silica gel column chromatography (DCM/MeOH/NH_4OH, 8.5/1.5/0.15 v/v) to yield a yellow solid (90.9 mg, 46%) which could *not* be confidently identified as the target compound **38**. [R_f = 0.40 (DCM/MeOH/NH_4OH, 8.5/1.5/0.07 v/v].
IR (ATR): ν_{max} cm^{-1}.
^{1}**H-NMR** (400 MHz, $CDCl_3$): δ .
^{13}**C-NMR** (100 MHz, $CDCl_3$): δ .

Have unfortunately yet to confidently isolate this compound and to confirm it by NMR.

7-(4-(4-((5*H*-indolo[3,2-c]quinolin-5-yl)methyl)-1H-1,2,3-triazol-1-yl)butoxy)-3-chloro-4-methyl-2*H*-chromen-2-one (39)

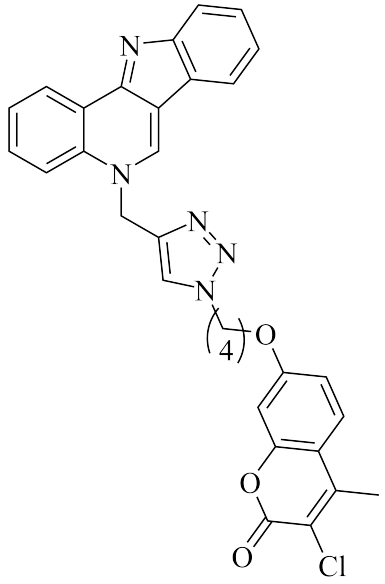

To a solution of 5-(prop-2-yn-1-yl)-5H-indolo[3,2-c]quinoline (**36**) (95.2 mg, 0.31 mmol) and 7-(4-azidobutoxy)-3-chloro-4-methyl-2H-chromen-2-one **33** (79.3 mg, 0.31 mmol) in DMF (1.8 mL), $CuSO_4$ x H2O (23.2 mg, 0.092 mmol) and (+)-sodium L-ascorbate (NaAsc) (36.8 mg, 0.19 mmol) was added. The reaction mixture was stirred at ambient temperature for 43 h. The mixture was concentrated under reduced pressure, evaporated onto celite and purified by silica gel column chromatography (DCM/MeOH, 1/0 $\rightarrow$ 9.75/0.25 v/v) to yield the target compound **39** as a yellow solid (52.0 mg, 30%). [R_f = 0.30 (DCM/MeOH/, 9/1 v/v].
mp: 249-251 °C.
IR (ATR): ν_{max} 2940, 2852, 1720, 1596, 1508, 1284, 1201, 1144. cm^{-1}.
^{1}**H-NMR** (400 MHz, $CDCl_3$): δ 10.43 (s, 1H), 8.85 (d, J = 7.3 Hz, 1H), 8.62 (d, J = 8.9 Hz, 1H), 8.42 (s, 2H, two overlapping signals), 8.12-8.08 (m, 1H), 8.02-7.98 (m, 1H), 7.92 (d, J = 7.9 Hz, 1H), 7.73-7.70 (m, 2H), 7.60-7.56 (m, 1H), 6.97-6.92 (m, 2H), 6.32 (s, 2H), 4.43 (t, J = 7.0 Hz, 2H), 4.04 (t, J = 6.3 Hz, 2H), 2.52 (s, 3H, overlaps with solvent residual signal), 1.97-1.90 (m, 2H), 1.70-1.64 (m, 2H).
^{13}**C-NMR** (100 MHz, $CDCl_3$): δ 161.5, 156.4, 152.6, 148.8, 144.9, 143.4, 141.0, 135.1, 132.3, 128.2, 127.0, 124.4, 124.3, 123.2, 122.2, 121.0, 119.5, 117.1, 116.2, 114.2, 114.0, 113.0, 112.7, 101.1, 67.6, 51.1, 49.2, 40.1 (overlaps with solvent residual signal), 26.3, 25.3, 16.1. One quaternary carbon signal missing.

Experimental - Incomplete

7-((6-(4-((5*H*-indolo[3,2-c]quinolin-5-yl)methyl)-1*H*-1,2,3-triazol-1-yl)hexyl)oxy)-3-chloro-4-methyl-2*H*-chromen-2-one (40)

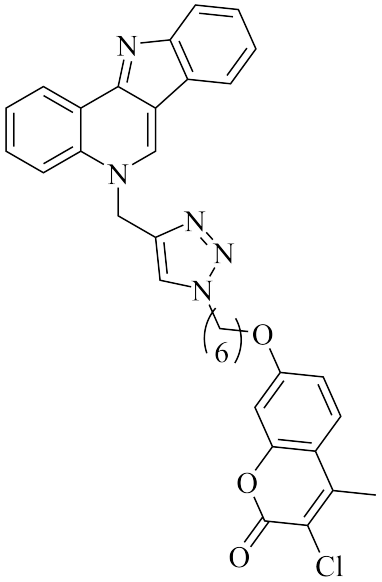

To a solution of 5-(prop-2-yn-1-yl)-5H-indolo[3,2-c]quinoline (**36**) (47.8 mg, 0.19 mmol) and *N*-(8-azidooctyl)-1,2,3,4-tetrahydroacridin-9-amine (**29**) (52.5 mg, 0.19 mmol) in DMF (1.2 mL), $CuSO_4$ x H2O (14 mg, 0.056 mmol) and (+)-sodium L-ascorbate (NaAsc) (22.2 mg, 0.11 mmol) was added. The reaction mixture was stirred at ambient temperature for 43 h. The mixture was concentrated under reduced pressure, evaporated onto celite and purified by silica gel column chromatography (DCM/MeOH/NH_4OH, 8.5/1.5/0.15 v/v) to yield target a yellow solid (90.9 mg, 46%) which could *not* be confidently identified as the target compound **38**. [R_f = 0.40 (DCM/MeOH/NH_4OH, 8.5/1.5/0.07 v/v].

Have unfortunately yet to confidently isolate this compound and to confirm it by NMR or in any other way.

7-((8-(4-((5*H*-indolo[3,2-c]quinolin-5-yl)methyl)-1*H*-1,2,3-triazol-1-yl)octyl)oxy)-3-chloro-4-methyl-2-textitH-chromen-2-one (41)

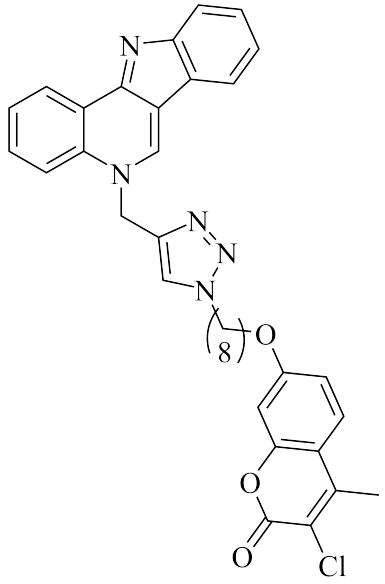

To a solution of 5-(prop-2-yn-1-yl)-5H-indolo[3,2-c]quinoline (**36**) (47.8 mg, 0.19 mmol) and *N*-(8-azidooctyl)-1,2,3,4-tetrahydroacridin-9-amine (**29**) (52.5 mg, 0.19 mmol) in DMF (1.2 mL), $CuSO_4$ x H2O (14 mg, 0.056 mmol) and (+)-sodium L-ascorbate (NaAsc) (22.2 mg, 0.11 mmol) was added. The reaction mixture was stirred at ambient temperature for 43 h. The mixture was concentrated under reduced pressure, evaporated onto celite and purified by silica gel column chromatography (DCM/MeOH/NH_4OH, 8.5/1.5/0.15 v/v) to yield target a yellow solid (90.9 mg, 46%) which could *not* be confidently identified as the target compound **38**. [R_f = 0.40 (DCM/MeOH/NH_4OH, 8.5/1.5/0.07 v/v].

Have unfortunately yet to confidently isolate this compound and to confirm it by NMR or in any other way.

References

[1] Patterson, C. World Alzheimer report 2018: the state of the art of dementia research: new frontiers. *Alzheimer's Disease International (ADI): London, UK* **2018**,

[2] Association, A., et al. 2017 Alzheimer's disease facts and figures. *Alzheimer's & Dementia* **2017**, *13*, 325–373.

[3] Association, A. 2020 Alzheimer's disease facts and figures. *Alzheimer's & Dementia* **2020**, *16*, 391–460.

[4] Schultz, C.; Del Tredici, K.; Braak, H. *Alzheimer's Disease*; Springer, 2004; pp 21–31.

[5] Merriam, A. E.; Aronson, M. K.; Gaston, P.; Wey, S.-L.; Katz, I. The psychiatric symptoms of Alzheimer's disease. *Journal of the American Geriatrics Society* **1988**, *36*, 7–22.

[6] Stelzmann, R. A.; Norman Schnitzlein, H.; Reed Murtagh, F. An English translation of Alzheimer's 1907 paper,"Über eine eigenartige Erkankung der Hirnrinde". *Clinical Anatomy: The Official Journal of the American Association of Clinical Anatomists and the British Association of Clinical Anatomists* **1995**, *8*, 429–431.

[7] Singh, S. K.; Srivastav, S.; Yadav, A. K.; Srikrishna, S.; Perry, G. Overview of Alzheimer's disease and some therapeutic approaches targeting Aβ by using several synthetic and herbal compounds. *Oxidative medicine and cellular longevity* **2016**, *2016*.

[8] McGeer, P.; Itagaki, S.; Tago, H.; McGeer, E. Occurrence of HLA-DR reactive microglia in Alzheimer's disease. *Annals of the New York Academy of Sciences* **1988**, *540*, 319–323.

[9] Serrano-Pozo, A.; Frosch, M. P.; Masliah, E.; Hyman, B. T. Neuropathological alterations in Alzheimer disease. *Cold Spring Harbor perspectives in medicine* **2011**, *1*, a006189.

[10] Tuppo, E. E.; Arias, H. R. The role of inflammation in Alzheimer's disease. *The international journal of biochemistry & cell biology* **2005**, *37*, 289–305.

[11] Von Bernhardi, R. Glial cell dysregulation: a new perspective on Alzheimer disease. *Neurotoxicity research* **2007**, *12*, 215–232.

[12] Cummings, J. L.; Morstorf, T.; Zhong, K. Alzheimer's disease drug-development pipeline: few candidates, frequent failures. *Alzheimer's research & therapy* **2014**, *6*, 37.

[13] Rogawski, M. A.; Wenk, G. L. The neuropharmacological basis for the use of memantine in the treatment of Alzheimer's disease. *CNS drug reviews* **2003**, *9*, 275–308.

[14] Thomas, S. J.; Grossberg, G. T. Memantine: a review of studies into its safety and efficacy in treating Alzheimer's disease and other dementias. *Clinical interventions in aging* **2009**, *4*, 367.

[15] Smith, D. A. Treatment of Alzheimer's disease in the long-term-care setting. *American Journal of Health-System Pharmacy* **2009**, *66*, 899–907.

[16] Tariot, P. N.; Federoff, H. J. Current treatment for Alzheimer disease and future prospects. *Alzheimer disease & associated disorders* **2003**, *17*, S105–S113.

[17] Sun, Y.; Lai, M.-S.; Lu, C.-J.; Chen, R.-C. How long can patients with mild or moderate Alzheimer's dementia maintain both the cognition and the therapy of cholinesterase inhibitors: a national population-based study. *European journal of neurology* **2008**, *15*, 278–283.

[18] Davies, P.; Maloney, A. Selective loss of central cholinergic neurons in Alzheimer's disease. *The Lancet* **1976**, *308*, 1403.

[19] Perry, E. K.; Gibson, P. H.; Blessed, G.; Perry, R. H.; Tomlinson, B. E. Neurotransmitter enzyme abnormalities in senile dementia: Choline acetyltransferase and glutamic acid decarboxylase activities in necropsy brain tissue. *Journal of the neurological sciences* **1977**, *34*, 247–265.

[20] Rylett, R.; Ball, M.; Colhoun, E. Evidence for high affinity choline transport in synaptosomes prepared from hippocampus and neocortex of patients with Alzheimer's disease. *Brain research* **1983**, *289*, 169–175.

[21] Drachman, D. A.; Leavitt, J. Human memory and the cholinergic system: a relationship to aging? *Archives of neurology* **1974**, *30*, 113–121.

[22] H Ferreira-Vieira, T.; M Guimaraes, I.; R Silva, F.; M Ribeiro, F. Alzheimer's disease: targeting the cholinergic system. *Current neuropharmacology* **2016**, *14*, 101–115.

[23] Francis, P. T.; Palmer, A. M.; Snape, M.; Wilcock, G. K. The cholinergic hypothesis of Alzheimer's disease: a review of progress. *Journal of Neurology, Neurosurgery & Psychiatry* **1999**, *66*, 137–147.

[24] Sussman, J. L.; Harel, M.; Frolow, F.; Oefner, C.; Goldman, A.; Toker, L.; Silman, I. Atomic structure of acetylcholinesterase from Torpedo californica: a prototypic acetylcholine-binding protein. *Science* **1991**, *253*, 872–879.

[25] Harel, M.; Schalk, I.; Ehret-Sabatier, L.; Bouet, F.; Goeldner, M.; Hirth, C.; Axelsen, P.; Silman, I.; Sussman, J. Quaternary ligand binding to aromatic residues in the active-site gorge of acetylcholinesterase. *Proceedings of the National Academy of Sciences* **1993**, *90*, 9031–9035.

[26] Cheung, J.; Rudolph, M. J.; Burshteyn, F.; Cassidy, M. S.; Gary, E. N.; Love, J.; Franklin, M. C.; Height, J. J. Structures of human acetylcholinesterase in complex with pharmacologically important ligands. *Journal of medicinal chemistry* **2012**, *55*, 10282–10286.

[27] Nachon, F.; Carletti, E.; Ronco, C.; Trovaslet, M.; Nicolet, Y.; Jean, L.; Renard, P.-Y. Crystal structures of human cholinesterases in complex with huprine W and tacrine: elements of specificity for anti-Alzheimer's drugs targeting acetyl-and butyrylcholinesterase. *Biochemical Journal* **2013**, *453*, 393–399.

[28] Kryger, G.; Silman, I.; Sussman, J. L. Structure of acetylcholinesterase complexed with E2020 (Aricept®): implications for the design of new anti-Alzheimer drugs. *Structure* **1999**, *7*, 297–307.

[29] Kovarik, Z.; Radić, Z.; Berman, H. A.; Simeon-Rudolf, V.; Reiner, E.; Taylor, P. Acetylcholinesterase active centre and gorge conformations analysed by combinatorial mutations and enantiomeric phosphonates. *Biochemical Journal* **2003**, *373*, 33–40.

[30] Rosenberry, T. L.; Brazzolotto, X.; Macdonald, I. R.; Wandhammer, M.; Trovaslet-Leroy, M.; Darvesh, S.; Nachon, F. Comparison of the binding of reversible inhibitors to human butyrylcholinesterase and acetylcholinesterase: A crystallographic, kinetic and calorimetric study. *Molecules* **2017**, *22*, 2098.

[31] Bourne, Y.; Radić, Z.; Sulzenbacher, G.; Kim, E.; Taylor, P.; Marchot, P. Substrate and product trafficking through the active center gorge of acetylcholinesterase analyzed by crystallography and equilibrium binding. *Journal of Biological Chemistry* **2006**, *281*, 29256–29267.

[32] Pang, Y.-P.; Quiram, P.; Jelacic, T.; Hong, F.; Brimijoin, S. Highly potent, selective, and low cost bis-tetrahydroaminacrine inhibitors of acetylcholinesterase steps toward novel drugs for treating Alzheimer's disease. *Journal of Biological Chemistry* **1996**, *271*, 23646–23649.

[33] Bourne, Y.; Radić, Z.; Kolb, H. C.; Sharpless, K. B.; Taylor, P.; Marchot, P. Structural insights into conformational flexibility at the peripheral site and within the active center gorge of AChE. *Chemico-biological interactions* **2005**, *157*, 159–165.

[34] Colletier, J. P.; Sanson, B.; Nachon, F.; Gabellieri, E.; Fattorusso, C.; Campiani, G.; Weik, M. Conformational Flexibility in the Peripheral Site of Torpedo c alifornica Acetylcholinesterase Revealed by the Complex Structure with a Bifunctional Inhibitor. *Journal of the American Chemical Society* **2006**, *128*, 4526–4527.

[35] Goyal, D.; Kaur, A.; Goyal, B. Benzofuran and indole: promising scaffolds for drug development in Alzheimer's disease. *ChemMedChem* **2018**, *13*, 1275–1299.

[36] Bolognesi, M. L.; Cavalli, A.; Valgimigli, L.; Bartolini, M.; Rosini, M.; Andrisano, V.; Recanatini, M.; Melchiorre, C. Multi-target-directed drug design strategy: from a dual binding site acetylcholinesterase inhibitor to a trifunctional compound against Alzheimer's disease. *Journal of medicinal chemistry* **2007**, *50*, 6446–6449.

[37] Nam, S. O.; Park, D. H.; Lee, Y. H.; Ryu, J. H.; Lee, Y. S. Synthesis of aminoalkyl-substituted coumarin derivatives as acetylcholinesterase inhibitors. *Bioorganic & medicinal chemistry* **2014**, *22*, 1262–1267.

[38] Tasso, B.; Catto, M.; Nicolotti, O.; Novelli, F.; Tonelli, M.; Giangreco, I.; Pisani, L.; Sparatore, A.; Boido, V.; Carotti, A., et al. Quinolizidinyl derivatives of bi-and tricyclic systems as potent inhibitors of acetyl-and butyrylcholinesterase with potential in Alzheimer's disease. *European journal of medicinal chemistry* **2011**, *46*, 2170–2184.

[39] Ece, A. Towards more effective acetylcholinesterase inhibitors: a comprehensive modelling study based on human acetylcholinesterase protein–drug complex. *Journal of Biomolecular Structure and Dynamics* **2020**, *38*, 565–572.

[40] Aziz-Aloya, R. B.; Seidman, S.; Timberg, R.; Sternfeld, M.; Zakut, H.; Soreq, H. Expression of a human acetylcholinesterase promoter-reporter construct in developing neuromuscular junctions of Xenopus embryos. *Proceedings of the National Academy of Sciences* **1993**, *90*, 2471–2475.

[41] Lane, R. M.; Potkin, S. G.; Enz, A. Targeting acetylcholinesterase and butyrylcholinesterase in dementia. *International Journal of Neuropsychopharmacology* **2006**, *9*, 101–124.

[42] Taylor, P.; Radic, Z. The cholinesterases: from genes to proteins. *Annual review of pharmacology and toxicology* **1994**, *34*, 281–320.

[43] Saxena, A.; Redman, A. M.; Jiang, X.; Lockridge, O.; Doctor, B. Differences in active site gorge dimensions of cholinesterases revealed by binding of inhibitors to human butyrylcholinesterase. *Biochemistry* **1997**, *36*, 14642–14651.

[44] Silver, A., et al. The biology of cholinesterases. **1974**,

[45] Perry, E. K.; Tomlinson, B. E.; Blessed, G.; Bergmann, K.; Gibson, P. H.; Perry, R. H. Correlation of cholinergic abnormalities with senile plaques and mental test scores in senile dementia. *Br Med J* **1978**, *2*, 1457–1459.

[46] Darvesh, S.; MacKnight, C.; Rockwood, K. Butyrylcholinesterase and cognitive function. *International psychogeriatrics* **2001**, *13*, 461.

[47] Macdonald, I. R.; Maxwell, S. P.; Reid, G. A.; Cash, M. K.; DeBay, D. R.; Darvesh, S. Quantification of butyrylcholinesterase activity as a sensitive and specific biomarker of Alzheimer's disease. *Journal of Alzheimer's Disease* **2017**, *58*, 491–505.

[48] Ballard, C. Advances in the treatment of Alzheimer's disease: benefits of dual cholinesterase inhibition. *European Neurology* **2002**, *47*, 64–70.

[49] Walker, L. C.; Ibegbu, C. C.; Todd, C. W.; Robinson, H. L.; Jucker, M.; LeVine III, H.; Gandy, S. Emerging prospects for the disease-modifying treatment of Alzheimer's disease. *Biochemical pharmacology* **2005**, *69*, 1001–1008.

[50] Hardy, J. A.; Higgins, G. A. Alzheimer's disease: the amyloid cascade hypothesis. *Science* **1992**, *256*, 184–186.

[51] Hardy, J.; Allsop, D. Amyloid deposition as the central event in the aetiology of Alzheimer's disease. *Trends in pharmacological sciences* **1991**, *12*, 383–388.

[52] Levy-Lahad, E.; Wasco, W.; Poorkaj, P.; Romano, D. M.; Oshima, J.; Pettingell, W. H.; Yu, C.-e.; Jondro, P. D.; Schmidt, S. D.; Wang, K., et al. Candidate gene for the chromosome 1 familial Alzheimer's disease locus. *Science* **1995**, *269*, 973–977.

[53] Sherrington, R.; Rogaev, E.; Liang, Y. a.; Rogaeva, E.; Levesque, G.; Ikeda, M.; Chi, H.; Lin, C.; Li, G.; Holman, K., et al. Cloning of a gene bearing missense mutations in early-onset familial Alzheimer's disease. *Nature* **1995**, *375*, 754–760.

[54] Wisniewski, K.; Wisniewski, H.; Wen, G. Occurrence of neuropathological changes and dementia of Alzheimer's disease in Down's syndrome. *Annals of Neurology: Official Journal of the American Neurological Association and the Child Neurology Society* **1985**, *17*, 278–282.

[55] Lott, I. T.; Head, E. Alzheimer disease and Down syndrome: factors in pathogenesis. *Neurobiology of aging* **2005**, *26*, 383–389.

[56] Bitan, G.; Kirkitadze, M. D.; Lomakin, A.; Vollers, S. S.; Benedek, G. B.; Teplow, D. B. Amyloid β-protein (Aβ) assembly: Aβ40 and Aβ42 oligomerize through distinct pathways. *Proceedings of the National Academy of Sciences* **2003**, *100*, 330–335.

[57] Jiang, N.; Wang, X.-B.; Li, Z.-R.; Li, S.-Y.; Xie, S.-S.; Huang, M.; Kong, L.-Y. Design of a structural framework with potential use to develop balanced multifunctional agents against Alzheimer's disease. *RSC advances* **2015**, *5*, 14242–14255.

[58] Honig, L. S.; Vellas, B.; Woodward, M.; Boada, M.; Bullock, R.; Borrie, M.; Hager, K.; Andreasen, N.; Scarpini, E.; Liu-Seifert, H., et al. Trial of solanezumab for mild dementia due to Alzheimer's disease. *New England Journal of Medicine* **2018**, *378*, 321–330.

[59] Tayeb, H. O.; Murray, E. D.; Price, B. H.; Tarazi, F. I. Bapineuzumab and solanezumab for Alzheimer's disease: is the 'amyloid cascade hypothesis' still alive? *Expert opinion on biological therapy* **2013**, *13*, 1075–1084.

[60] Vassar, R.; Bennett, B. D.; Babu-Khan, S.; Kahn, S.; Mendiaz, E. A.; Denis, P.; Teplow, D. B.; Ross, S.; Amarante, P.; Loeloff, R., et al. β-Secretase cleavage of Alzheimer's amyloid precursor protein by the transmembrane aspartic protease BACE. *science* **1999**, *286*, 735–741.

[61] Albert, J. S. *Progress in medicinal chemistry*; Elsevier, 2009; Vol. 48; pp 133–161.

[62] De Ferrari, G. V.; Canales, M. A.; Shin, I.; Weiner, L. M.; Silman, I.; Inestrosa, N. C. A structural motif of acetylcholinesterase that promotes amyloid β-peptide fibril formation. *Biochemistry* **2001**, *40*, 10447–10457.

[63] Alvarez, A.; Opazo, C.; Alarcón, R.; Garrido, J.; Inestrosa, N. C. Acetylcholinesterase promotes the aggregation of amyloid-β-peptide fragments by forming a complex with the growing fibrils. *Journal of molecular biology* **1997**, *272*, 348–361.

[64] Inestrosa, N. C.; Alvarez, A.; Perez, C. A.; Moreno, R. D.; Vicente, M.; Linker, C.; Casanueva, O. I.; Soto, C.; Garrido, J. Acetylcholinesterase accelerates assembly of amyloid-β-peptides into Alzheimer's fibrils: possible role of the peripheral site of the enzyme. *Neuron* **1996**, *16*, 881–891.

[65] Toiber, D.; Berson, A.; Greenberg, D.; Melamed-Book, N.; Diamant, S.; Soreq, H. N-acetylcholinesterase-induced apoptosis in Alzheimer's disease. *PloS one* **2008**, *3*, e3108.

[66] Inestrosa, N. C.; Dinamarca, M. C.; Alvarez, A. Amyloid–cholinesterase interactions: implications for Alzheimer's disease. *The FEBS journal* **2008**, *275*, 625–632.

[67] Gaweska, H.; Fitzpatrick, P. F. Structures and mechanism of the monoamine oxidase family. *Biomolecular concepts* **2011**, *2*, 365–377.

[68] Shih, J.; Chen, K.; Ridd, M. Monoamine oxidase: from genes to behavior. *Annual review of neuroscience* **1999**, *22*, 197–217.

[69] Shih, J.; Chen, K. Regulation of MAO-A and MAO-B gene expression. *Current medicinal chemistry* **2004**, *11*, 1995–2005.

[70] Cases, O.; Seif, I.; Grimsby, J.; Gaspar, P.; Chen, K.; Pournin, S.; Muller, U.; Aguet, M.; Babinet, C.; Shih, J. C., et al. Aggressive behavior and altered amounts of brain serotonin and norepinephrine in mice lacking MAOA. *Science* **1995**, *268*, 1763–1766.

[71] Bortolato, M.; Chen, K.; Shih, J. C. Monoamine oxidase inactivation: from pathophysiology to therapeutics. *Advanced drug delivery reviews* **2008**, *60*, 1527–1533.

[72] Baldessarini, R. J. Current status of antidepressants: clinical pharmacology and therapy. *The Journal of clinical psychiatry* **1989**,

[73] Foley, P.; Gerlach, M.; Youdim, M.; Riederer, P. MAO-B inhibitors: multiple roles in the therapy of neurodegenerative disorders? *Parkinsonism & related disorders* **2000**, *6*, 25–47.

[74] Mangoni, A.; Grassi, M.; Frattola, L.; Piolti, R.; Bassi, S.; Motta, A.; Marcone, A.; Smirne, S. Effects of a MAO-B inhibitor in the treatment of Alzheimer disease. *European neurology* **1991**, *31*, 100–107.

[75] Oreland, L.; Gottfries, C.-G. Brain and brain monoamine oxidase in aging and in dementia of Alzheimer's type. *Progress in Neuro-Psychopharmacology and Biological Psychiatry* **1986**, *10*, 533–540.

[76] Fowler, J.; Volkow, N.; Wang, G.-J.; Logan, J.; Pappas, N.; Shea, C.; MacGregor, R. Age-related increases in brain monoamine oxidase B in living healthy human subjects. *Neurobiology of aging* **1997**, *18*, 431–435.

[77] Heinonen, E.; Lammintausta, R. A review of the pharmacology of selegiline. *Acta Neurologica Scandinavica* **1991**, *84*, 44–59.

[78] Maruyama, W.; Weinstock, M.; Youdim, M. B.; Nagai, M.; Naoi, M. Anti-apoptotic action of anti-Alzheimer drug, TV3326 [(N-propargyl)-(3R)-aminoindan-5-yl]-ethyl methyl carbamate, a novel cholinesterase-monoamine oxidase inhibitor. *Neuroscience letters* **2003**, *341*, 233–236.

[79] Schedin-Weiss, S.; Inoue, M.; Hromadkova, L.; Teranishi, Y.; Yamamoto, N. G.; Wiehager, B.; Bogdanovic, N.; Winblad, B.; Sandebring-Matton, A.; Frykman, S., et al. Monoamine oxidase B is elevated in Alzheimer disease neurons, is associated with γ-secretase and regulates neuronal amyloid β-peptide levels. *Alzheimer's research & therapy* **2017**, *9*, 1–19.

[80] Heneka, M. T.; Carson, M. J.; El Khoury, J.; Landreth, G. E.; Brosseron, F.; Feinstein, D. L.; Jacobs, A. H.; Wyss-Coray, T.; Vitorica, J.; Ransohoff, R. M., et al. Neuroinflammation in Alzheimer's disease. *The Lancet Neurology* **2015**, *14*, 388–405.

[81] Swerdlow, R. H. Mitochondria and mitochondrial cascades in Alzheimer's disease. *Journal of Alzheimer's Disease* **2018**, *62*, 1403–1416.

[82] Oshiro, S.; Morioka, M. S.; Kikuchi, M. Dysregulation of iron metabolism in Alzheimer's disease, Parkinson's disease, and amyotrophic lateral sclerosis. *Advances in pharmacological sciences* **2011**, *2011*.

[83] Workgroup, A. A. C. H.; Khachaturian, Z. S. Calcium hypothesis of Alzheimer's disease and brain aging: a framework for integrating new evidence into a comprehensive theory of pathogenesis. *Alzheimer's & Dementia* **2017**, *13*, 178–182.

[84] Markesbery, W. R. Oxidative stress hypothesis in Alzheimer's disease. *Free Radical Biology and Medicine* **1997**, *23*, 134–147.

[85] Bush, A. I.; Tanzi, R. E. Therapeutics for Alzheimer's disease based on the metal hypothesis. *Neurotherapeutics* **2008**, *5*, 421–432.

[86] Carmo Carreiras, M.; Mendes, E.; Jesus Perry, M.; Paula Francisco, A.; Marco-Contelles, J. The multifactorial nature of Alzheimer's disease for developing potential therapeutics. *Current topics in medicinal chemistry* **2013**, *13*, 1745–1770.

[87] Morphy, R.; Kay, C.; Rankovic, Z. From magic bullets to designed multiple ligands. *Drug discovery today* **2004**, *9*, 641–651.

[88] Gong, C.-X.; Liu, F.; Iqbal, K. Multifactorial hypothesis and multi-targets for Alzheimer's disease. *Journal of Alzheimer's Disease* **2018**, *64*, S107–S117.

[89] Viegas-Junior, C.; Danuello, A.; da Silva Bolzani, V.; Barreiro, E. J.; Fraga, C. A. M. Molecular hybridization: a useful tool in the design of new drug prototypes. *Current medicinal chemistry* **2007**, *14*, 1829–1852.

[90] González, J. F.; Alcántara, A. R.; Doadrio, A. L.; Sánchez-Montero, J. M. Developments with multi-target drugs for Alzheimer's disease: an overview of the current discovery approaches. *Expert opinion on drug discovery* **2019**, *14*, 879–891.

[91] Oset-Gasque, M. J.; Marco-Contelles, J. Alzheimer's disease, the "one-molecule, one-target" paradigm, and the multitarget directed ligand approach. 2018.

[92] Talevi, A. Multi-target pharmacology: possibilities and limitations of the "skeleton key approach" from a medicinal chemist perspective. *Frontiers in pharmacology* **2015**, *6*, 205.

[93] Cavalli, A.; Bolognesi, M. L.; Minarini, A.; Rosini, M.; Tumiatti, V.; Recanatini, M.; Melchiorre, C. Multi-target-directed ligands to combat neurodegenerative diseases. *Journal of medicinal chemistry* **2008**, *51*, 347–372.

[94] Bolognesi, M. L.; Minarini, A.; Rosini, M.; Tumiatti, V.; Melchiorre, C. From dual binding site acetylcholinesterase inhibitors to multi-target-directed ligands (MTDLs): a step forward in the treatment of Alzheimer's disease. *Mini reviews in medicinal chemistry* **2008**, *8*, 960–967.

[95] Guzior, N.; Wieckowska, A.; Panek, D.; Malawska, B. Recent development of multifunctional agents as potential drug candidates for the treatment of Alzheimer's disease. *Current medicinal chemistry* **2015**, *22*, 373–404.

[96] Sharma, P.; Srivastava, P.; Seth, A.; Tripathi, P. N.; Banerjee, A. G.; Shrivastava, S. K. Comprehensive review of mechanisms of pathogenesis involved in Alzheimer's disease and potential therapeutic strategies. *Progress in neurobiology* **2019**, *174*, 53–89.

[97] dos Santos, P.; Leide, C.; Ozela, P. F.; de Fatima de Brito Brito, M.; Pinheiro, A. A.; Padilha, E. C.; Braga, F. S.; de Paula, d. S.; Carlos, H.; dos Santos, C. B. R., et al. Alzheimer's disease: a review from the pathophysiology to diagnosis, new perspectives for pharmacological treatment. *Current medicinal chemistry* **2018**, *25*, 3141–3159.

[98] Sameem, B.; Saeedi, M.; Mahdavi, M.; Shafiee, A. A review on tacrine-based scaffolds as multi-target drugs (MTDLs) for Alzheimer's disease. *European journal of medicinal chemistry* **2017**, *128*, 332–345.

[99] Mathew, B.; Parambi, D. G.; Mathew, G. E.; Uddin, M. S.; Inasu, S. T.; Kim, H.; Marathakam, A.; Unnikrishnan, M. K.; Carradori, S. Emerging therapeutic potentials of dual-acting MAO and AChE inhibitors in Alzheimer's and Parkinson's diseases. *Archiv der Pharmazie* **2019**, *352*, 1900177.

[100] Jalili-Baleh, L.; Babaei, E.; Abdpour, S.; Bukhari, S. N. A.; Foroumadi, A.; Ramazani, A.; Sharifzadeh, M.; Abdollahi, M.; Khoobi, M. A review on flavonoid-based scaffolds as multi-target-directed ligands (MTDLs) for Alzheimer's disease. *European journal of medicinal chemistry* **2018**, *152*, 570–589.

[101] Anand, P.; Singh, B.; Singh, N. A review on coumarins as acetylcholinesterase inhibitors for Alzheimer's disease. *Bioorganic & medicinal chemistry* **2012**, *20*, 1175–1180.

[102] O'Reilly, R. A.; Aggeler, P. M.; Hoag, M. S.; Leong, L. Studies on the coumarin anticoagulant drugs: the assay of warfarin and its biologic application. *Thrombosis and Haemostasis* **1962**, *8*, 082–095.

[103] Kostova, I.; Bhatia, S.; Grigorov, P.; Balkansky, S.; S Parmar, V.; K Prasad, A.; Saso, L. Coumarins as antioxidants. *Current medicinal chemistry* **2011**, *18*, 3929–3951.

[104] Parvatkar, P.; Tilve, S. *Bioactivities and synthesis of indoloquinoline alkaloids: cryptolepine, isocryptolepine and neocryptolepine*; Nova Science Publishers, New York, 2012.

[105] T Parvatkar, P.; S Parameswaran, P.; G Tilve, S. Isolation, biological activities and synthesis of indoloquinoline alkaloids: cryptolepine, isocryptolepine and neocryptolepine. *Current Organic Chemistry* **2011**, *15*, 1036–1057.

[106] Bozorov, K.; Zhao, J.; Aisa, H. A. 1, 2, 3-Triazole-containing hybrids as leads in medicinal chemistry: A recent overview. *Bioorganic & medicinal chemistry* **2019**, *27*, 3511–3531.

[107] Li, J.-C.; Zhang, J.; Rodrigues, M. C.; Ding, D.-J.; Longo, J. P. F.; Azevedo, R. B.; Muehlmann, L. A.; Jiang, C.-S. Synthesis and evaluation of novel 1, 2, 3-triazole-based acetylcholinesterase inhibitors with neuroprotective activity. *Bioorganic & Medicinal Chemistry Letters* **2016**, *26*, 3881–3885.

[108] Albert, A.; Gledhill, W. Improved syntheses of aminoacridines. Part IV. Substituted 5-aminoacridines. *J. Soc. Chem. Ind* **1945**, *44*, 169–172.

[109] Albert, A.; Royer, R. 245. Acridine syntheses and reactions. Part V. A new dehalogenation of 5-chloroacridine and its derivatives. *Journal of the Chemical Society (Resumed)* **1949**, 1148–1151.

[110] Shaw, F.; Bentley, G. The pharmacology of some new anti-cholinesterases. *Australian Journal of Experimental Biology & Medical Science* **1953**, *31*.

[111] Thomsen, T.; Zendeh, B.; Fischer, J.; Kewitz, H. In vitro effects of various cholinesterase inhibitors on acetyl-and butyrylcholinesterase of healthy volunteers. *Biochemical pharmacology* **1991**, *41*, 139–141.

[112] Summers, W. K.; Majovski, L. V.; Marsh, G. M.; Tachiki, K.; Kling, A. Oral tetrahydroaminoacridine in long-term treatment of senile dementia, Alzheimer type. *New England Journal of Medicine* **1986**, *315*, 1241–1245.

[113] Crismon, M. L. Tacrine: first drug approved for Alzheimer's disease. *Annals of Pharmacotherapy* **1994**, *28*, 744–751.

[114] Watkins, P. B.; Zimmerman, H. J.; Knapp, M. J.; Gracon, S. I.; Lewis, K. W. Hepatotoxic effects of tacrine administration in patients with Alzheimer's disease. *Jama* **1994**, *271*, 992–998.

[115] Osseni, R.; Debbasch, C.; Christen, M.-O.; Rat, P.; Warnet, J.-M. Tacrine-induced reactive oxygen species in a human liver cell line: the role of anethole dithiolethione as a scavenger. *Toxicology in vitro* **1999**, *13*, 683–688.

[116] Woltjer, R. L.; Milatovic, D. *Toxicology of Organophosphate & Carbamate Compounds*; Elsevier, 2006; pp 25–33.

[117] Wu, W.-Y.; Dai, Y.-C.; Li, N.-G.; Dong, Z.-X.; Gu, T.; Shi, Z.-H.; Xue, X.; Tang, Y.-P.; Duan, J.-A. Novel multitarget-directed tacrine derivatives as potential candidates for the treatment of Alzheimer's disease. *Journal of enzyme inhibition and medicinal chemistry* **2017**, *32*, 572–587.

[118] Roldan-Pena, J. M.; Romero-Real, V.; Hicke, J.; Maya, I.; Franconetti, A.; Lagunes, I.; Padron, J. M.; Petralla, S.; Poeta, E.; Naldi, M., et al. Tacrine-O-protected phenolics heterodimers as multitarget-directed ligands against Alzheimer's disease: Selective subnanomolar BuChE inhibitors. *European journal of medicinal chemistry* **2019**, *181*, 111550.

[119] Chen, Y.; Sun, J.; Huang, Z.; Liao, H.; Peng, S.; Lehmann, J.; Zhang, Y. Design, synthesis and evaluation of tacrine–flurbiprofen–nitrate trihybrids as novel anti-Alzheimer's disease agents. *Bioorganic & medicinal chemistry* **2013**, *21*, 2462–2470.

[120] Cen, J.; Guo, H.; Hong, C.; Lv, J.; Yang, Y.; Wang, T.; Fang, D.; Luo, W.; Wang, C. Development of tacrine-bifendate conjugates with improved cholinesterase inhibitory and pro-cognitive efficacy and reduced hepatotoxicity. *European Journal of Medicinal Chemistry* **2018**, *144*, 128–136.

[121] Chen, Y.; Sun, J.; Fang, L.; Liu, M.; Peng, S.; Liao, H.; Lehmann, J.; Zhang, Y. Tacrine–ferulic acid–nitric oxide (NO) donor trihybrids as potent, multifunctional acetyl-and butyrylcholinesterase inhibitors. *Journal of medicinal chemistry* **2012**, *55*, 4309–4321.

[122] Girek, M.; Szymański, P. Tacrine hybrids as multi-target-directed ligands in Alzheimer's disease: influence of chemical structures on biological activities. *Chemical Papers* **2019**, *73*, 269–289.

[123] Tumiatti, V.; Minarini, A.; Bolognesi, M.; Milelli, A.; Rosini, M.; Melchiorre, C. Tacrine derivatives and Alzheimer's disease. *Current medicinal chemistry* **2010**, *17*, 1825–1838.

[124] Romero, A.; Cacabelos, R.; Oset-Gasque, M. J.; Samadi, A.; Marco-Contelles, J. Novel tacrine-related drugs as potential candidates for the treatment of Alzheimer's disease. *Bioorganic & medicinal chemistry letters* **2013**, *23*, 1916–1922.

[125] Wang, L.; Moraleda, I.; Iriepa, I.; Romero, A.; López-Muñoz, F.; Chioua, M.; Inokuchi, T.; Bartolini, M.; Marco-Contelles, J. 5-Methyl-N-(8-(5, 6, 7, 8-tetrahydroacridin-9-ylamino) octyl)-5 H-indolo [2, 3-b] quinolin-11-amine: a highly potent human cholinesterase inhibitor. *MedChemComm* **2017**, *8*, 1307–1317.

[126] Zha, X.; Lamba, D.; Zhang, L.; Lou, Y.; Xu, C.; Kang, D.; Chen, L.; Xu, Y.; Zhang, L.; De Simone, A., et al. Novel tacrine–benzofuran hybrids as potent multitarget-directed ligands for the treatment of Alzheimer's disease: design, synthesis, biological evaluation, and X-ray crystallography. *Journal of Medicinal Chemistry* **2016**, *59*, 114–131.

[127] Rydberg, E. H.; Brumshtein, B.; Greenblatt, H. M.; Wong, D. M.; Shaya, D.; Williams, L. D.; Carlier, P. R.; Pang, Y.-P.; Silman, I.; Sussman, J. L. Complexes of Alkylene-linked Tacrine dimers with Torpedo c alifornica acetylcholinesterase: Binding of Bis (5)-tacrine produces a dramatic rearrangement in the active-site gorge. *Journal of medicinal chemistry* **2006**, *49*, 5491–5500.

[128] Costa, J. S. d.; Pisoni, D. S.; Silva, C. B. d.; Petzhold, C. L.; Russowsky, D.; Ceschi, M. A. Lewis acid promoted Friedländer condensation reactions between anthranilonitrile and ketones for the synthesis of tacrine and its analogues. *Journal of the Brazilian Chemical Society* **2009**, *20*, 1448–1454.

[129] Proctor, G.; Harvey, A. Synthesis of tacrine analogues and their structure-activity relationships. *Current medicinal chemistry* **2000**, *7*, 295–302.

[130] Nikseresht, A.; Ghasemi, S.; Parak, S. [Cu3 (BTC) 2]: A metal–organic framework as an environment-friendly and economically catalyst for the synthesis of tacrine analogues by Friedländer reaction under conventional and ultrasound irradiation. *Polyhedron* **2018**, *151*, 112–117.

[131] McKenna, M. T.; Proctor, G. R.; Young, L. C.; Harvey, A. L. Novel tacrine analogues for potential use against Alzheimer's disease: potent and selective acetylcholinesterase inhibitors and 5-HT uptake inhibitors. *Journal of medicinal chemistry* **1997**, *40*, 3516–3523.

[132] Xie, S.-S.; Wang, X.-B.; Li, J.-Y.; Yang, L.; Kong, L.-Y. Design, synthesis and evaluation of novel tacrine–coumarin hybrids as multifunctional cholinesterase inhibitors against Alzheimer's disease. *European journal of medicinal chemistry* **2013**, *64*, 540–553.

[133] Scheiner, M.; Dolles, D.; Gunesch, S.; Hoffmann, M.; Nabissi, M.; Marinelli, O.; Naldi, M.; Bartolini, M.; Petralla, S.; Poeta, E., et al. Dual-Acting Cholinesterase–Human Cannabinoid Receptor 2 Ligands Show Pronounced Neuroprotection in Vitro and Overadditive and Disease-Modifying Neuroprotective Effects in Vivo. *Journal of medicinal chemistry* **2019**, *62*, 9078–9102.

[134] Pan, T.; Xie, S.; Zhou, Y.; Hu, J.; Luo, H.; Li, X.; Huang, L. Dual functional cholinesterase and PDE4D inhibitors for the treatment of Alzheimer's disease: Design, synthesis and evaluation of tacrine-pyrazolo [3, 4-b] pyridine hybrids. *Bioorganic & medicinal chemistry letters* **2019**, *29*, 2150–2152.

[135] Oukoloff, K.; Coquelle, N.; Bartolini, M.; Naldi, M.; Le Guével, R.; Bach, S.; Josselin, B.; Ruchaud, S.; Catto, M.; Pisani, L., et al. Design, biological evaluation and X-ray crystallography of nanomolar multifunctional ligands targeting simultaneously acetylcholinesterase and glycogen synthase kinase-3. *European journal of medicinal chemistry* **2019**, *168*, 58–77.

[136] Wieckowska, A.; Wichur, T.; Godyn, J.; Bucki, A.; Marcinkowska, M.; Siwek, A.; Wieckowski, K.; Zareba, P.; Knez, D.; Gluch-Lutwin, M., et al. Novel multitarget-directed ligands aiming at symptoms and causes of Alzheimer's disease. *ACS chemical neuroscience* **2018**, *9*, 1195–1214.

[137] Marco-Contelles, J.; Pérez-Mayoral, E.; Samadi, A.; Carreiras, M. d. C.; Soriano, E. Recent advances in the Friedlander reaction. *Chemical reviews* **2009**, *109*, 2652–2671.

[138] Vogel, A. Darstellung von Benzoesäure aus der Tonka-Bohne und aus den Meliloten- oder Steinklee-Blumen. *Annalen der Physik* **1820**, *64*, 161–166.

[139] Kontogiorgis, C.; Detsi, A.; Hadjipavlou-Litina, D. Coumarin-based drugs: a patent review (2008–present). *Expert opinion on therapeutic patents* **2012**, *22*, 437–454.

[140] Fylaktakidou, K. C.; Hadjipavlou-Litina, D. J.; Litinas, K. E.; Nicolaides, D. N. Natural and synthetic coumarin derivatives with anti-inflammatory/antioxidant activities. *Current pharmaceutical design* **2004**, *10*, 3813–3833.

[141] de Souza, S. M.; Delle Monache, F.; Smânia, A. Antibacterial activity of coumarins. *Zeitschrift fuer Naturforschung C* **2005**, *60*, 693–700.

[142] Ito, C.; Itoigawa, M.; Onoda, S.; Hosokawa, A.; Ruangrungsi, N.; Okuda, T.; Tokuda, H.; Nishino, H.; Furukawa, H. Chemical constituents of Murraya siamensis: three coumarins and their anti-tumor promoting effect. *Phytochemistry* **2005**, *66*, 567–572.

[143] MacLeod, S.; Sellers, E. Pharmacodynamic and pharmacokinetic drug interactions with coumarin anticoagulants. *Drugs* **1976**, *11*, 461–470.

[144] Zaid, H.; Raiyn, J.; Nasser, A.; Saad, B.; Rayan, A. Physicochemical properties of natural based products versus synthetic chemicals. *The Open Nutraceuticals Journal* **2010**, *3*.

[145] Piazzi, L.; Cavalli, A.; Colizzi, F.; Belluti, F.; Bartolini, M.; Mancini, F.; Recanatini, M.; Andrisano, V.; Rampa, A. Multi-target-directed coumarin derivatives: hAChE and BACE1 inhibitors as potential anti-Alzheimer compounds. *Bioorganic & medicinal chemistry letters* **2008**, *18*, 423–426.

[146] Zhou, X.; Wang, X.-B.; Wang, T.; Kong, L.-Y. Design, synthesis, and acetylcholinesterase inhibitory activity of novel coumarin analogues. *Bioorganic & medicinal chemistry* **2008**, *16*, 8011–8021.

[147] Brühlmann, C.; Ooms, F.; Carrupt, P.-A.; Testa, B.; Catto, M.; Leonetti, F.; Altomare, C.; Carotti, A. Coumarins derivatives as dual inhibitors of acetylcholinesterase and monoamine oxidase. *Journal of Medicinal Chemistry* **2001**, *44*, 3195–3198.

[148] Radić, Z.; Reiner, E.; Taylor, P. Role of the peripheral anionic site on acetylcholinesterase: inhibition by substrates and coumarin derivatives. *Molecular pharmacology* **1991**, *39*, 98–104.

[149] Soto-Ortega, D. D.; Murphy, B. P.; Gonzalez-Velasquez, F. J.; Wilson, K. A.; Xie, F.; Wang, Q.; Moss, M. A. Inhibition of amyloid-β aggregation by coumarin analogs can be manipulated by functionalization of the aromatic center. *Bioorganic & medicinal chemistry* **2011**, *19*, 2596–2602.

[150] Abdelhafez, O. M.; Amin, K. M.; Ali, H. I.; Abdalla, M. M.; Batran, R. Z. Monoamine oxidase A and B inhibiting effect and molecular modeling of some synthesized coumarin derivatives. *Neurochemistry international* **2013**, *62*, 198–209.

[151] Gnerre, C.; Catto, M.; Leonetti, F.; Weber, P.; Carrupt, P.-A.; Altomare, C.; Carotti, A.; Testa, B. Inhibition of monoamine oxidases by functionalized coumarin derivatives: biological activities, QSARs, and 3D-QSARs. *Journal of medicinal chemistry* **2000**, *43*, 4747–4758.

[152] Rendenbach-Müller, B.; Schlecker, R.; Traut, M.; Weifenbach, H. Synthesis of coumarins as subtype-selective inhibitors of monoamine oxidase. *Bioorganic & Medicinal Chemistry Letters* **1994**, *4*, 1195–1198.

[153] Chimenti, F.; Secci, D.; Bolasco, A.; Chimenti, P.; Bizzarri, B.; Granese, A.; Carradori, S.; Yánez, M.; Orallo, F.; Ortuso, F., et al. Synthesis, molecular modeling, and selective inhibitory activity against human monoamine oxidases of 3-carboxamido-7-substituted coumarins. *Journal of medicinal chemistry* **2009**, *52*, 1935–1942.

[154] Catto, M.; Nicolotti, O.; Leonetti, F.; Carotti, A.; Favia, A. D.; Soto-Otero, R.; Méndez-Álvarez, E.; Carotti, A. Structural insights into monoamine oxidase inhibitory potency and selectivity of 7-substituted coumarins from ligand-and target-based approaches. *Journal of medicinal chemistry* **2006**, *49*, 4912–4925.

[155] Marumoto, S.; Miyazawa, M. Structure–activity relationships for naturally occurring coumarins as β-secretase inhibitor. *Bioorganic & medicinal chemistry* **2012**, *20*, 784–788.

[156] Garino, C.; Tomita, T.; Pietrancosta, N.; Laras, Y.; Rosas, R.; Herbette, G.; Maigret, B.; Quéléver, G.; Iwatsubo, T.; Kraus, J.-L. Naphthyl and coumarinyl biarylpiperazine derivatives as highly potent human β-secretase inhibitors. Design, synthesis, and enzymatic BACE-1 and cell assays. *Journal of medicinal chemistry* **2006**, *49*, 4275–4285.

[157] Garino, C.; Pietrancosta, N.; Laras, Y.; Moret, V.; Rolland, A.; Quéléver, G.; Kraus, J.-L. BACE-1 inhibitory activities of new substituted phenyl-piperazine coupled to various heterocycles: chromene, coumarin and quinoline. *Bioorganic & medicinal chemistry letters* **2006**, *16*, 1995–1999.

[158] He, Q.; Liu, J.; Lan, J.-S.; Ding, J.; Sun, Y.; Fang, Y.; Jiang, N.; Yang, Z.; Sun, L.; Jin, Y., et al. Coumarin-dithiocarbamate hybrids as novel multitarget AChE and MAO-B inhibitors against Alzheimer's disease: Design, synthesis and biological evaluation. *Bioorganic Chemistry* **2018**, *81*, 512–528.

[159] Heravi, M. M.; Khaghaninejad, S.; Mostofi, M. *Advances in heterocyclic chemistry*; Elsevier, 2014; Vol. 112; pp 1–50.

[160] Vekariya, R. H.; Patel, H. D. Recent advances in the synthesis of coumarin derivatives via knoevenagel condensation: A review. *Synthetic Communications* **2014**, *44*, 2756–2788.

[161] Liu, Y.-Y.; Thom, E.; Liebman, A. A. Coumarins via the wittig reaction. Synthesis of methoxsalen-5-14C. *Journal of Heterocyclic Chemistry* **1979**, *16*, 799–801.

[162] Murray, R.; Ballantyne, M. Claisen rearrangements—I: Synthesis of the coumarin, pinnarin. *Tetrahedron* **1970**, *26*, 4667–4671.

[163] Patel, H. S.; Patel, S. R. Coumarin polymers derived from salicylaldehyde-formaldehyde polymer. *Journal of Macromolecular Science—Chemistry* **1984**, *21*, 343–352.

[164] Drewes, S. E.; Njamela, O. L.; Emslie, N. D.; Ramesar, N.; Field, J. S. Intramolecular Baylis-Hillman reaction: a pathway to substituted coumarins. *Synthetic communications* **1993**, *23*, 2807–2815.

[165] Osman, H.; Arshad, A.; Lam, C. K.; Bagley, M. C. Microwave-assisted synthesis and antioxidant properties of hydrazinyl thiazolyl coumarin derivatives. *Chemistry Central Journal* **2012**, *6*, 32.

[166] Harishkumar, H. N.; Mahadevan, K. M.; Kumar, H. C. K.; Satyanarayan, N. D. A facile, choline chloride/urea catalyzed solid phase synthesis of coumarins via Knoevenagel condensation. *Organic Communications* **2011**, *4*, 26.

[167] Potdar, M. K.; Mohile, S. S.; Salunkhe, M. M. Coumarin syntheses via Pechmann condensation in Lewis acidic chloroaluminate ionic liquid. *Tetrahedron Letters* **2001**, *42*, 9285–9287.

[168] Bose, D. S.; Rudradas, A.; Babu, M. H. The indium (III) chloride-catalyzed von Pechmann reaction: a simple and effective procedure for the synthesis of 4-substituted coumarins. *Tetrahedron Letters* **2002**, *43*, 9195–9197.

[169] Pisani, L.; Muncipinto, G.; Miscioscia, T. F.; Nicolotti, O.; Leonetti, F.; Catto, M.; Caccia, C.; Salvati, P.; Soto-Otero, R.; Mendez-Alvarez, E., et al. Discovery of a novel class of potent coumarin monoamine oxidase B inhibitors: development and biopharmacological profiling of 7-[(3-chlorobenzyl) oxy]-4-[(methylamino) methyl]-2 H-chromen-2-one methanesulfonate (NW-1772) as a highly potent, selective, reversible, and orally active monoamine oxidase B inhibitor. *Journal of medicinal chemistry* **2009**, *52*, 6685–6706.

[170] Zak, J.; Ron, D.; Riva, E.; Harding, H. P.; Cross, B. C.; Baxendale, I. R. Establishing a Flow Process to Coumarin-8-Carbaldehydes as Important Synthetic Scaffolds. *Chemistry–A European Journal* **2012**, *18*, 9901–9910.

[171] Lan, J.-S.; Ding, Y.; Liu, Y.; Kang, P.; Hou, J.-W.; Zhang, X.-Y.; Xie, S.-S.; Zhang, T. Design, synthesis and biological evaluation of novel coumarin-N-benzyl pyridinium hybrids as multi-target agents for the treatment of Alzheimer's disease. *European Journal of Medicinal Chemistry* **2017**, *139*, 48–59.

[172] Xie, S.-S.; Wang, X.; Jiang, N.; Yu, W.; Wang, K. D.; Lan, J.-S.; Li, Z.-R.; Kong, L.-Y. Multi-target tacrine-coumarin hybrids: cholinesterase and monoamine oxidase B inhibition properties against Alzheimer's disease. *European Journal of Medicinal Chemistry* **2015**, *95*, 153–165.

[173] Jiang, N.; Huang, Q.; Liu, J.; Liang, N.; Li, Q.; Li, Q.; Xie, S.-S. Design, synthesis and biological evaluation of new coumarin-dithiocarbamate hybrids as multifunctional agents for the treatment of Alzheimer's disease. *European journal of medicinal chemistry* **2018**, *146*, 287–298.

[174] Lavrado, J.; Moreira, R.; Paulo, A. Indoloquinolines as scaffolds for drug discovery. *Current medicinal chemistry* **2010**, *17*, 2348–2370.

[175] Paulo, A.; Gomes, E. T.; Steele, J.; Warhurst, D. C.; Houghton, P. J. Antiplasmodial activity of Cryptolepis sanguinolenta alkaloids from leaves and roots. *Planta medica* **2000**, *66*, 30–34.

[176] Oliver-Bever, B. *Medicinal plants in tropical West Africa*; Cambridge university press, 1986.

[177] Konrath, E. L.; Passos, C. d. S.; Klein-Júnior, L. C.; Henriques, A. T. Alkaloids as a source of potential anticholinesterase inhibitors for the treatment of A lzheimer's disease. *Journal of Pharmacy and Pharmacology* **2013**, *65*, 1701–1725.

[178] Bongarzone, S.; Bolognesi, M. L. The concept of privileged structures in rational drug design: focus on acridine and quinoline scaffolds in neurodegenerative and protozoan diseases. *Expert opinion on drug discovery* **2011**, *6*, 251–268.

[179] Nuthakki, V. K.; Mudududdla, R.; Sharma, A.; Kumar, A.; Bharate, S. B. Synthesis and biological evaluation of indoloquinoline alkaloid cryptolepine and its bromo-derivative as dual cholinesterase inhibitors. *Bioorganic Chemistry* **2019**, *90*, 103062.

[180] Hartz, A. M.; Miller, D. S.; Bauer, B. Restoring blood-brain barrier P-glycoprotein reduces brain amyloid-β in a mouse model of Alzheimer's disease. *Molecular pharmacology* **2010**, *77*, 715–723.

[181] Brohm, D.; Metzger, S.; Bhargava, A.; Müller, O.; Lieb, F.; Waldmann, H. Natural products are biologically validated starting points in structural space for compound library development: solid-phase synthesis of dysidiolide-derived phosphatase inhibitors. *Angewandte Chemie International Edition* **2002**, *41*, 307–311.

[182] Chen, X.; Decker, M. Multi-target compounds acting in the central nervous system designed from natural products. *Current medicinal chemistry* **2013**, *20*, 1673–1685.

[183] Paterson, I.; Anderson, E. A. The renaissance of natural products as drug candidates. *Science* **2005**, *310*, 451–453.

[184] Dhanabal, T.; Sangeetha, R.; Mohan, P. Heteroatom directed photoannulation: synthesis of indoloquinoline alkaloids: cryptolepine, cryptotackieine, cryptosanguinolentine, and their methyl derivatives. *Tetrahedron* **2006**, *62*, 6258–6263.

[185] Agarwal, P. K.; Sawant, D.; Sharma, S.; Kundu, B. New route to the synthesis of the isocryptolepine alkaloid and its related skeletons using a modified Pictet–Spengler reaction. *European Journal of Organic Chemistry* **2009**, *2009*, 292–303.

[186] Thobokholt, E. N.; Larghi, E. L.; Bracca, A. B.; Kaufman, T. S. Isolation and synthesis of cryptosanguinolentine (isocryptolepine), a naturally-occurring bioactive indoloquinoline alkaloid. *RSC Advances* **2020**, *10*, 18978–19002.

[187] Boganyi, B.; Kaman, J. A concise synthesis of indoloquinoline skeletons applying two consecutive Pd-catalyzed reactions. *Tetrahedron* **2013**, *69*, 9512–9519.

[188] Helgeland, I. T. U.; Sydnes, M. O. A Concise Synthesis of Isocryptolepine by C–C Cross-Coupling Followed by a Tandem C–H Activation and C–N Bond Formation. *Synopen* **2017**, *1*, 0041–0044.

[189] Håheim, K. S.; Helgeland, I. T. U.; Lindbäck, E.; Sydnes, M. O. Mapping the reactivity of the quinoline ring-system–Synthesis of the tetracyclic ring-system of isocryptolepine and regioisomers. *Tetrahedron* **2019**, *75*, 2949–2957.

[190] Timári, G.; Soós, T.; Hajos, G. A convenient synthesis of two new indoloquinoline alkaloids. *Synlett* **1997**, *1997*, 1067–1068.

[191] Singh, M. S. *Reactive intermediates in organic chemistry: Structure, Mechanism, and Reactions*; John Wiley & Sons, 2014.

[192] Taheri Kal Koshvandi, A.; Heravi, M. M.; Momeni, T. Current Applications of Suzuki–Miyaura Coupling Reaction in The Total Synthesis of Natural Products: An update. *Applied Organometallic Chemistry* **2018**, *32*, e4210.

[193] Suzuki, A. Cross-coupling reactions of organoboranes: an easy way to construct C-C bonds (Nobel Lecture). *Angewandte Chemie International Edition* **2011**, *50*, 6722–6737.

[194] Wu, X.-F.; Anbarasan, P.; Neumann, H.; Beller, M. From noble metal to Nobel prize: palladium-catalyzed coupling reactions as key methods in organic synthesis. *Angewandte Chemie International Edition* **2010**, *49*, 9047–9050.

[195] Boström, J.; Brown, D. G.; Young, R. J.; Keserü, G. M. Expanding the medicinal chemistry synthetic toolbox. *Nature Reviews Drug Discovery* **2018**, *17*, 709–727.

[196] Suzuki, A. Cross-coupling reactions via organoboranes. *Journal of organometallic chemistry* **2002**, *653*, 83–90.

[197] Suzuki, A. Organoborane coupling reactions (Suzuki coupling). *Proceedings of the Japan Academy, Series B* **2004**, *80*, 359–371.

[198] Miyaura, N.; Suzuki, A. Palladium-catalyzed cross-coupling reactions of organoboron compounds. *Chemical reviews* **1995**, *95*, 2457–2483.

[199] Miyaura, N.; Yamada, K.; Suzuki, A. A new stereospecific cross-coupling by the palladium-catalyzed reaction of 1-alkenylboranes with 1-alkenyl or 1-alkynyl halides. *Tetrahedron Letters* **1979**, *20*, 3437–3440.

[200] Suzuki, A. Recent advances in the cross-coupling reactions of organoboron derivatives with organic electrophiles, 1995–1998. *Journal of Organometallic Chemistry* **1999**, *576*, 147–168.

[201] Zhao, Y.-L.; Li, Y.; Li, S.-M.; Zhou, Y.-G.; Sun, F.-Y.; Gao, L.-X.; Han, F.-S. A highly practical and reliable nickel catalyst for Suzuki–Miyaura coupling of aryl halides. *Advanced Synthesis & Catalysis* **2011**, *353*, 1543–1550.

[202] Bellina, F.; Carpita, A.; Rossi, R. Palladium catalysts for the Suzuki cross-coupling reaction: an overview of recent advances. *Synthesis* **2004**, *2004*, 2419–2440.

[203] Amatore, C.; Jutand, A.; Le Duc, G. Kinetic Data for the Transmetalation/Reductive Elimination in Palladium-Catalyzed Suzuki–Miyaura Reactions: Unexpected Triple Role of Hydroxide Ions Used as Base. *Chemistry–A European Journal* **2011**, *17*, 2492–2503.

[204] Beletskaya, I. P.; Alonso, F.; Tyurin, V. The Suzuki-Miyaura reaction after the Nobel prize. *Coordination Chemistry Reviews* **2019**, *385*, 137–173.

[205] Biswas, B.; Kulsi, G. Solving the Riddle-the Mechanism of Suzuki Cross Coupling: A Review. *Asian J. Adv. Basic Sci* **2016**, *4*, 131–140.

[206] Wu, P.; Fokin, V. V. Catalytic azide-alkyne cycloaddition: Reactivity and applications. *Aldrichimica Acta* **2007**, *40*, 7–17.

[207] Tornøe, C. W.; Sanderson, S. J.; Mottram, J. C.; Coombs, G. H.; Meldal, M. Combinatorial Library of Peptidotriazoles: Identification of [1, 2, 3]-Triazole Inhibitors against a Recombinant Leishmania m exicana Cysteine Protease. *Journal of Combinatorial Chemistry* **2004**, *6*, 312–324.

[208] Whiting, M.; Muldoon, J.; Lin, Y.-C.; Silverman, S. M.; Lindstrom, W.; Olson, A. J.; Kolb, H. C.; Finn, M.; Sharpless, K. B.; Elder, J. H., et al. Inhibitors of HIV-1 protease by using in situ click chemistry. *Angewandte Chemie* **2006**, *118*, 1463–1467.

[209] Najafi, Z.; Mahdavi, M.; Saeedi, M.; Karimpour-Razkenari, E.; Asatouri, R.; Vafadarnejad, F.; Moghadam, F. H.; Khanavi, M.; Sharifzadeh, M.; Akbarzadeh, T. Novel tacrine-1, 2, 3-triazole hybrids: in vitro, in vivo biological evaluation and docking study of cholinesterase inhibitors. *European Journal of Medicinal Chemistry* **2017**, *125*, 1200–1212.

[210] Bourne, Y.; Kolb, H. C.; Radić, Z.; Sharpless, K. B.; Taylor, P.; Marchot, P. Freeze-frame inhibitor captures acetylcholinesterase in a unique conformation. *Proceedings of the National Academy of Sciences* **2004**, *101*, 1449–1454.

[211] Agalave, S. G.; Maujan, S. R.; Pore, V. S. Click chemistry: 1, 2, 3-triazoles as pharmacophores. *Chemistry–An Asian Journal* **2011**, *6*, 2696–2718.

[212] Michael, A. Ueber die einwirkung von diazobenzolimid auf acetylendicarbonsäuremethylester. *Journal für praktische Chemie* **1893**, *48*, 94–95.

[213] Huisgen, R. Kinetics and mechanism of 1, 3-dipolar cycloadditions. *Angewandte Chemie International Edition in English* **1963**, *2*, 633–645.

[214] Huisgen, R. 1, 3-dipolar cycloadditions. Past and future. *Angewandte Chemie International Edition in English* **1963**, *2*, 565–598.

[215] Tornøe, C. W.; Christensen, C.; Meldal, M. Peptidotriazoles on solid phase:[1, 2, 3]-triazoles by regiospecific copper (I)-catalyzed 1, 3-dipolar cycloadditions of terminal alkynes to azides. *The Journal of organic chemistry* **2002**, *67*, 3057–3064.

[216] Rostovtsev, V. V.; Green, L. G.; Fokin, V. V.; Sharpless, K. B. A stepwise huisgen cycloaddition process: copper (I)-catalyzed regioselective "ligation" of azides and terminal alkynes. *Angewandte Chemie* **2002**, *114*, 2708–2711.

[217] Meldal, M.; Tornøe, C. W. Cu-catalyzed azide- alkyne cycloaddition. *Chemical reviews* **2008**, *108*, 2952–3015.

[218] Hein, J. E.; Fokin, V. V. Copper-catalyzed azide–alkyne cycloaddition (CuAAC) and beyond: new reactivity of copper (I) acetylides. *Chemical Society Reviews* **2010**, *39*, 1302–1315.

[219] Presolski, S. I.; Hong, V.; Cho, S.-H.; Finn, M. Tailored ligand acceleration of the Cu-catalyzed azide- alkyne cycloaddition reaction: practical and mechanistic implications. *Journal of the American Chemical Society* **2010**, *132*, 14570–14576.

[220] Meldal, M.; Diness, F. Recent Fascinating Aspects of the CuAAC Click Reaction. *Trends in Chemistry* **2020**,

[221] Worrell, B.; Malik, J.; Fokin, V. V. Direct evidence of a dinuclear copper intermediate in Cu (I)-catalyzed azide-alkyne cycloadditions. *Science* **2013**, *340*, 457–460.

[222] Zhu, L.; Brassard, C. J.; Zhang, X.; Guha, P. M.; Clark, R. J. On the Mechanism of Copper (I)-Catalyzed Azide–Alkyne Cycloaddition. *The Chemical Record* **2016**, *16*, 1501–1517.

[223] Himo, F.; Lovell, T.; Hilgraf, R.; Rostovtsev, V. V.; Noodleman, L.; Sharpless, K. B.; Fokin, V. V. Copper (I)-catalyzed synthesis of azoles. DFT study predicts unprecedented reactivity and intermediates. *Journal of the American Chemical Society* **2005**, *127*, 210–216.

[224] Lewis, W. G.; Green, L. G.; Grynszpan, F.; Radić, Z.; Carlier, P. R.; Taylor, P.; Finn, M.; Sharpless, K. B. Click chemistry in situ: acetylcholinesterase as a reaction vessel for the selective assembly of a femtomolar inhibitor from an array of building blocks. *Angewandte Chemie* **2002**, *114*, 1095–1099.

[225] Manetsch, R.; Krasiński, A.; Radić, Z.; Raushel, J.; Taylor, P.; Sharpless, K. B.; Kolb, H. C. In situ click chemistry: enzyme inhibitors made to their own specifications. *Journal of the American Chemical Society* **2004**, *126*, 12809–12818.

[226] Hooper, C.; Killick, R.; Lovestone, S. The GSK3 hypothesis of Alzheimer's disease. *Journal of neurochemistry* **2008**, *104*, 1433–1439.

[227] Gottlieb, H. E.; Kotlyar, V.; Nudelman, A. NMR chemical shifts of common laboratory solvents as trace impurities. *The Journal of organic chemistry* **1997**, *62*, 7512–7515.

[228] Maspero, M.; Volpato, D.; Cirillo, D.; Chen, N. Y.; Messerer, R.; Sotriffer, C.; De Amici, M.; Holzgrabe, U.; Dallanoce, C. Tacrine-xanomeline and tacrine-iperoxo hybrid ligands: Synthesis and biological evaluation at acetylcholinesterase and M1 muscarinic acetylcholine receptors. *Bioorganic Chemistry* **2020**, *96*, 103633.

[229] Więckowska, A.; Kołaczkowski, M.; Bucki, A.; Godyń, J.; Marcinkowska, M.; Więckowski, K.; Zaręba, P.; Siwek, A.; Kazek, G.; Głuch-Lutwin, M., et al. Novel multi-target-directed ligands for Alzheimer's disease: combining cholinesterase inhibitors and 5-HT6 receptor antagonists. Design, synthesis and biological evaluation. *European Journal of Medicinal Chemistry* **2016**, *124*, 63–81.

[230] Sethna, S. M.; Shah, N. M. The Chemistry of Coumarins. *Chemical Reviews* **1945**, *36*, 1–62.

[231] Tian, Y.; Liang, Z.; Xu, H.; Mou, Y.; Guo, C. Design, synthesis and cytotoxicity of novel dihydroartemisinin-coumarin hybrids via click chemistry. *Molecules* **2016**, *21*, 758.

[232] Najafi, Z.; Mahdavi, M.; Saeedi, M.; Karimpour-Razkenari, E.; Edraki, N.; Sharifzadeh, M.; Khanavi, M.; Akbarzadeh, T. Novel tacrine-coumarin hybrids linked to 1, 2, 3-triazole as anti-Alzheimer's compounds: In vitro and in vivo biological evaluation and docking study. *Bioorganic chemistry* **2019**, *83*, 303–316.

[233] Dubovitskii, S.; Radchenko, O.; Norikov, V. Synthesis of isocryptolepine, an alkaloid fromCryptolepis sanguinolenta. *Russian chemical bulletin* **1996**, *45*, 2656–2657.

[234] Fulmer, G. R.; Miller, A. J.; Sherden, N. H.; Gottlieb, H. E.; Nudelman, A.; Stoltz, B. M.; Bercaw, J. E.; Goldberg, K. I. NMR chemical shifts of trace impurities: common laboratory solvents, organics, and gases in deuterated solvents relevant to the organometallic chemist. *Organometallics* **2010**, *29*, 2176–2179.

[235] Sun, Y.; Chen, J.; Chen, X.; Huang, L.; Li, X. Inhibition of cholinesterase and monoamine oxidase-B activity by Tacrine–Homoisoflavonoid hybrids. *Bioorganic & medicinal chemistry* **2013**, *21*, 7406–7417.

5 Appendix

Spectra for novel compounds

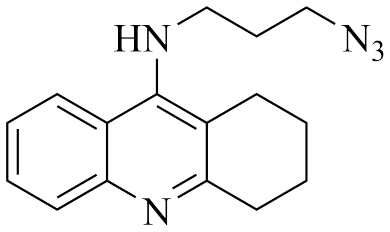

31

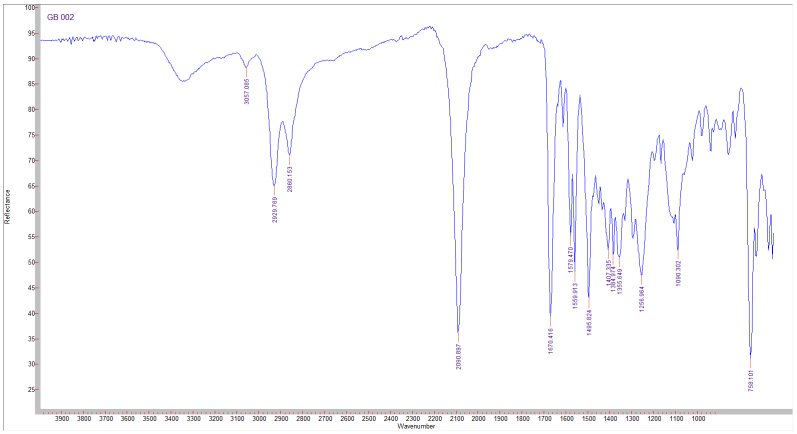

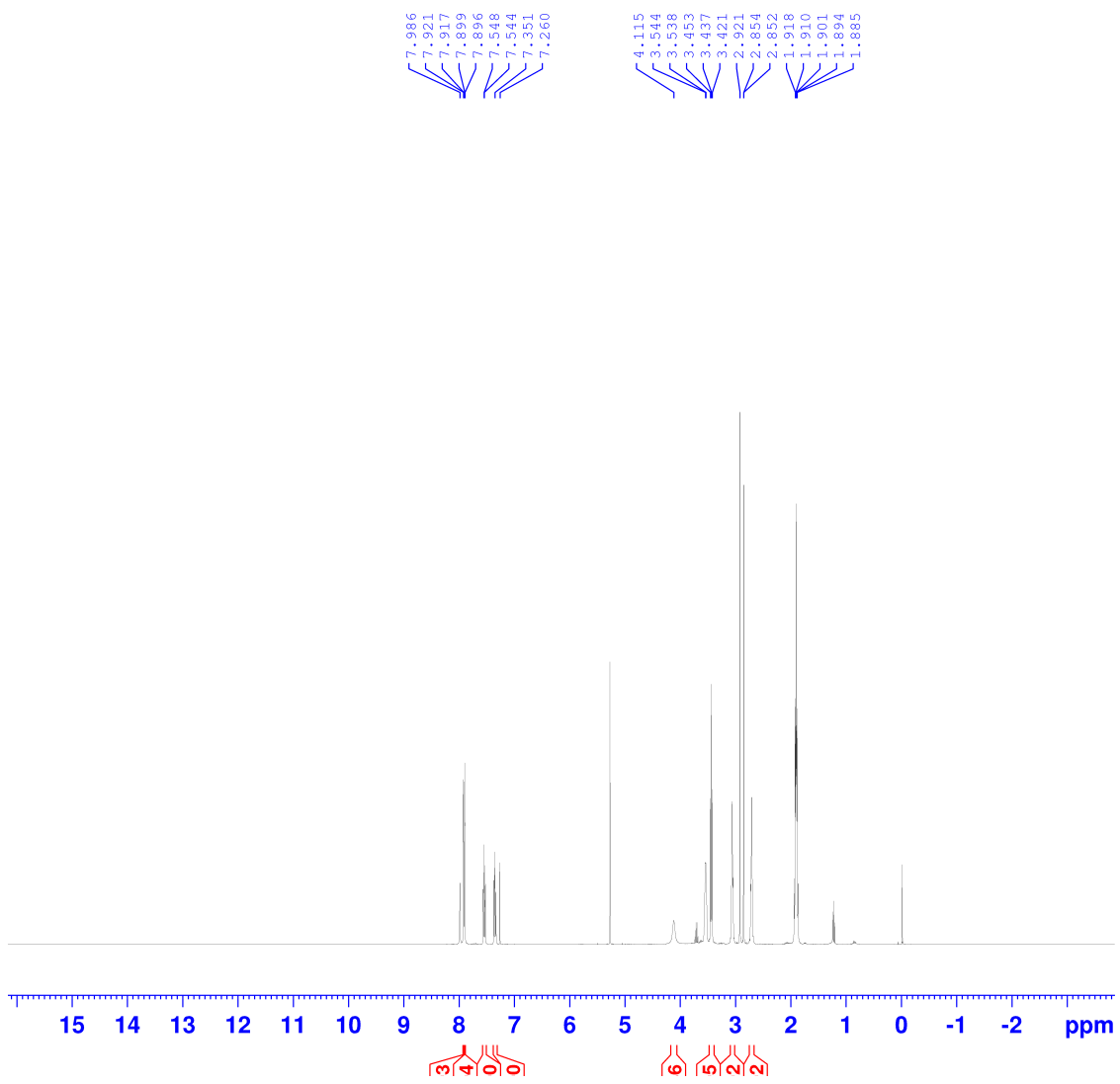
7.986
7.921
7.917
7.899
7.896
7.548
7.544
7.351
7.260
4.115
3.544
3.538
3.453
3.437
3.421
2.921
2.854
2.852
1.918
1.910
1.901
1.894
1.885
15 14 13 12 11 10 9 8 7 6 5 4 3 2 1 0 -1 -2 ppm
3 4 0 0
6 5 2 2

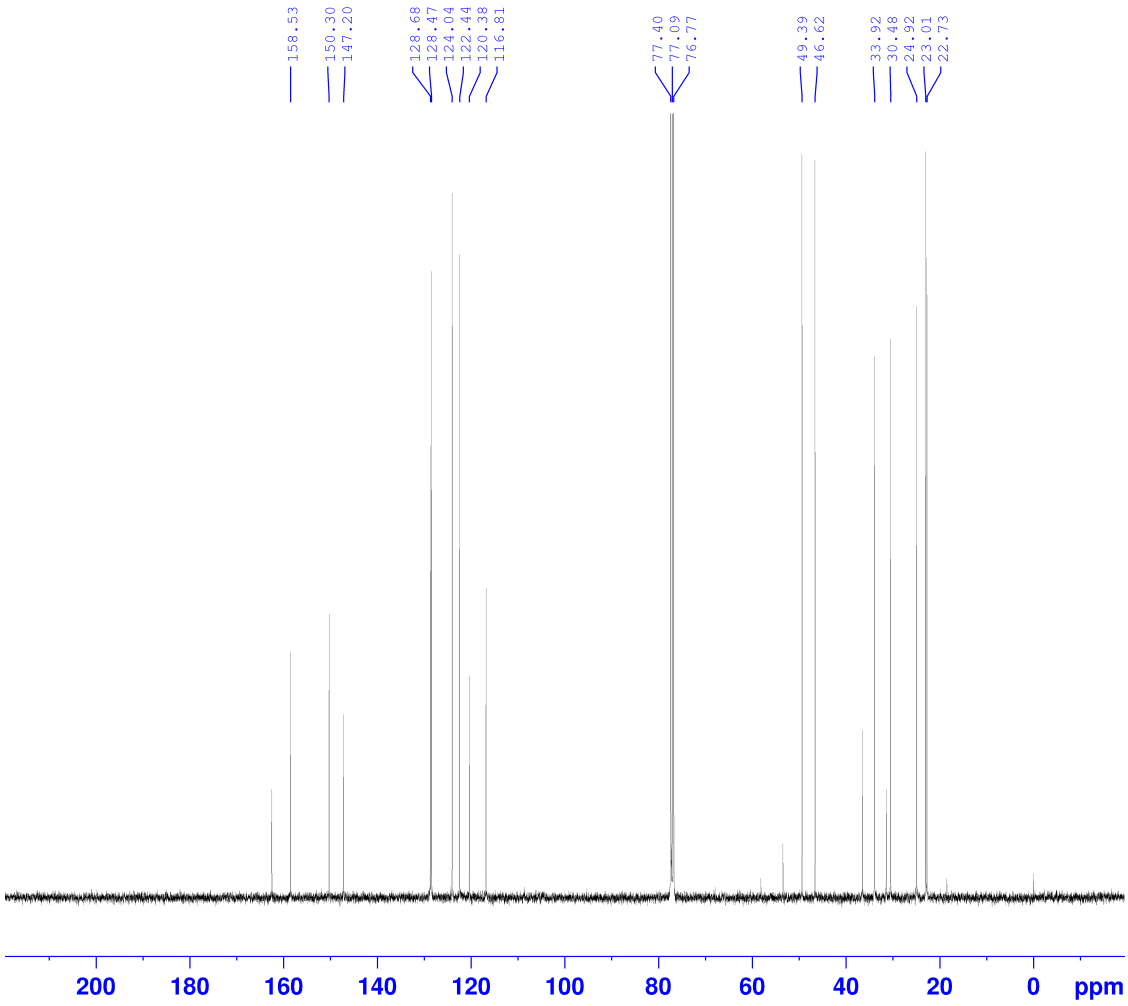
158.53
150.30
147.20
128.68
128.47
124.04
122.44
120.38
116.81
77.40
77.09
76.77
49.39
46.62
33.92
30.48
24.92
23.01
22.73
200
180
160
140
120
100
80
60
40
20
0
ppm

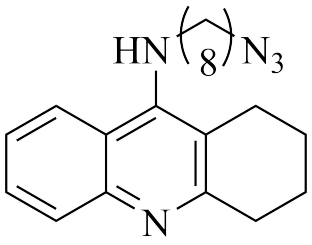
HN
8
N3
N

33

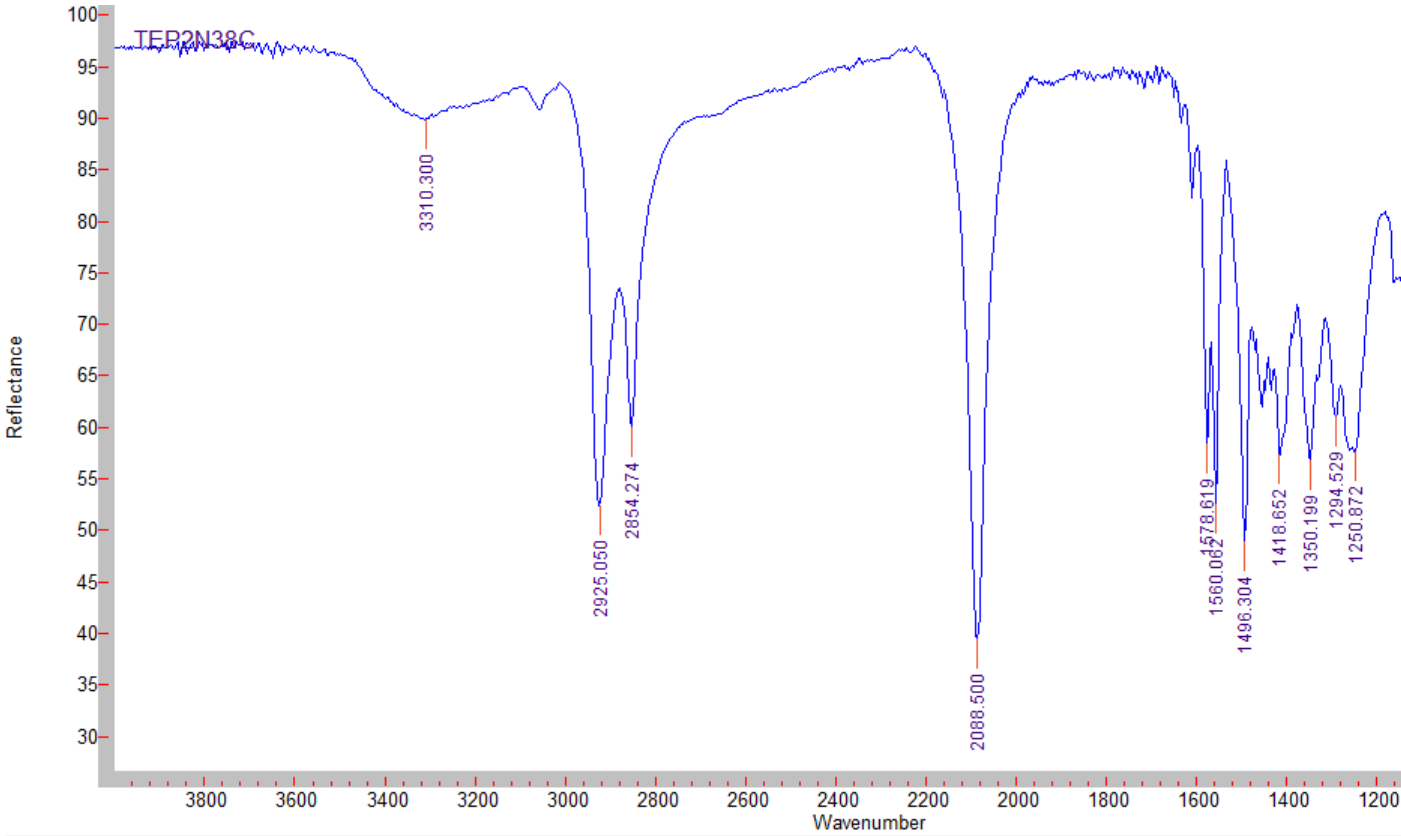
TEP2N38C
Reflectance
Wavenumber
3310.300
2925.050
2854.274
2088.500
1578.619
1560.082
1496.304
1418.652
1350.199
1294.529
1250.872

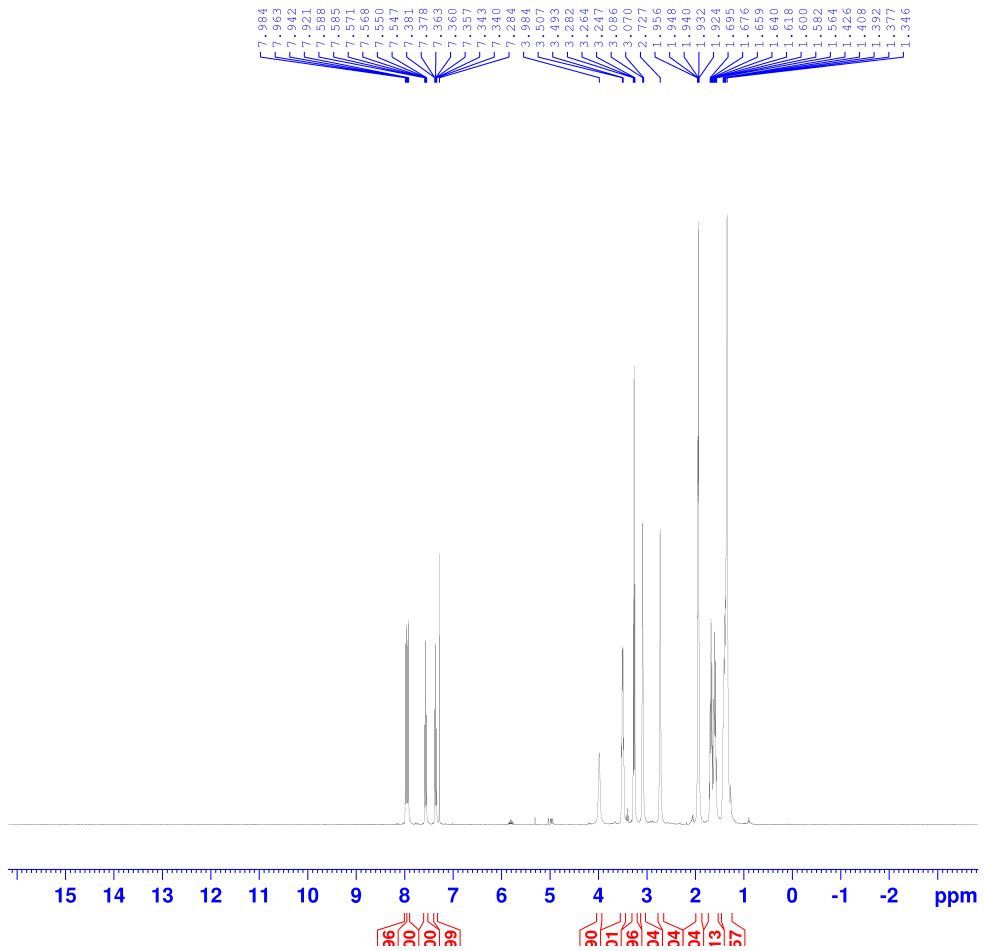
7.984
7.963
7.942
7.921
7.588
7.585
7.571
7.568
7.550
7.547
7.381
7.378
7.363
7.360
7.357
7.343
7.340
7.284
3.984
3.507
3.493
3.282
3.264
3.247
3.086
3.070
2.727
2.256
1.948
1.940
1.932
1.924
1.695
1.676
1.659
1.640
1.618
1.600
1.582
1.564
1.426
1.408
1.392
1.377
1.346
15 14 13 12 11 10 9 8 7 6 5 4 3 2 1 0 -1 -2 ppm

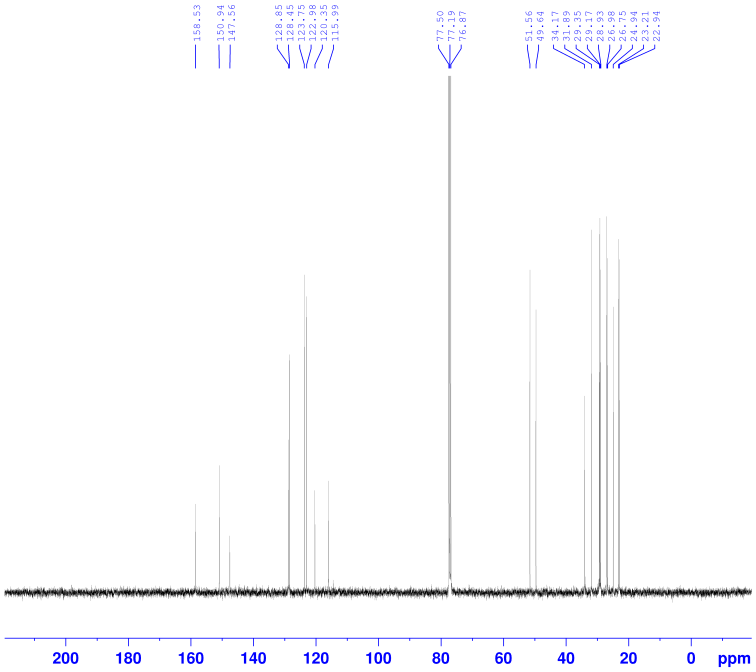
158.53
150.94
147.56
128.85
128.45
123.75
122.98
120.35
118.99
77.50
77.19
76.87
51.56
49.64
34.17
31.89
29.35
29.13
28.73
26.98
26.75
24.94
23.21
22.94
200
180
160
140
120
100
80
60
40
20
0
ppm

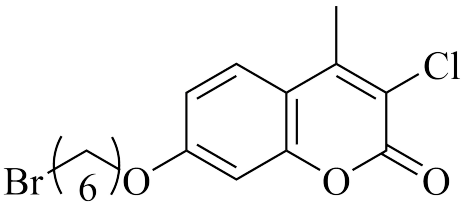
Cl
Br
6
O
O
O

35

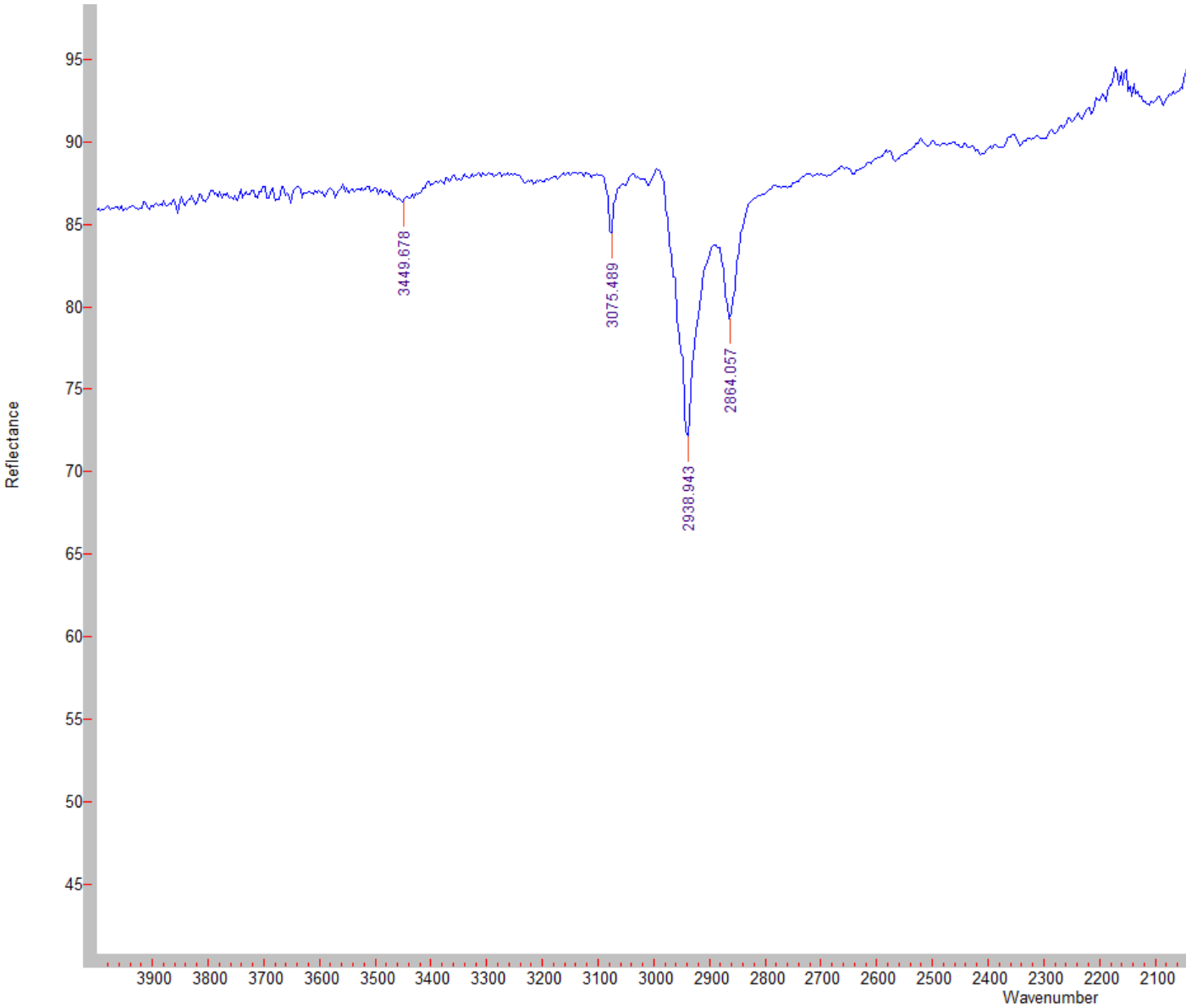
Reflectance
95
90
85
80
75
70
65
60
55
50
45
3449.678
3075.489
2938.943
2864.057
3900 3800 3700 3600 3500 3400 3300 3200 3100 3000 2900 2800 2700 2600 2500 2400 2300 2200 2100
Wavenumber

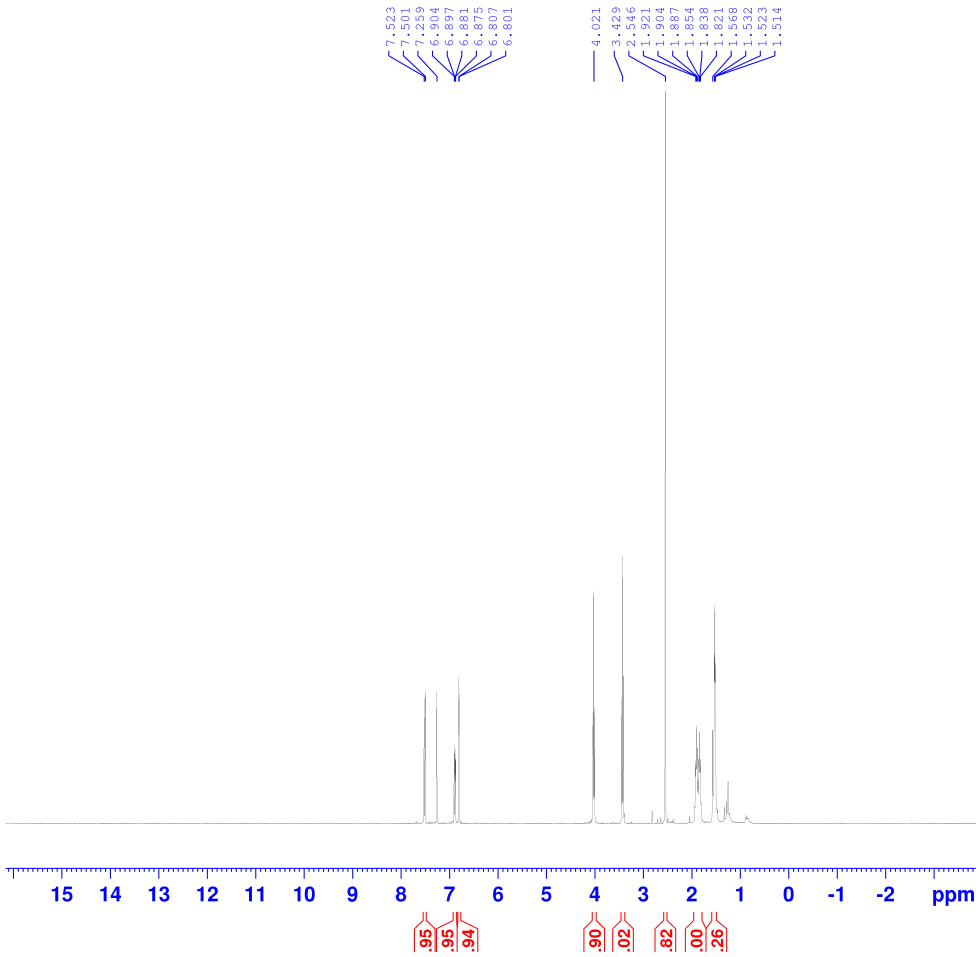
7.523
7.501
7.259
6.904
6.897
6.881
6.875
6.807
6.801
4.021
3.429
2.546
1.921
1.904
1.887
1.854
1.838
1.821
1.568
1.532
1.523
1.514
15 14 13 12 11 10 9 8 7 6 5 4 3 2 1 0 -1 -2 ppm
.95
.95
.94
.90
.02
.82
.00
.26

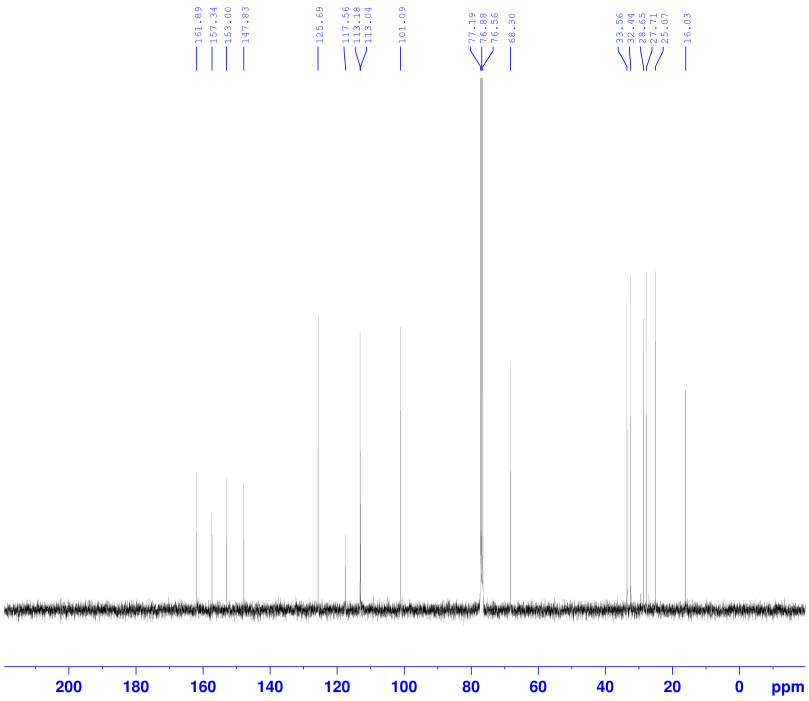
161.89
157.34
153.00
147.83
125.69
117.56
113.18
113.04
101.09
77.19
76.88
76.56
68.30
33.56
32.44
28.65
27.71
25.07
16.03
200
180
160
140
120
100
80
60
40
20
0
ppm

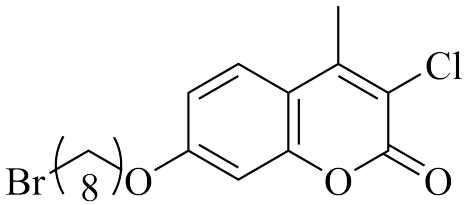
Cl
Br
8
O
O
O

36

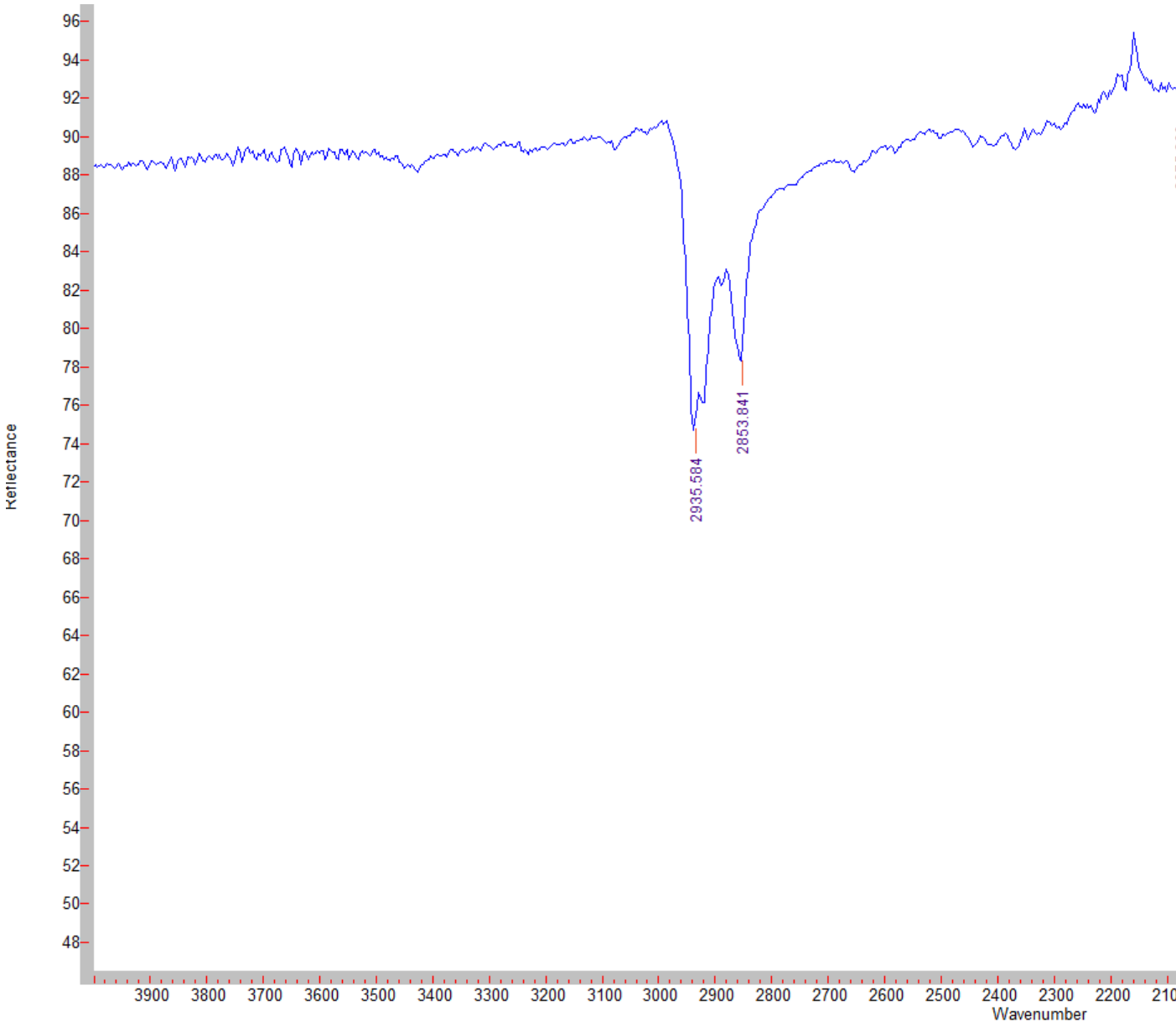
Reflectance
96
94
92
90
88
86
84
82
80
78
76
74
72
70
68
66
64
62
60
58
56
54
52
50
48
2935.584
2853.841
3900
3800
3700
3600
3500
3400
3300
3200
3100
3000
2900
2800
2700
2600
2500
2400
2300
2200
Wavenumber

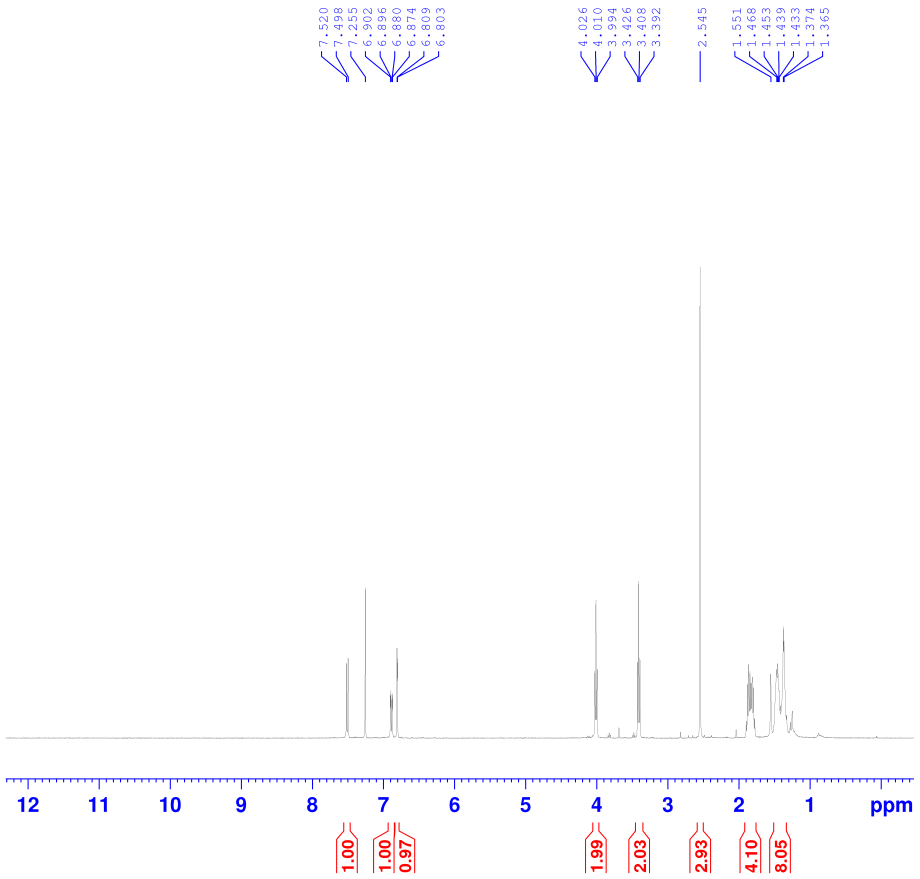
7.520
7.498
7.255
6.902
6.896
6.880
6.874
6.809
6.803
4.026
4.010
3.994
3.426
3.408
3.392
2.545
1.551
1.468
1.453
1.439
1.433
1.374
1.365
12
11
10
9
8
7
6
5
4
3
2
1
ppm
1.00
1.00
0.97
1.99
2.03
2.93
4.10
8.05

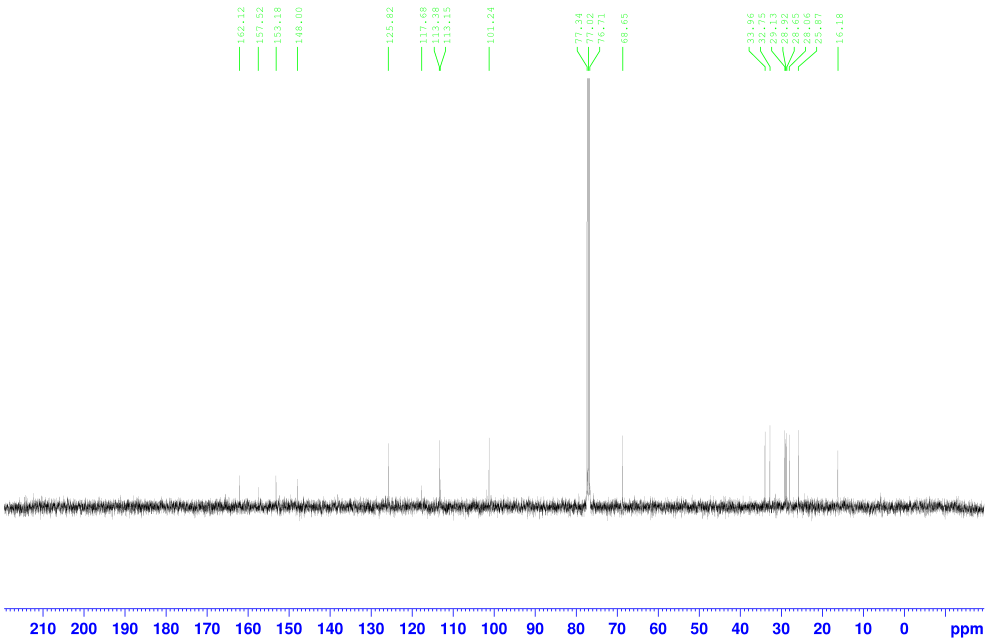
162.12
157.52
153.18
148.00
125.82
117.68
113.38
113.15
101.24
77.34
77.02
76.71
68.65
33.96
32.75
29.13
28.92
28.65
28.06
25.97
16.18
210 200 190 180 170 160 150 140 130 120 110 100 90 80 70 60 50 40 30 20 10 0 ppm

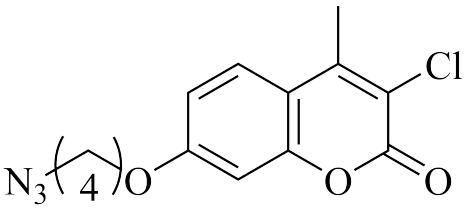
Cl
N3
4
O
O
O

37

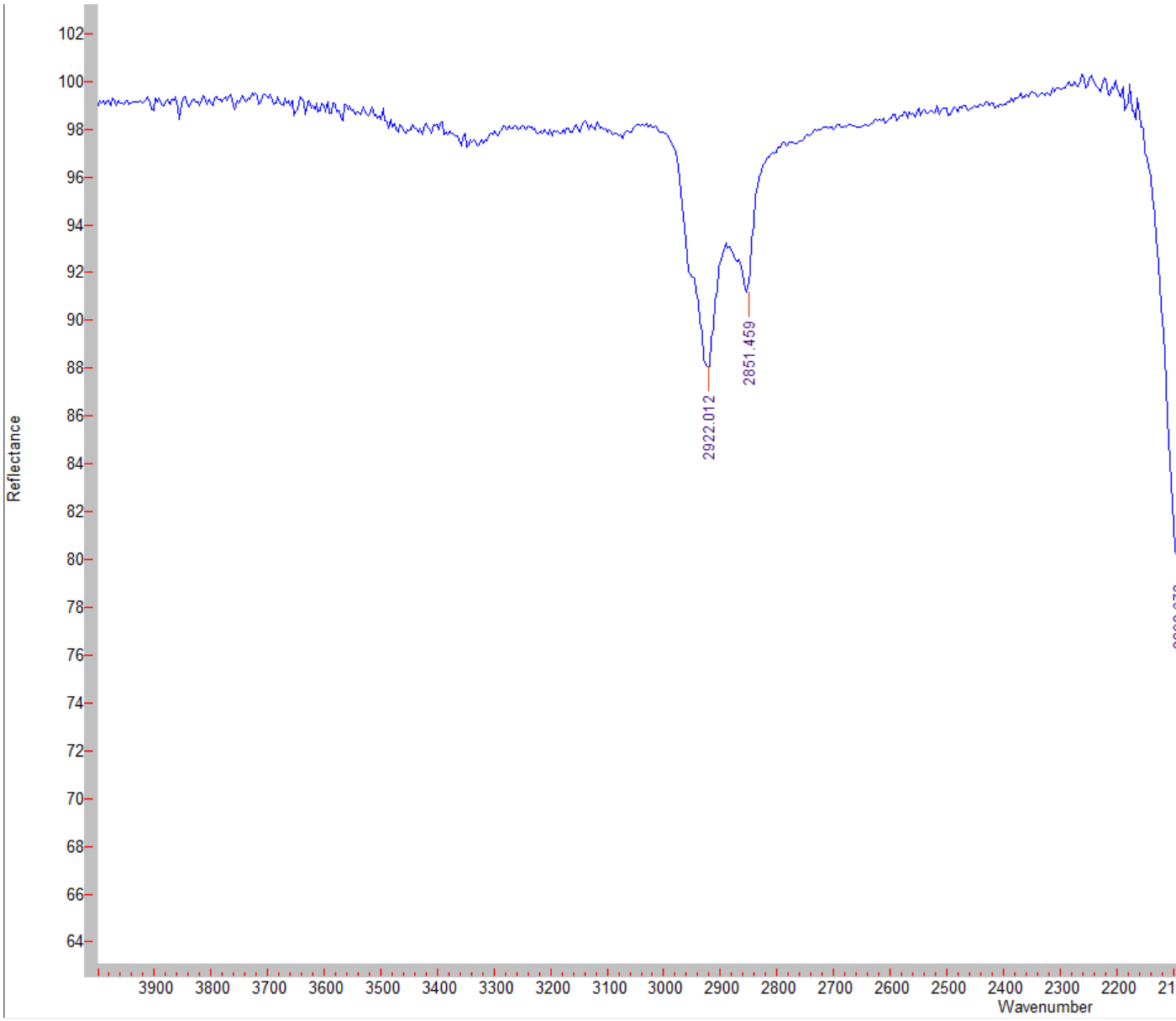
Reflectance
102
100
98
96
94
92
90
88
86
84
82
80
78
76
74
72
70
68
66
64
2922.012
2851.459
3900 3800 3700 3600 3500 3400 3300 3200 3100 3000 2900 2800 2700 2600 2500 2400 2300 2200
Wavenumber

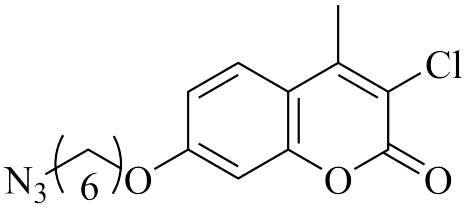
Cl
N3
6
O
O
O

38

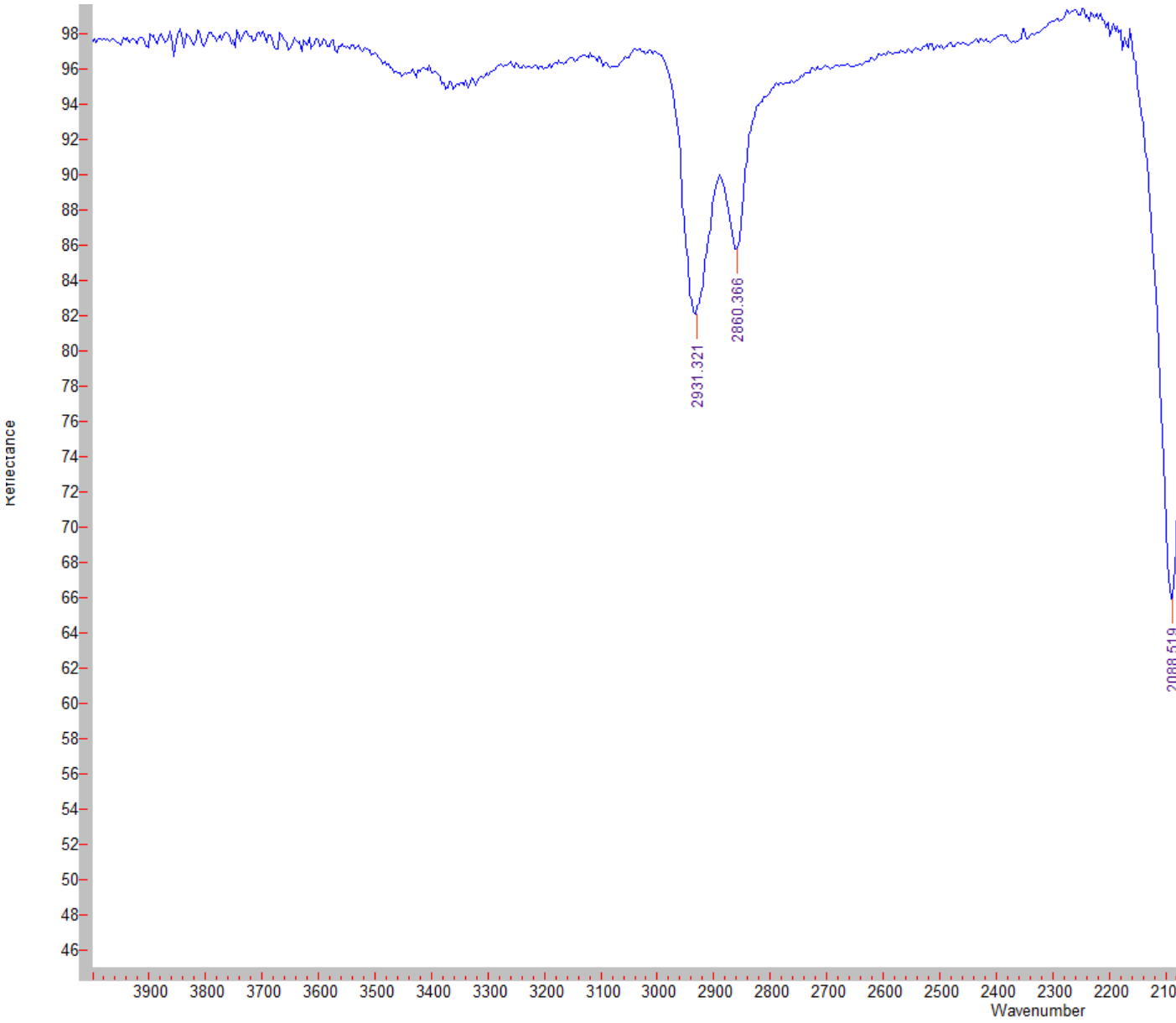
Reflectance
98
96
94
92
90
88
86
84
82
80
78
76
74
72
70
68
66
64
62
60
58
56
54
52
50
48
46
2931.321
2860.366
3900 3800 3700 3600 3500 3400 3300 3200 3100 3000 2900 2800 2700 2600 2500 2400 2300 2200 210
Wavenumber

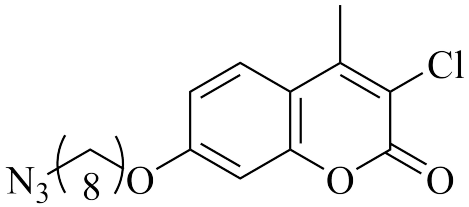
Cl
N3
8
O
O
O

39

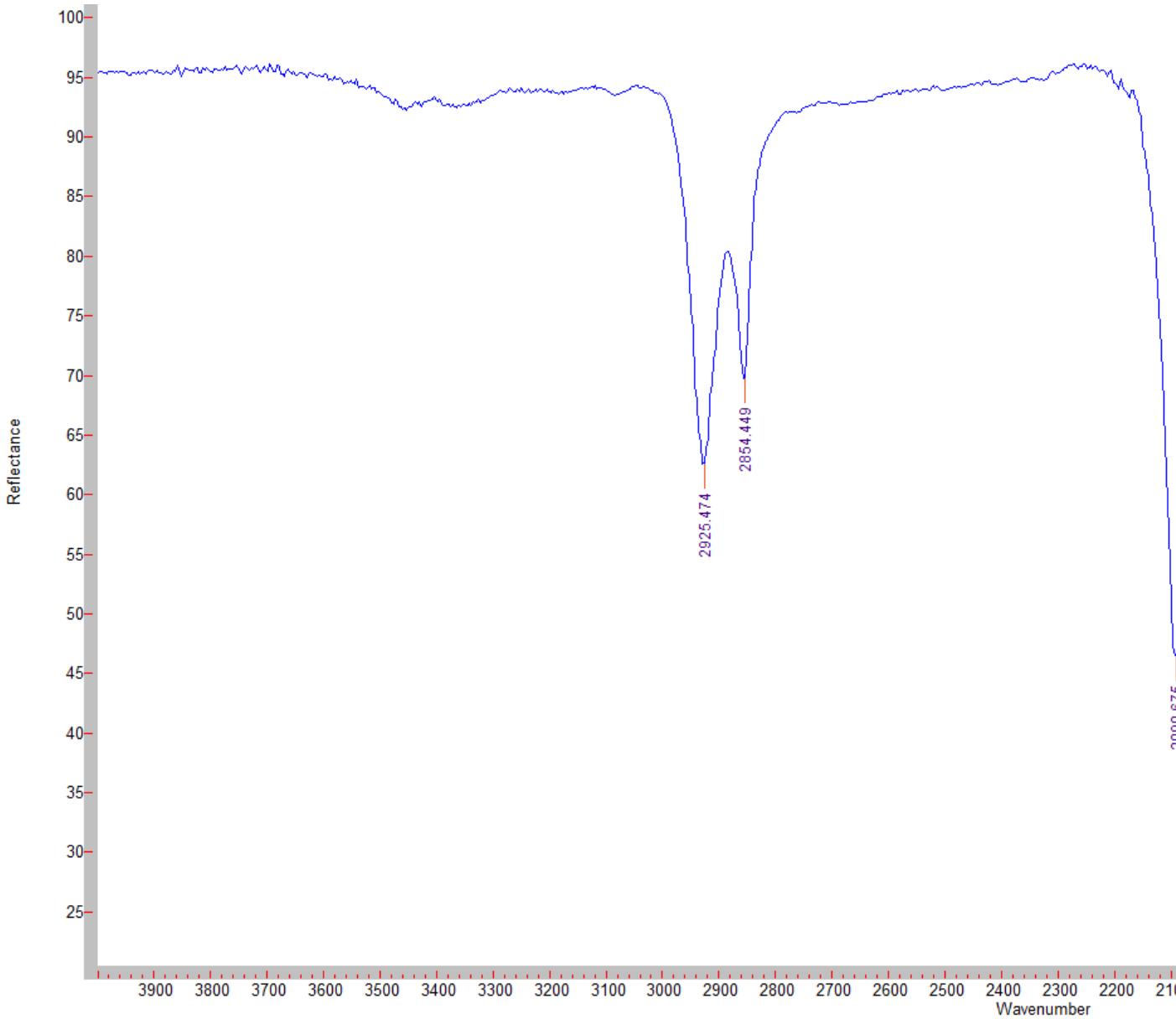
Reflectance
100
95
90
85
80
75
70
65
60
55
50
45
40
35
30
25
2925.474
2854.449
3900
3800
3700
3600
3500
3400
3300
3200
3100
3000
2900
2800
2700
2600
2500
2400
2300
2200
Wavenumber

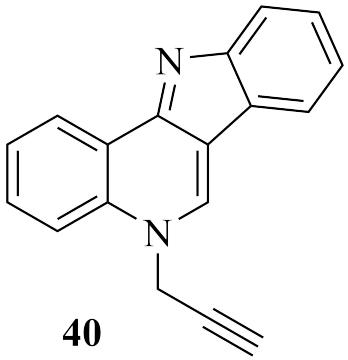
N
N

40

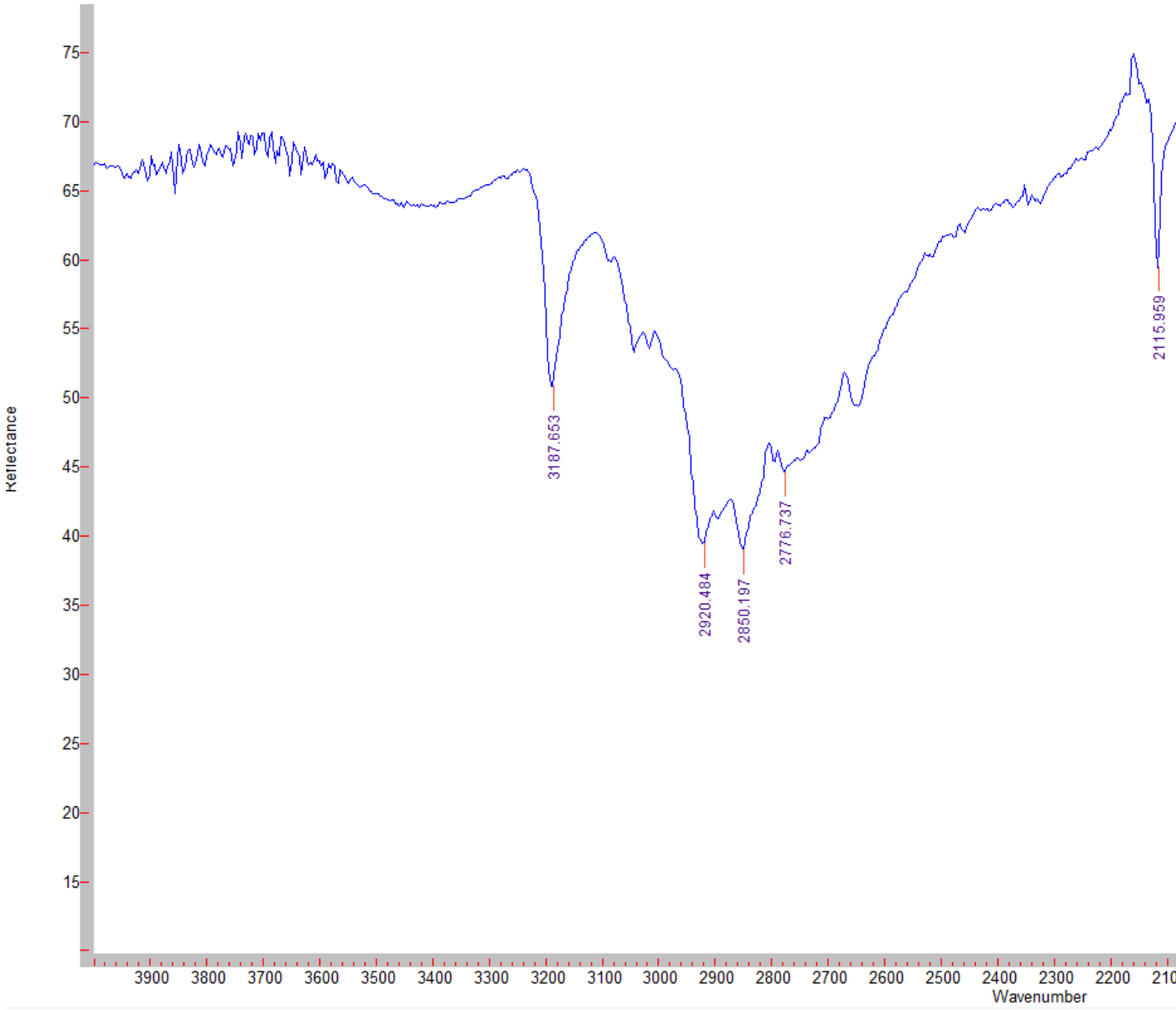
Reflectance
75
70
65
60
55
50
45
40
35
30
25
20
15
3187.653
2920.484
2850.197
2776.737
2115.959
3900 3800 3700 3600 3500 3400 3300 3200 3100 3000 2900 2800 2700 2600 2500 2400 2300 2200 210
Wavenumber

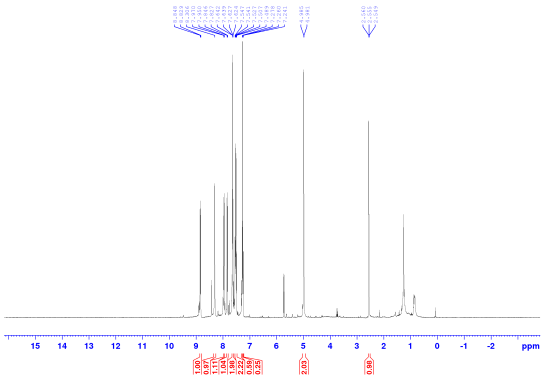
15 14 13 12 11 10 9 8 7 6 5 4 3 2 1 0 -1 -2 ppm

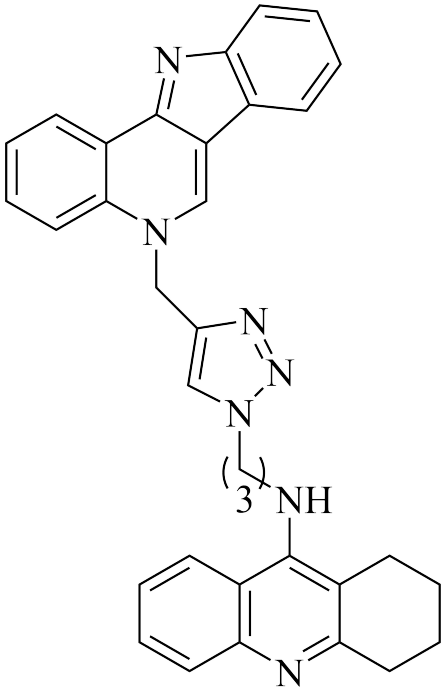
N
N
N
N
N
3
NH
N

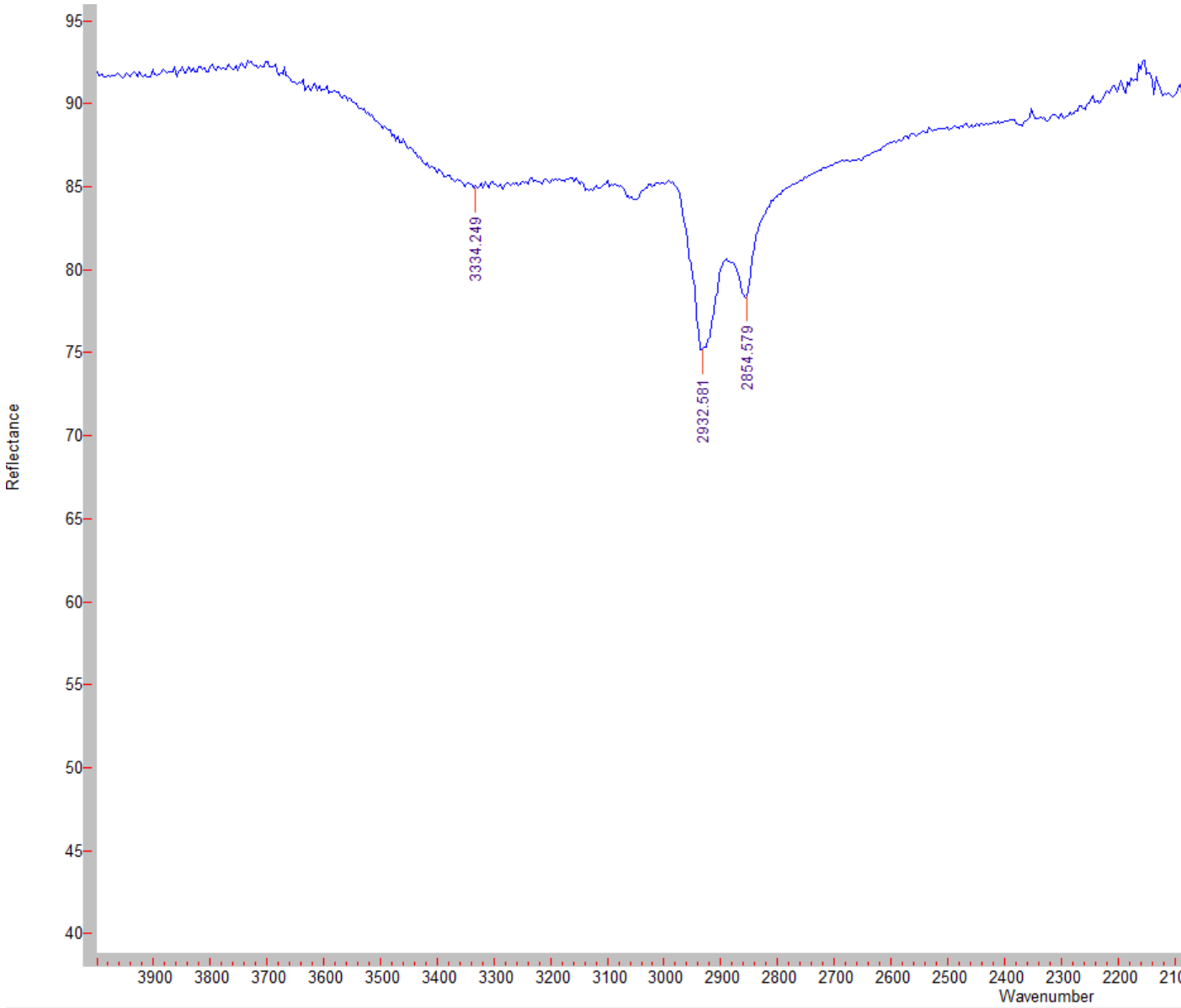
Reflectance
95
90
85
80
75
70
65
60
55
50
45
40
3334.249
2932.581
2854.579
3900 3800 3700 3600 3500 3400 3300 3200 3100 3000 2900 2800 2700 2600 2500 2400 2300 2200
Wavenumber

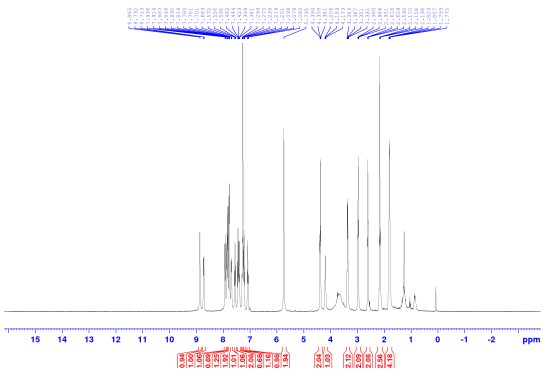

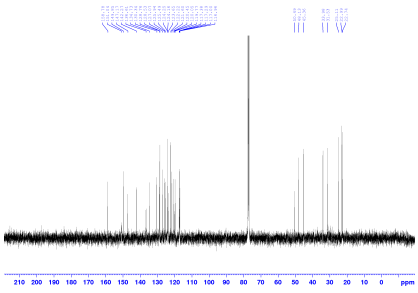

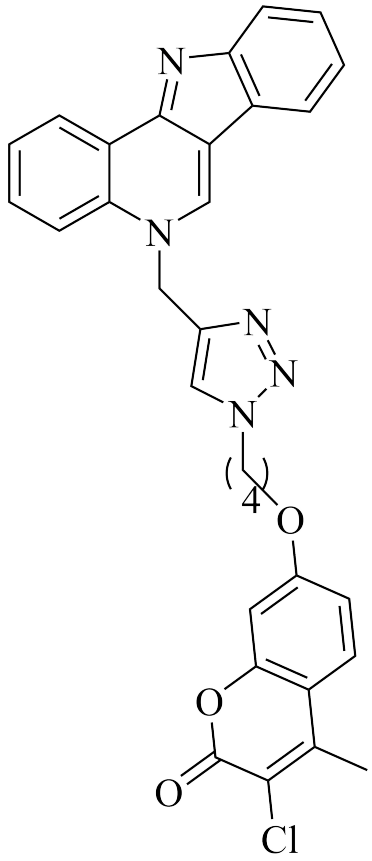
N
N
N
N
4
O
O
O
Cl

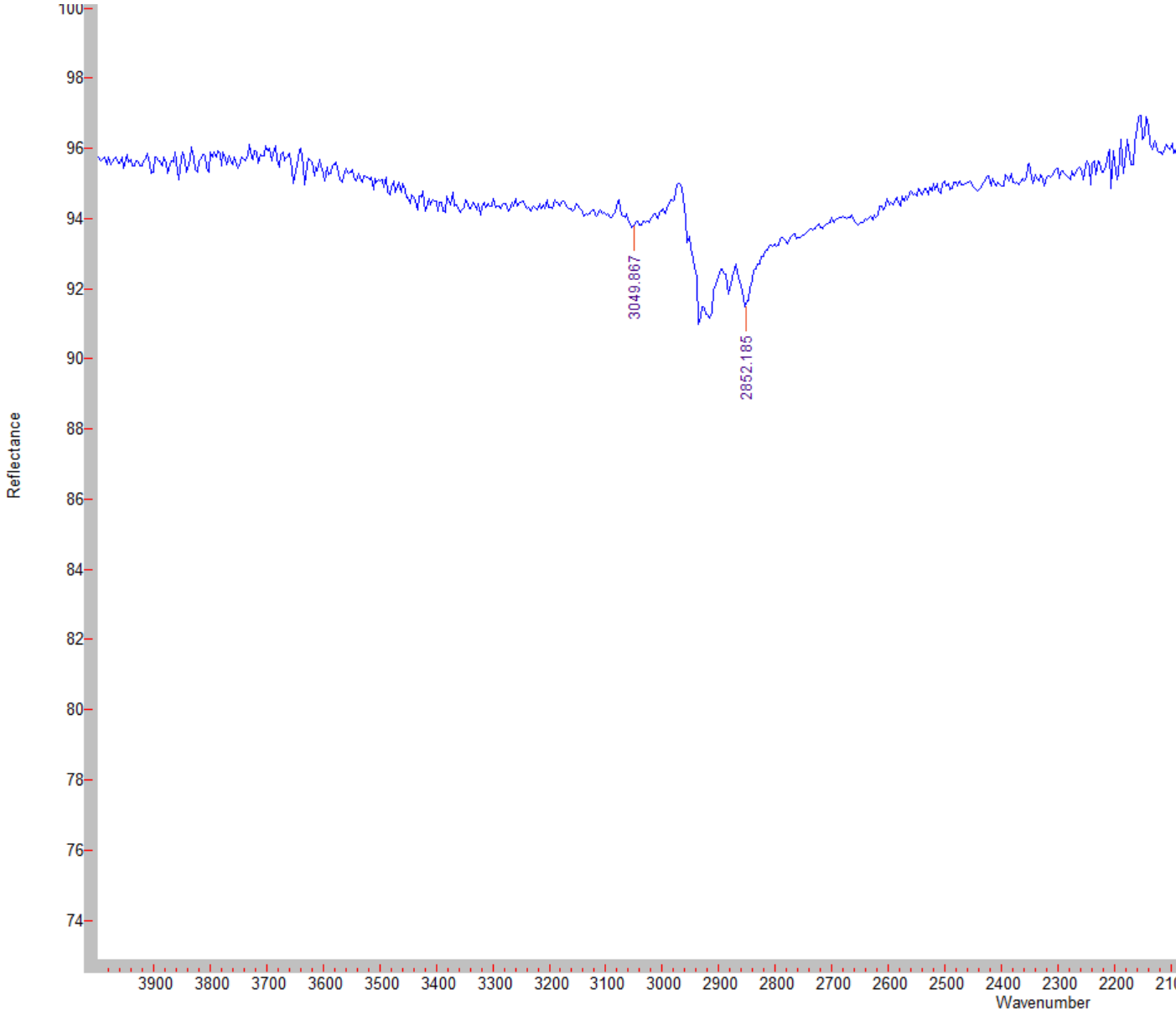
100
98
96
94
92
90
88
86
84
82
80
78
76
74
Reflectance
3049.867
2852.185
3900 3800 3700 3600 3500 3400 3300 3200 3100 3000 2900 2800 2700 2600 2500 2400 2300 2200
Wavenumber

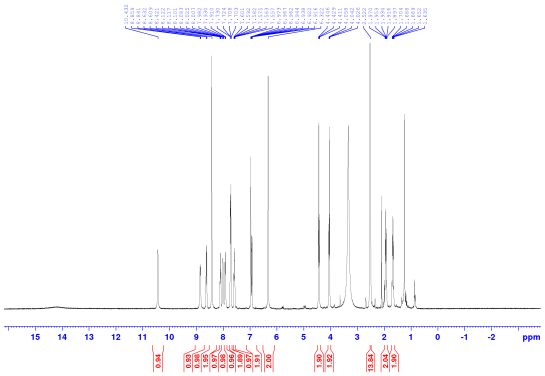
15 14 13 12 11 10 9 8 7 6 5 4 3 2 1 0 -1 -2 ppm

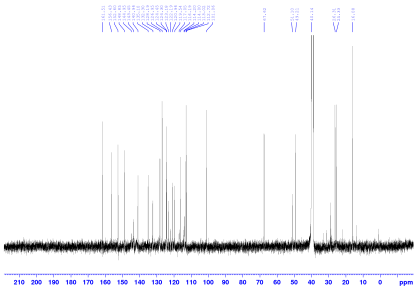
210 200 190 180 170 160 150 140 130 120 110 100 90 80 70 60 50 40 30 20 10 0 ppm